P-08-59

Forsmark site investigation

Large-scale confirmatory multiple-hole tracer test

Anna Lindquist, Calle Hjerne,
Rune Nordqvist, Eva Wass
Geosigma AB

May 2008

Svensk Kärnbränslehantering AB
Swedish Nuclear Fuel
and Waste Management Co
Box 250, SE-101 24 Stockholm
Tel +46 8 459 84 00

ISSN 1651-4416
SKB P-08-59

Forsmark site investigation

Large-scale confirmatory multiple-hole tracer test

Anna Lindquist, Calle Hjerne,
Rune Nordqvist, Eva Wass
Geosigma AB

May 2008

Keywords: Tracer test, Dilution test, Sorption, AP PF 400-07-020.

Abstract

A large scale tracer test has been carried out within the Forsmark site investigation area during the summer 2007. The borehole HFM14 was pumped and non-sorbing tracers were injected in six isolated sections in six different surrounding boreholes. The distance from the injection sections to the pumping borehole varied from 72 m to 512 m. The pumping lasted 15 weeks with a flow rate of 350 l/min. Prior to the tracer test groundwater flow measurements were carried out in the sections of current interest (by dilution measurements) both before and during pumping, on one hand to confirm the response to the pumping and on the other hand since the groundwater flow was necessary for further calculations.

In the borehole closest to the pumping hole, HFM15, an additional tracer test was made towards the end of the pumping period. This time one non-sorbing tracer (Uranine) and one sorbing tracer (Cesium) was used.

Tracer breakthrough was obtained from five of the six boreholes. Only from HFM32, the most remote of the six holes, the tracer did not appear in HFM14. From the additional tracer test in HFM15, tracer breakthrough was obtained for both Uranine and Cs.

Transport models (advection-dispersion model and advection-dispersion model including matrix diffusion) were used to evaluate transport parameters from the measured results. In the case of evaluation of Cs in the additional tracer test, linear sorption was also included in the models.

The additional test with Uranine and Cs indicates a weak sorption of Cs, with the retardation factor R=2.2.

The results from the tracer test are quantitatively in good accordance with the results from the hydraulic interference test performed in conjunction with the pumping.

Sammanfattning

Ett storskaligt spårförsök har genomförts inom platsundersökningsområdet i Forsmark under sommaren 2007. Pumpning gjordes i HFM14 och injektion av sex olika icke-sorberande spårämnen gjordes i avgränsade sektioner i sex omkringliggande borrhål. Avståndet från borrhålen där spårämne tillsattes till pumphålet varierade mellan 72 och 512 m. Pumpningen pågick i 15 veckor och flödet var 350 l/min. Innan själva spårförsöket startade mättes grundvattenflödet i de aktuella sektionerna (med utspädningsmätningar) både före och under pumpning, dels för att säkerställa att de svarade på pumpningen, dels för att grundvattenflödet var nödvändigt för vidare beräkningar.

I det närmsta borrhålet, HFM15, gjordes mot slutet av pumpningen ytterligare ett spårämnesförsök, denna gång med ett icke-sorberande ämne (Uranin) och ett sorberande (Cesium).

Spårämnesgenombrott erhölls från fem av de sex borrhålen. Endast från HFM32 som låg längst bort, uteblev genombrottet. Från det andra försöket i HFM15 erhölls genombrott av både Uranin och Cs.

Transportmodeller (advektions-dispersions modellen samt i några fall även advektions-dispersions modellen med matrisdiffusion) användes för att utifrån de uppmätta resultaten bestämma transportparametrar. Vid utvärdering av försöket med Cs inkluderades också en linjär sorption i modellerna.

Försöket med Uranin och Cs i HFM15 indikerar en svag fördröjning av Cs, med retardationsfaktorn R=2.2.

Resultaten från spårförsöket är kvantitativt överensstämmande med resultaten från det hydrauliska interferenstestet som utfördes i samband med pumpningen.

Contents

1 Introduction

This document reports the results gained by the multiple-hole tracer test with pumping in HFM14, which is one of the activities performed within the site investigation at Forsmark. The work was carried out in accordance with activity plan AP PF 400-07-020. In Table 1-1 controlling documents for performing this activity are listed. Both activity plan and method descriptions are SKB's internal controlling documents. The obtained data from the activity are reported to the database Sicada, where they are traceable by the activity plan number.

The field work was performed during 15 weeks from June to October 2007. The field work involved groundwater flow measurements (both during natural conditions prior to the pumping and during the pumping in HFM14) in the six investigated sections by dilution measurements, a multiple-hole tracer test and an additional tracer test using Uranine together with the sorbing tracer Cesium in HFM15.

A map of the investigation area in Forsmark and the boreholes involved in this tracer test is shown in Figure 1-1. Six different borehole sections in six different boreholes were included in the tracer test surrounding the pumping borehole HFM14. They are listed in Table 1-2 below. The distances given in Table 2-1 are the distances between HFM14 at borehole length 20 m and the middle of each tested section. An interference test was also performed in connection with the tracer test. The pumping test and the interference test are described in a separate report /1/.

Table 1-1. Controlling documents for performance of the activity.

Activity plan	**Number**	**Version**
Storskaligt spårförsök med pumpning i hammarborrhål 14.	AP PF 400-07-020	1.0
Method descriptions	**Number**	**Version**
Metodbeskrivning för flerhålsförsök.	SKB MD 530.006	1.0
System för hydrologisk och metrologisk datainsamling.	SKB MD 368.010	1.0
Vattenprovtagning och utspädningsmätning i observationshål.		

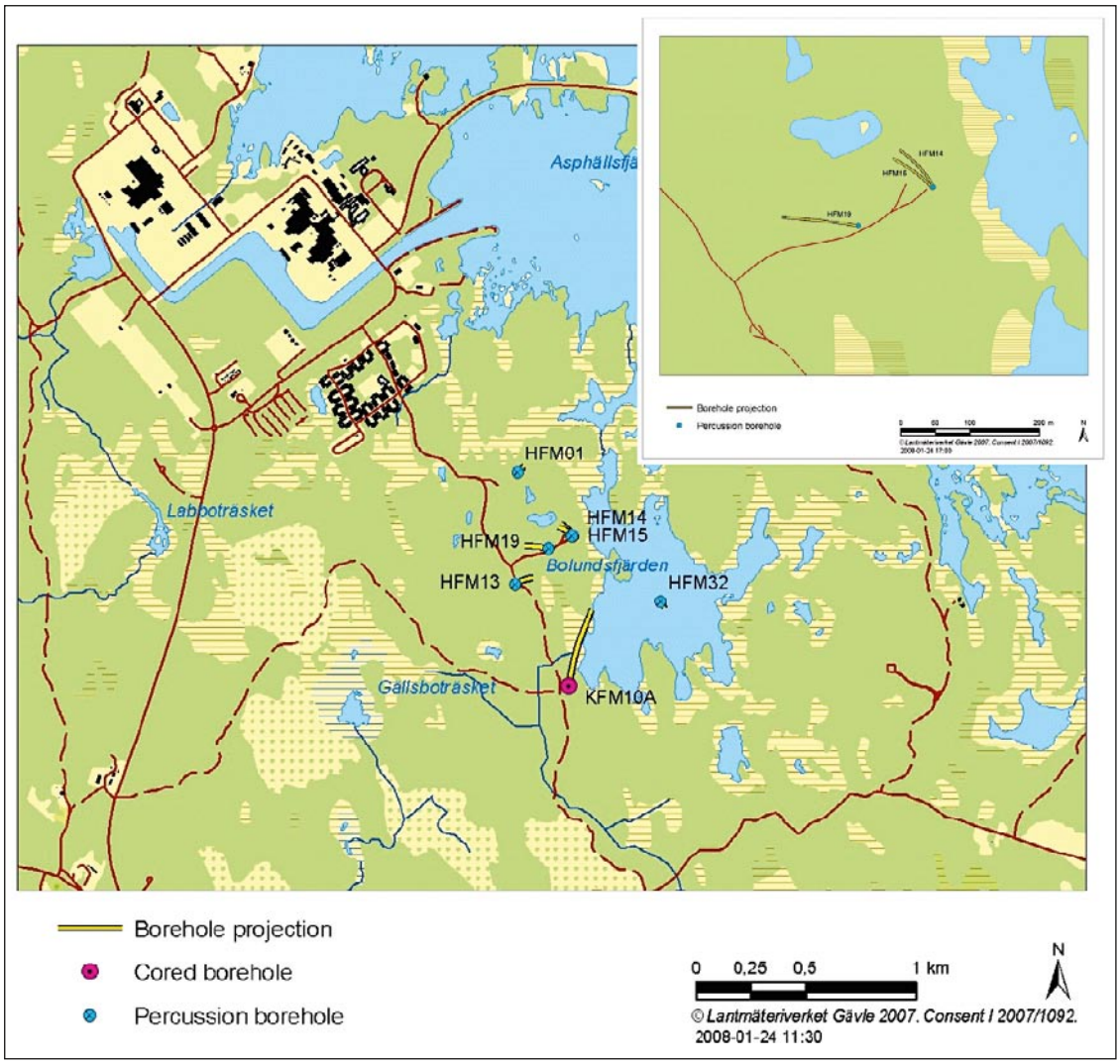

Figure 1-1. *Map over Forsmark site investigation area and the seven boreholes involved in the tracer test. The small figure shows a detailed map of the boreholes near drill site 5.*

Table 1-2. Injection boreholes involved in the tracer test.

Borehole	Section number	Section length (mbl)*	Distance from HFM14 at 20 mbl* (m)
HFM01	2	33.5–45.5	378
HFM13	1	159–173	297
HFM15	1	85–95	72
HFM19	1	168–182	246
HFM32	3	26–31	512
KFM10A	2	430–440	493

*mbl = metres borehole length.

2 Objective and scope

The objective of the activity is to partly verify the hydrogeological model by confirming the connection between the pumping borehole and a number of boreholes that are assumed to have a connection with the pumping borehole. Transport properties were also approximately determined for these flow paths.

Also, a qualitative combined interpretation with the results from the interference test (described in a separate report /1/) is included in the activity.

An earlier tracer test in zone A2 at vertical depth c 400 m indicated a low retardation factor for Cs /2/. It was therefore decided to test the sorption of Cs in the shallow part of the zone. This was done by conducting an extra tracer injection of Cs and Uranine in borehole HFM15 during the end of the tracer test experiment.

2.1 Borehole data

Geometrical data of the boreholes involved in the tracer test are presented in Table 2-1. The reference point of the boreholes is always top of casing (ToC). The Swedish National coordinate system (RT90 2.5 gon V 0:–15) is used in the x-y-plane together with RHB70 in the z-direction. Northing and Easting refer to the top of the boreholes at top of casing. All section positions are given as length along the borehole (not vertical distance from ToC).

2.2 Tests performed

During summer 2006 an interference test with pumping in HFM14 was conducted. In conjunction with this test groundwater flow measurements were performed in 10 borehole sections /3/. The results showed that four of these were suitable as injection sections in a tracer test. These four sections (HFM13:1, HFM15:1, HFM19:1 and HFM32:3) together with two other that were not permanently installed with equipment for groundwater level monitoring and circulation in 2006 (HFM01:2 and KFM10A:2) were selected as possible injection sections.

Firstly another campaign of groundwater flow measurements were performed to confirm the results from 2006, and to decide whether the two new sections were suitable to be part of the tracer test. They commenced 2–3 days before the pumping started and continued during 4 days of pumping to detect flow responses. Only sections that were clearly affected by the pumping in HFM14 were appropriate to be part of the tracer test.

Table 2-1. Geometrical data of the boreholes involved in the test.

Borehole	Coordinate Northing (m)	Easting (m)	Elevation (m)	Inclination (degrees)	Bearing (degrees)
HFM14	6699313.139	1631734.586	3.912	–59.96	331.75
HFM01	6699605.181	1631484.552	1.731	–77.51	34.06
HFM13	6699093.678	1631474.404	5.687	–58.97	51.19
HFM15	6699312.444	1631733.081	3.878	–44.25	314.31
HFM19	6699257.585	1631626.925	3.656	–58.30	280.92
HFM32	6699015.036	1632137.068	0.974	–86.06	116.15
KFM10A	6698629.174	1631715.900	4.507	–50.13	10.42

The pumping in HFM14 started at 10:46 on June 28 and continued until 10:30 on October 8. The pumping test was performed as a constant flow rate test and is further described in a separate report /1/. The flow rate was c 350 l/min.

After completion of the groundwater flow measurements the tracer test started by injection of the different tracers and sampling in the pumping borehole.

Towards the end of the test period an additional tracer injection with Uranine and Cesium (Cs) as tracers was performed in HFM15.

3 Equipment

3.1 General

The six boreholes used as injection boreholes are permanently instrumented with 1–4 inflatable packers isolating 2–5 borehole sections each. Drawings of the instrumentation in core and percussion boreholes are presented in Figure 3-1.

All isolated borehole sections are connected to the HMS-system for pressure monitoring. In general, the sections used for tracer tests are equipped with three polyamide tubes. Two are used for injection, sampling and circulation in the borehole section and one is used for pressure monitoring.

3.2 Groundwater flow measurements

A schematic drawing of the dilution tracer test equipment is shown in Figure 3-2. The basic idea is to cause an internal circulation in the borehole section. The circulation makes it possible to obtain a homogeneous tracer concentration in the borehole section and to sample the tracer outside the borehole in order to monitor the dilution of the tracer with time.

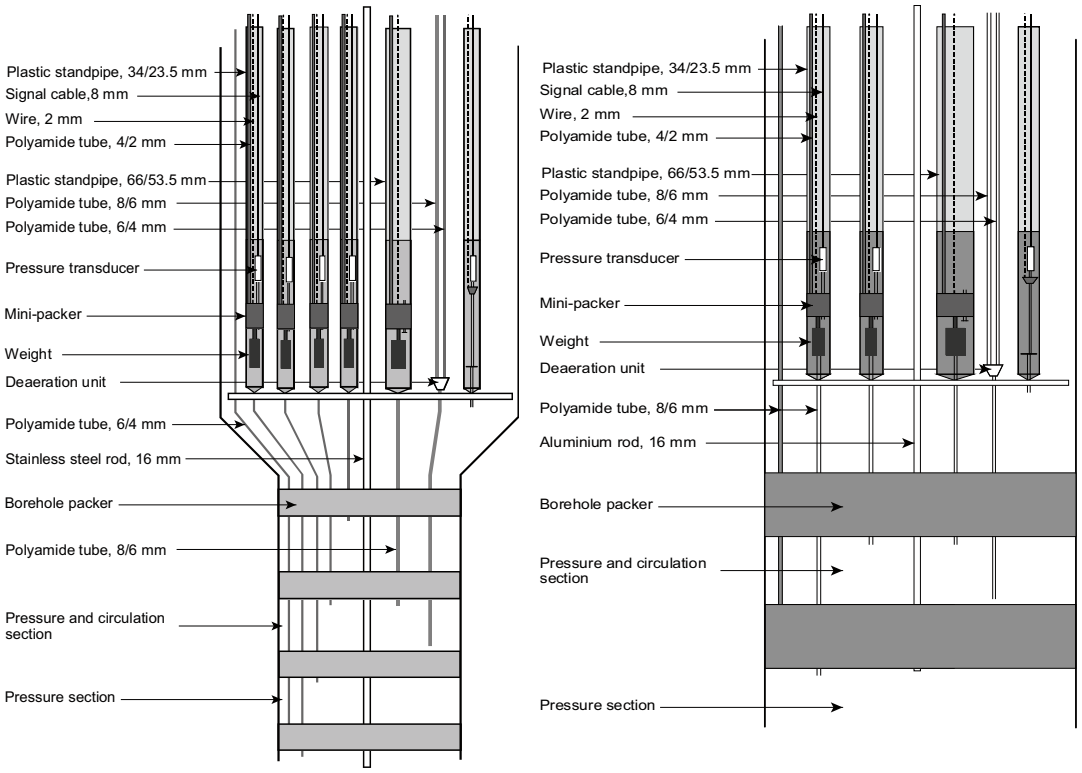

Figure 3-1. *Explanatory sketch of permanent instrumentation in core boreholes (left) and percussion boreholes (right) with circulation sections.*

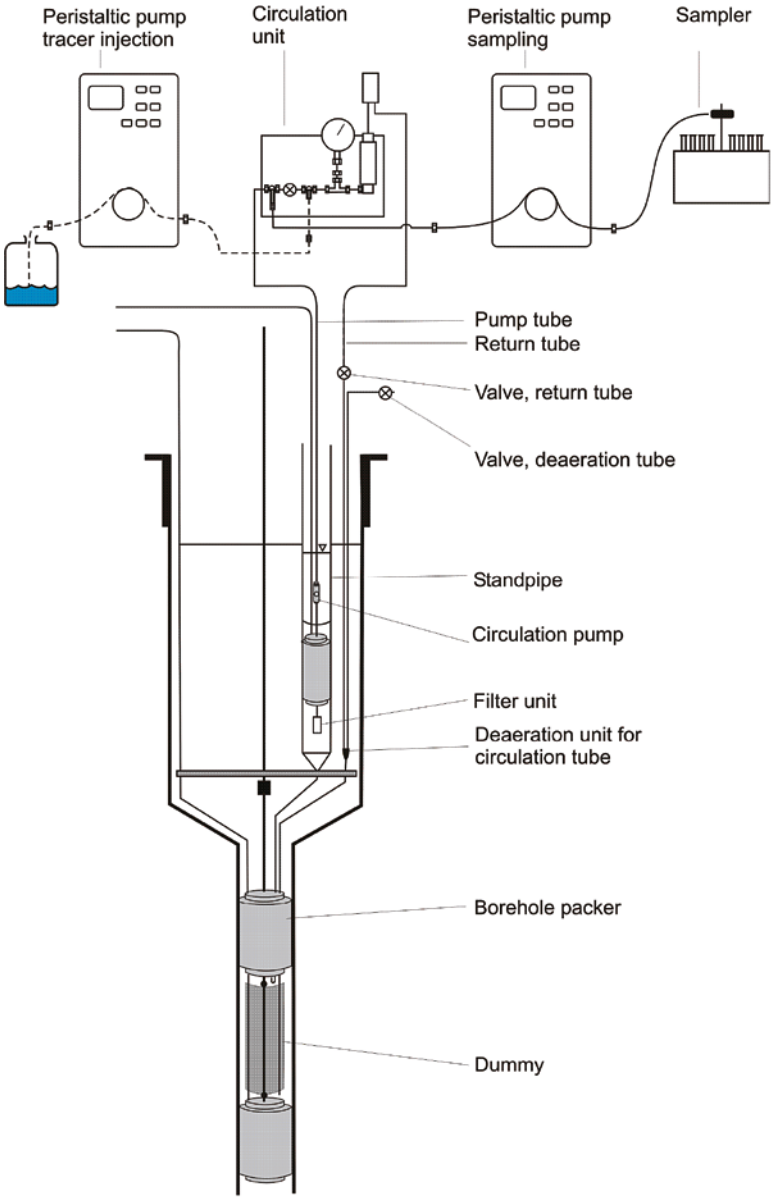

Figure 3-2. *Schematic drawing of the equipment used in tracer dilution measurements.*

Circulation is controlled by a down-hole pump with adjustable capacity and measured by a flow meter. Tracer injections are made with a peristaltic pump and sampling is performed by continuously extracting a small volume of water from the system through another peristaltic pump (constant leak) to a fractional sampler. The circulation unit and the sampling equipment are also shown in Figure 3-3. The equipment and test procedure is described in detail in SKB MD 368.010, SKB internal document, see Table 1-1.

The tracer used was a fluorescent dye tracer, Uranine (Sodium Fluorescein), from Merck (purum quality).

Figure 3-3. *Circulation unit, peristaltic pump and fractional sampler used at the injection sections in the groundwater flow measurements and the tracer test.*

3.3 Tracer test

The same equipment as used in the dilution measurements, with a few additions and alterations, was employed for sampling, injection and circulation in the six tested boreholes during the tracer test. The tracer solution was mixed and stored in 25 l cans, two or three cans per tracer. The tracer injection was accomplished by use of an additional pump at the surface, pumping the tracer solution from the cans into the circulation loop, whereas the circulation pump in the borehole was used to pump water from the section. The pumped water was collected in cans which were weighed and analysed for its tracer concentration. A schematic view of the injection procedure and the equipment used is shown in Figure 3-4.

Samples were collected from the withdrawal borehole HFM14 by two different automatic programmable samplers producing discrete samples. One of the samplers consists of 24 magnetic valves and a control unit allowing selection of time period between openings/samples and open time (to get an appropriate sample volume), see Figure 3-5. Samples were collected in 125 ml plastic (HDPE) bottles. The other sampler producing 500 ml discrete samples is supplied with 24 bottles and was only used as an extra sampler. When the ordinary magnetic valve sampler functioned well, the sampled water in the 500 ml bottles was poured out.

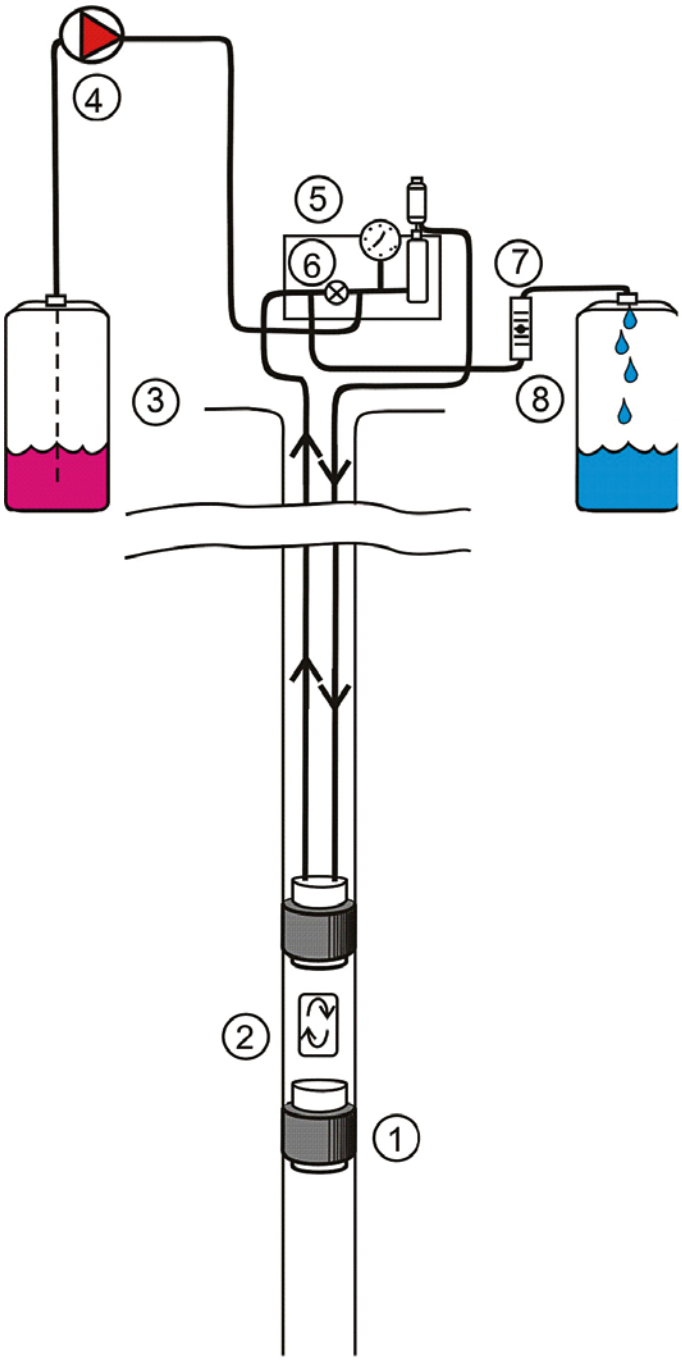

1. Packer
2. Circulation pump
3. Tracer
4. Injection pump
5. Circulation unit
6. Closed valve
7. Flow meter
8. Water pumped from section

Figure 3-4. *Schematic view of equipment used for the tracer injections.*

Figure 3-5. *The automatic sampling equipment (24 magnetic valves) used at the withdrawal hole HFM14.*

3.3.1 Additional tracer test with a sorbing and a non-sorbing tracer

An additional injection was performed in HFM15 (see Figure 1-1). In this case the injection procedure and the equipment used were different. The circulation pump was removed and the tracer was injected with excess pressure through both the tube where the pump is normally placed and through the return hose. A schematic view of the injection equipment is shown in Figure 3-6.

The sampling at the withdrawal borehole HFM14 was also slightly altered. During this part of the test the magnetic valve sampler was used for samples intended for metal analysis and the other sampler was used for the Uranine samples. A portion of each sample in the 500 ml bottles was poured into 19 ml tubes kept for analyses and the rest was emptied and the bottles were re-used.

3.3.2 Tracers used

Six different tracers were used, one for each section. Five of the tracers consisted of DTPA-complexes of the rare earth metals (lantanoids) Europium (Eu), Terbium (Tb), Gadolinium (Gd), Dysprosium (Dy) and Holmium (Ho). The sixth tracer was Rhenium (Re) which was prepared by dissolving the salt ReCl in water. Also Uranine (c 0.5 ppm) was added to all tracer solutions to enable visual monitoring of the increase/decrease of tracer concentration in the injection section during and after the injection. The tracers will only be referred to as Eu, Tb, Gd, Dy Ho and Re in this report. In Table 3-1 the tracer used in each borehole is presented together with the initial concentration (C_{00}) of the tracer solutions.

The DTPA-complexes were prepared at the Geosigma laboratory in Uppsala by mixing DTPA, NaOH, the chloride salt of each metal and, if needed, some HCl to correct the pH and also in some cases NaCl to obtain a density equal to the borehole water. The tracer solutions were stored in 25 l cans, two or three per tracer.

The tracer solution for the additional test was prepared by mixing Uranine and CsCl with water. The solution was stored in a 25 l can. Since the tracer was added as a sub-flow, the concentration in the can was much higher than the actual injection concentration. The concentrations are displayed in Table 3-2.

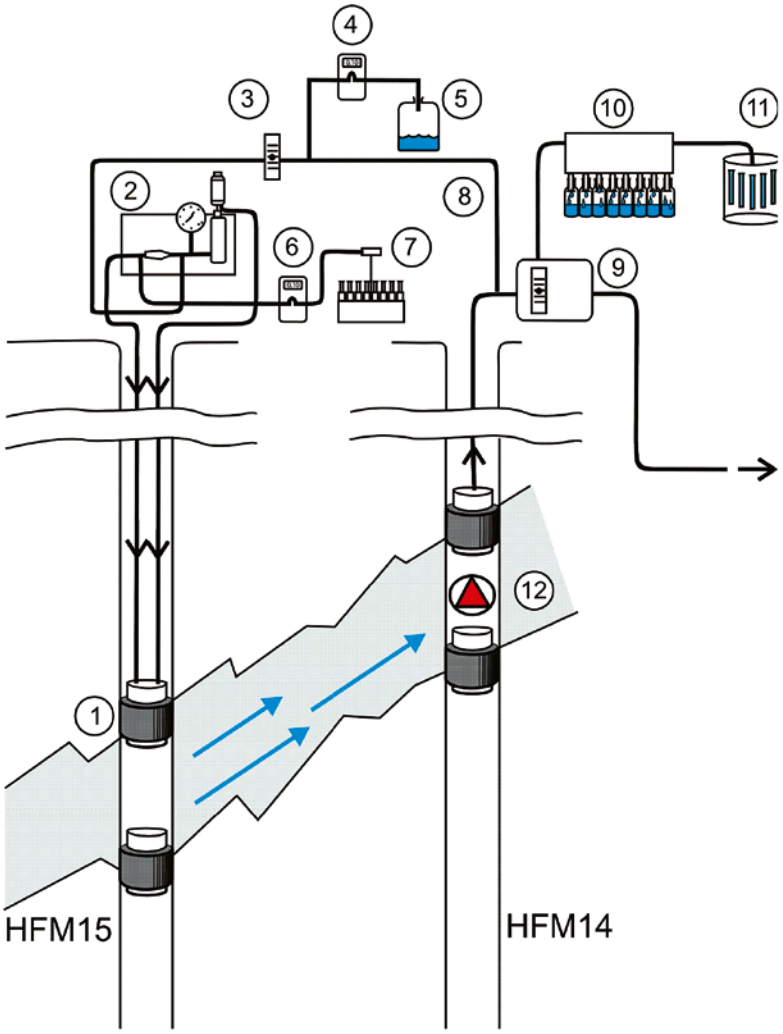

Figure 3-6. *Overview of equipment and injection procedure for the additional tracer test.*

Table 3-1. Tracers used in the different boreholes.

Borehole: section	Tracer	C_{00} (g/l)
HFM01:2	Eu	0.494
HFM13:1	Tb	0.740
HFM15:1	Gd	0.176
HFM19:1	Dy	2.513
HFM32:3	Re	1.781
KFM10A:2	Ho	1.519

Table 3-2. Tracers used for the additional injection in HFM15.

Borehole: section	Tracer	Concentrate (g/l)	Injection concentration (g/l)
HFM15:1	Uranine	14.27	0.051
HFM15:1	Cs	49.7	0.177

3.4 Interpretation tools

The models used for evaluation of the tracer test and calculation of transport parameters are described below.

3.4.1 Transport models

Advection-dispersion model with sorption in a single pathway

This model is described by the standard governing equation for one-dimensional advection-dispersive transport with linear equilibrium sorption:

$$D_L \frac{\partial^2 C}{\partial x^2} - v\frac{\partial C}{\partial x} = R\frac{\partial C}{\partial t} \tag{3-1}$$

where C is concentration [e.g. M/L^3], x is distance along transport path [L], t is time [T], v is the average water velocity [L/T] along the flow path, D_L is the longitudinal dispersion coefficient [L^2/T] and R is the retardation factor.

The following initial and boundary conditions are applied:

$$C(x,0) = 0 \tag{3-2}$$

$$\frac{\partial C(\infty,t)}{\partial x} = 0 \tag{3-3}$$

$$-D_L\frac{\partial C}{\partial x} + vC = vC_0 \quad x = 0 \tag{3-4}$$

where C_0 is the concentrations of the in-flowing water across the inlet boundary. The above boundary and initial conditions result in a solution for a constant injection of tracer. For a tracer pulse with constant concentration of limited duration (t_{inj}), the resulting tracer concentration may be calculated as:

$$C(x,t) = M(x,t) \qquad 0 < t \le t_{inj} \tag{3-5}$$

$$C(x,t) = M(x,t) - M(x,\, t - t_{inj}) \qquad t > t_{inj} \tag{3-6}$$

where $M(x,t)$ is the solution for a step-input injection with constant injection concentration. A more complex temporal variation in the tracer injection may be calculated in an analogous way by summation of a several such injection periods. A solution to the above equations, for a step input of constant concentration, is given by /4/ as follows:

$$\begin{aligned} M(x,t) = {} & \frac{1}{2}\,erfc\left[\frac{Rx - vt}{2(D_L Rt)^{1/2}}\right] + \left[\frac{v^2 t}{\pi D_L R}\right]^{1/2} \exp\left[-\frac{(Rx - vt)^2}{4D_L Rt}\right] \\ & -\frac{1}{2}\left[1 + \frac{vx}{D_L} + \frac{v^2 t}{D_L R} + \right]\exp\left[\frac{vx}{D_L}\right] erfc\left[\frac{Rx + vt}{2(D_L Rt)^{1/2}}\right] \end{aligned} \tag{3-7}$$

where *erfc* is the complimetary error function.

The advection-dispersion model with sorption is herein referred to as the AD model.

The results from AD model evaluation are in this report presented using mean residence time, t_m (= x/v), Peclet number, Pe (=x/a_L) and retardation factor (R). Further, the proportionality factor, pf , which describes the fraction of the injected tracer mass that arrives at the sampling section, is obtained from the model fitting.

Advection-dispersion model in multiple pathways

This model is essentially the same as the preceding one (AD-1) except that tracer transport is assumed to occur in two, or more, separate pathways and mix in the pumping section. This is calculated by summing up the contribution from the different pathways as (for n pathways):

$$C(x,t) = \sum_{i=1}^{n} pf_i \cdot C_i(x,t) \tag{3-8}$$

where $C_i(x,t,)$ represents the partial tracer breakthrough from each individual pathway and pf_i is a proportionality factor that describes the contribution from each pathway.

It may here be noted that the pf parameter also represents dilution effects in the pumping section as well as other proportional tracer losses. Thus, this parameter is often relevant to include also when applying the advection-dispersion model for a single pathway.

Advection-dispersion model with matrix diffusion (one pathway)

In this model, the governing equation for the AD model is extended by adding a term that represents diffusion of tracer into a hydraulically stagnant matrix:

$$R\frac{\partial C}{\partial t} = - v\frac{\partial C}{\partial x} + D_L\frac{\partial^2 C}{\partial x^2} + \frac{2\,D_e}{\delta}\frac{\partial C_p}{\partial y} \tag{3-9}$$

with the transport in the matrix given by:

$$\frac{\partial C_p}{\partial t} - \frac{D_e}{R_d n_p}\frac{\partial^2 C_p}{\partial y^2} = 0 \tag{3-10}$$

where n_p is the matrix porosity, D_e is the effective diffusion coefficient [L^2/T], δ is the fracture aperture [L] of the flowing fracture, $C_p\ (y)$ is the tracer concentration in the matrix, R_d is the matrix retardation factor and y is a spatial coordinate perpendicular to the direction of the flowing transport path. The matrix diffusion model used here is also presented by /5/ and /6/. The model with advection-dispersion with sorption and matrix diffusion is herein referred to as the AD-MD model.

The boundary and initial conditions are:

$C(x,0) = 0$ (3-11)

$C(\infty,t) = 0$ (3-12)

$C(0,t) = C_0$ (3-13)

$C_p(0,x,t) = C(x,t)$ (3-14)

$C_p(\infty,x,t) = 0$ (3-15)

$C_p(y,x,0) = 0$ (3-16)

When this matrix diffusion model is employed for interpretation of tracer breakthrough curves, all unknown parameters in Equations 3-8 and 3-9 can not be evaluated independently. Instead, it is common to use a lumped parameter, *A*, which describes the effect of matrix diffusion. The parameter *A* may be written as:

$$A = \frac{\delta \cdot R}{2\sqrt{n_p D_e R_d}} \tag{3-17}$$

With this definition, the matrix diffusion effect increases with decreasing values of *A*.

3.4.2 Parameter estimation method

Estimated parameter values are obtained by non-linear least-squares regression. The basic non-linear least-squares regression minimises the sum of squared differences between the modelled (Y^M) and the observed (Y^O) variables and may be formulated as:

$$\min S = \mathbf{E_R}^T \mathbf{W} \mathbf{E_R} \tag{3-18}$$

where $\mathbf{E_R}$ is a vector of residuals ($\mathbf{Y}^O - \mathbf{Y}^M$) and $\mathbf{W}$ is a vector of reliability weights on observations.

The specific method for carrying out the regression employed in this study is often referred to as the Marquardt-Levenberg method. This method is a Newton-type optimisation algorithm that finds the parameter values that minimises the sum of squared errors between model and measurement values in an iterative manner. A basic Newton-type search algorithm used may be written as:

$$\mathbf{B}_{r+1} = \mathbf{B}_r + (\mathbf{X}_r^T \mathbf{W} \mathbf{X}_r)^{-1} \mathbf{X}_r^T (\mathbf{Y}^O - \mathbf{Y}_r^M) \tag{3-19}$$

where $\mathbf{B}$ is a vector of parameter estimates, $\mathbf{X}$ is a parameter sensitivity matrix, and the subscripts r and r+1 refer to the iteration number. The Marquardt-Levenberg method is an extension that enhances the convergence properties of the search algorithm by restricting the search direction.

Given an initial parameter estimate (B_r), the model variable vector (Y^M) and the sensitivity matrix (X) are calculated and a new vector of estimates (B_{r+1}) is obtained. Equation 3-18 is then repeated until a local optimal solution is found. The local minimum is defined by some convergence criterion, for example when parameter estimates are essentially identical between iterations. Finding a local minimum does not guarantee that the global minimum is found. When this appears to be a problem, several sets of initial estimates may be tried. When some knowledge about the parameters to be estimated and the physical system is already available, the initial estimates are often good enough for ensuring that a global minimum is found.

An important element of the above procedure is the matrix containing the parameter sensitivities. Parameter sensitivity is defined as the partial derivative of the dependent (simulated) variable with respect to a parameter. A sensitivity matrix contains one row for each observation and one column for each estimated parameter, as in the following example with three observations and two parameters.

$$\mathbf{X} = \begin{pmatrix} \frac{\partial y_1}{\partial b_1} & \frac{\partial y_1}{\partial b_2} \\ \frac{\partial y_2}{\partial b_1} & \frac{\partial y_2}{\partial b_2} \\ \frac{\partial y_3}{\partial b_1} & \frac{\partial y_3}{\partial b_2} \end{pmatrix} \tag{3-20}$$

Parameter sensitivities may be used to determine the precision of the estimated parameter values. Two diagnostic measures are given below regarding parameter uncertainty that may be obtained as a result of regression /7/.

The *standard errors* of parameter estimates are obtained by taking the square roots of the diagonals in the parameter covariance matrix, which is given by:

$$s^2(\mathbf{X}^T\mathbf{W}\mathbf{X})^{-1} \tag{3-21}$$

with s^2 being the error variance:

$$s^2 = \frac{\sum_{i=1}^{N} w_i \, (y_i^O - y_i^M)^2}{N - P} \tag{3-22}$$

where N is the number of measurements, P the number of parameters to be estimated and w_i the weight on observation i.

The linear correlation $r(p_1,p_2)$ between two parameters with values of p_1 and p_2, respectively, is given by:

$$r(p_1, p_2) = \frac{Cov(p_1, p_2)}{\sqrt{Var(p_1)\,Var(p_2)}} \tag{3-23}$$

where the variance and covariance terms are elements of the $s^2(\mathbf{X}^T\mathbf{W}\mathbf{X})^{-1}$ matrix. The correlation is a measure of the inter-dependence between two parameter estimates, and correlation values range between –1 and 1. Values close to either –1 or 1 mean that a change in one parameter value may be compensated for by a similar change in another parameter value to maintain the same fit (sum of squares) between model and measurements. The standard errors and parameter correlation values are the main diagnostic measures used in this analysis when examining the parameter estimation results from evaluation of the tracer tests.

3.4.3 Handling of tracer injection data

Measured groundwater flows and tracer concentration in the injection section were used to calculate the tracer input function for the evaluation models, see Section 4.6.2. The input function was approximated by a large number of step input periods that were superimposed as described in Equation 3-6. Each injection period is given an input value that is proportional to the injected tracer mass/time.

3.4.4 Other derived transport parameters

In accordance with the SKB method description for two-well tracer tests (SKB MD 530.006), some further transport parameters are derived, mainly based on the average residence time (t_m) determined from the model evaluation described above. The derived parameters are:

- fracture aperture (mass balance aperture),
- hydraulic fracture conductivity,
- flow porosity.

The fracture aperture, δ [L], is determined from:

$$\delta = \frac{Qt_m}{\pi (r^2 - r_w^2)} \tag{3-24}$$

where Q is the average pumping rate [L^3/T], r is the travel distance [L] and r_w is the borehole radius [L]. The hydraulic fracture conductivity, K_{fr} [L/T] is calculated using:

$$K_{fr} = \ln\left(\frac{r}{r_w}\right)\frac{\left(r^2 - r_w^2\right)}{2t_m \Delta h} \tag{3-25}$$

where Δh is the head difference [L] between the injection and pumping sections. The flow porosity, ε_f; is determined from:

$$\varepsilon_f = \frac{K}{K_{fr}} \tag{3-26}$$

where K is the hydraulic conductivity of the packed-off section determined from a steady-state evaluation of the interference test /8/.

4 Execution

4.1 General

The work involved preparations in terms of planning and scoping calculations, field work, analyses of collected samples, data handling, modelling and determination of transport parameters.

The work was carried out in accordance with the method descriptions SKB MD 368.010 and SKB MD 530.006 (SKB internal documents), see Table 1-1.

4.2 Scoping calculations

In June and July 2006 a number of groundwater flow measurements were performed during both natural conditions and during pumping in HFM14 as reported in /3/. Based on the results it was concluded that the sections HFM15:1 and HFM19:1 seemed suitable as injection sections during at tracer test with pumping in HFM14. HFM32:3 and HFM13:1 were also suggested as possible injection sections, although, the flow responses in these sections were not as significant. Since the performance of the test in 2006 some additional boreholes were permanently installed with equipment for groundwater level monitoring and circulation, and could therefore be of interest as injection sections in the large scale tracer test. In particular, HFM01:2 and KFM10A:2 were studied in the scoping calculations.

In order to optimize the test some scoping calculations were performed during the planning stage. The scoping and planning of the test was focused on three key issues to successfully perform the large scale test, injection method, travel time and tracer to be used. Since several injection sections may be used, the chosen injection method must be practical to use at multiple locations at the same time or be rather short in terms of time. The travel time from the injection section to HFM14 has to be reasonably short since the test is limited in time due to general planning of the site investigations at Forsmark. Finally, due to the large scale of the test, the dilution from the injection to the pumping section will be considerable, and for that reason the dynamic range of the tracers has to be large in order to detect breakthrough.

The scoping calculations indicated that a tracer test with simultaneous injection of a non-sorbing tracer and a sorbing tracer should not be possible. Hence it was decided to perform the tracer test only using non-sorbing tracers. However, the results indicated a short travel time between HFM15 and HFM14 which opened the possibilities of performing an additional tracer test with a sorbing tracer at the end of the pumping period.

4.2.1 Injection method

Three tracer injection methods were considered initially:

1. Injection with additional pressure.
2. Injection by adding a small volume with high concentration during circulation.
3. Injection by exchange of water.

Injection with additional pressure, i.e. the tracer is pushed out in the rock formation, was used successfully in a tracer test between KFM02A and KFM02B during the spring of 2007 /2/. An advantage with the method is that the injection pulse becomes distinct and there is a low probability of remaining tracer in the section. However, the method requires a rather complicated infrastructure with pumps and water tanks etc which is a clear disadvantage, especially when multiple injection sections may be used. Besides, after the injection of tracer, water without tracer will be injected, and consequently the total time for tracer injection in each borehole

will be rather long. Additionally, an increased pressure during the injection may also push the tracers further from the pumping hole causing a lower recovery in the test. Hence, injection with additional pressure was considered to be less favourable in the large scale tracer test with pumping in HFM14.

Injection by adding a small volume with high concentration during circulation is basically the same method used as during the measurements of the groundwater flow. It should therefore be very easy to perform this practically, because the equipment needed would already be in place. However, the initial concentration in the injection section (C_0) necessary to detect a breakthrough in HFM14 would probably have to be very high. Hence, there is a great risk that the concentration in the injection solution (C_{00}) had to exceed the solubility limit in some cases. Injection by adding a small volume with high concentration during circulation was therefore considered as unsuitable in this case.

The third method, injection by exchange of water, is rather easy to perform as the tracer solution with the ideal initial concentration C_0 is injected while the existing section water is being pumped with the same flow rate. After exchange of at least one section volume, the borehole section is circulated and the concentration is decaying as the tracer is transported away. The tracer injection pulse will not be as distinct as with injection with additional pressure, since no water without tracer is added after the tracer injection. But, on the other hand, the exchange method only requires the equipment used for groundwater flow rate measurements and some containers for the injection solution and for collection of return water. Hence, injection by exchange of water was chosen initially for the scoping calculations.

4.2.2 Travel time and dilution

The duration of the test was originally planned to be 8 weeks. The pumping flow rate in HFM14 was decided based on the pumping test in HFM14 performed in 2006 to 350 l/min. The residence time may be estimated according to Equation 4-1 (SKB MD 530.006):

$$t_m = \frac{\delta\pi (r^2 - r_w^2)}{Q} \qquad (4\text{-}1)$$

where t_m is mean residence time (s), δ is fracture aperture (m), r is travel distance (m), r_w is borehole radius (m) and Q is mean pumping rate (m^3/s).

Equation 4-1 requires an assumption of fracture aperture. No such data of the fracture aperture was available during the scoping calculations. In order to estimate the fracture aperture, the cubic law was used based on the reported transmissivities from the injection sections. However, from experience it is commonly known that the cubic law underestimates the fracture aperture considerably.

Other important factors for the detection of tracer in the pumping hole besides the mean residence time are the dilution of the tracer and the dispersivity. If it is assumed that 100% of the injected tracer is recovered in HFM14, the dilution is rather straight forward to calculate for the sections included in the test during 2006 (HFM15, HFM19 HFM13 and HFM32). However, no measurements of flow rate in KFM10A and HFM01 during pumping in HFM14 existed at the time of scoping calculations, why assumptions had to be made. The dispersivity is often assumed to be the travel distance divided by 10. However, significantly higher dispersivities have been reported, for example in the tracer test between KFM02A and KFM02B /2/.

A number of simulations where performed with the AD model in a single pathway, described in Section 3.4, in order to calculate reasonable maximum concentrations and time to the maximum concentration. Some results are presented in Table 4-1 for different assumptions regarding the dispersivity and fracture aperture which may be viewed as guidelines for the range of dilution and travel times. Noticeable is that most times are within the 8 weeks (1,344 h) time span originally set for the test. The quota of maximum concentration C and initial injection concentration C_0 is in the range of 1e–4 to 2e–7 in these cases.

Table 4-1. Calculated maximum concentrations and times to maximum concentrations for different assumptions of dispersivity, apertures and injections section while pumping 350 l/min in HFM14.

	HFM13:1	HFM15:1	HFM19:1	HFM32:3	KFM10A:2	HFM01:2
Assumed travel distance, r (m)	297	72	247	512	450	377
Assumed flow rate [ml/min]	11	64	220	19	19	41
	Dispersivity = r/5, Aperture = cubic law*5					
Max conc C/C_0	1.E–05	1.E–04	4.E–05	4.E–06	1.E–05	3.E–05
Time to max conc [h]	70	4	28	123	90	48
	Dispersivity = r/2, Aperture = cubic law*30					
Max conc C/C_0	3.E–06	5.E–05	6.E–06	5.E–07	3.E–06	5.E–06
Time to max conc [h]	215	12	103	464	246	151
	Dispersivity = r/2, Aperture = cubic law*100					
Max conc C/C_0	9.E–07	2.E–05	2.E–06	2.E–07	1.E–06	1.E–06
Time to max conc [h]	560	31	354	1,465	589	458

4.2.3 Tracers

The expected dilution from the injection sections to the pumping borehole was quite high as seen in Table 4-1, whereas the solubility has to be rather good and the background level has to be rather low of the tracers used. DTPA-complexes of the rare earth metals (lantanoids) Europium (Eu), Terbium (Tb), Gadolinium (Gd), Dysprosium (Dy) and Holmium (Ho) have previously successfully been used in tracer tests and fulfil the requirements of good solubility and low background levels. Also the tracer Rhenium (Re) fulfils these requirements.

The six tracers were optimized for the different injection sections with respect to the expected dilution, costs, available amount, solubility and background level. The selection was made so that the maximum concentration in HFM14 should be 100 times that of the expected background level if the dispersivity is equal to half the assumed travel distance and the aperture is according to 30 times the cubic law. The result were that Eu was assigned to HFM01, Tb to HFM13, Gd to HFM15, Dy to HFM19, Re to HFM32 and Ho to KFM10A.

4.3 Preparations

Equipment functioning checks were performed in the field before starting any tracer injections. All equipment was well-functioning.

All the tracer solutions were prepared at the Geosigma laboratory in Uppsala and stored in 25 l cans.

4.4 Execution of field work

4.4.1 Ground water flow measurements

The groundwater flow measurements were performed before the tracer test begun. The time periods for the measurements are presented in Table 4-2. The duration of the test during the period with natural gradient ranged from 46 to 72 hours, and the corresponding time during the period with stressed gradient (during pumping) from 60 to 98 hours.

The pumping in HFM14 started at 10:46 on June 28 and the flow rate was kept at c 350 l/min after an initial period of regulation to obtain a suitable flow rate. The pumping and the pressure responses in the surrounding boreholes are further described in a separate report /1/.

Table 4-2. Measurement periods for the groundwater flow measurements.

Section	Gw flow measurement natural gradient (start)	(stop)	Gw flow measurement stressed gradient (start)	(stop)
HFM01:2	2007-06-25 13:40	2007-06-28 10:46	2007-06-28 10:46	2007-07-02 12:30
HFM13:1	2007-06-26 13:05	2007-06-28 10:46	2007-06-28 10:46	2007-07-02 10:35
HFM15:1	2007-06-25 13:47	2007-06-28 10:46	2007-06-28 10:46	2007-07-02 11:14
HFM19:1	2007-06-26 13:01	2007-06-28 10:46	2007-06-28 10:46	2007-07-02 10:46
HFM32:3	2007-06-26 10:36	2007-06-28 10:46	2007-06-28 10:46	2007-07-01 19:52
KFM10A:2	2007-06-25 10:56	2007-06-28 10:46	2007-06-28 10:46	2007-07-02 09:30

The tests were made by injecting a slug of tracer (Uranine, 500 mg/l) in the selected borehole section and allowing the natural groundwater flow to dilute the tracer. The tracer was injected during a time period equivalent to the time it takes to circulate one section volume. The injection/circulation flow ratio was set to 1/1,000, implying that the start concentration in the borehole section would be about 0.5 mg/l. The tracer solution was continuously circulated and sampled using the equipment described in Section 3.2.

All samples attended for analysis of Uranine was buffered with c 1% Titrisol buffer solution (pH 9). Earlier experiences have showed that the buffer prevents decomposition of the dye.

The samples were analysed for dye tracer content at the Geosigma Laboratory using a Jasco FP 777 Spectrofluorometer.

4.4.2 Tracer test

The principle test layout is shown in Figure 4-1.

The injections were performed through an exchange procedure without excess pressure. An additional pump was employed to inject the tracer, and the circulation pump in the borehole was used to extract water from the section at the same rate. The pumped water was collected in cans. The injection procedure is illustrated in Figure 3-4 in Section 3-3. During the exchange procedure samples for analysis of Uranine were taken every 15 minutes from the pumped water to monitor the injection procedure. The volume of tracer injected was c 1.5 times the section volume. Hence, the exchange continued for a time that equalled circulation of 1.5 section volumes. Some data on the tracer injections are presented in Table 4-3. After the injection the circulation was started and samples were continuously withdrawn from the injection section using the same equipment as used during the groundwater flow measurements. The automatic sampling continued for 2 weeks, after which, samples were collected from the injection sections 1–2 times per week throughout the measurement period.

1% HNO_3 was added to the bottles and tubes for samples to be analysed for metals in order to keep the DTPA-complexes stable and prevent sorption on the plastic walls of the bottles.

The sampling of the pumped water from HFM14 was started prior to the tracer injections in order to collect data on background concentrations. To be sure to detect the first arrivals of the tracers, the sample interval was shorter during the first days of the test. After 7 days the interval between samples was set to 6 hours.

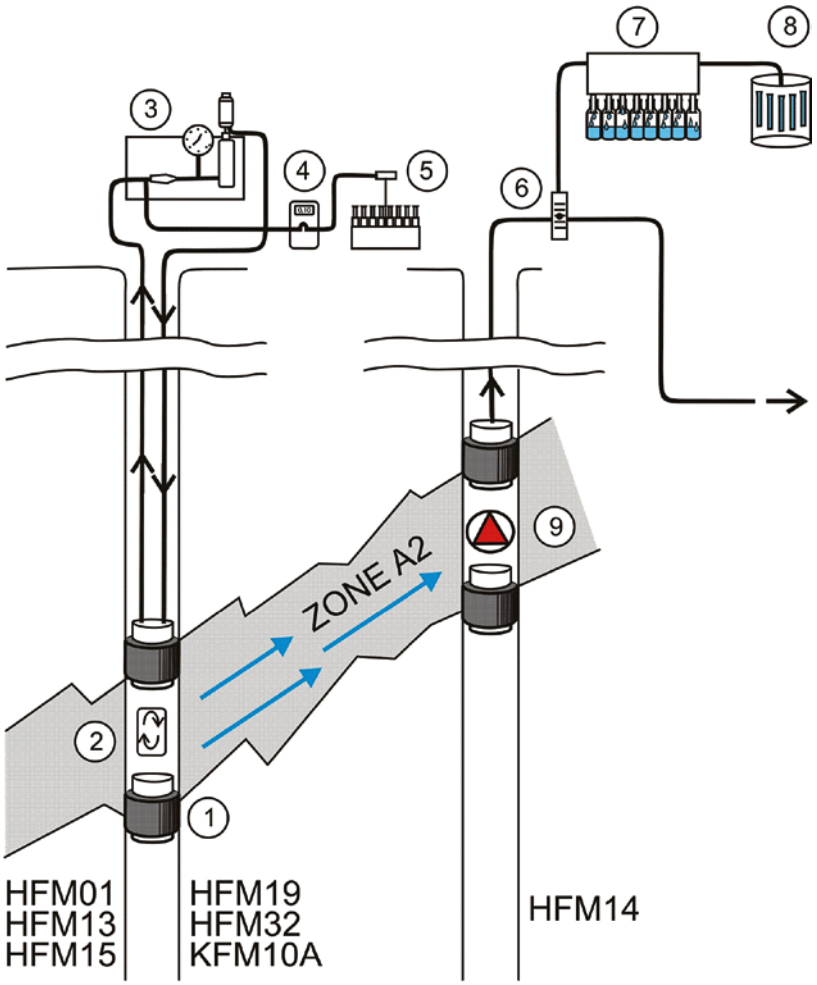

1. Packer
2. Circulation pump
3. Circulation unit
4. Peristaltic pump for sample withdrawal
5. Fractional sampler
6. Flow meter connected to logger
7. Automatic sampler
8. Automatic sampler
9. Pump

Figure 4-1. *Principle layout of the tracer test.*

Table 4-3. Data on tracer injections.

Borehole: section	Tracer	Section volume (l)	Volume tracer injected (l)	Injection start YYYY-MM-DD hh:mm	Injection stop YYYY-MM-DD hh:mm	Injection time (min)
HFM01:2	Eu	39.55	48.4	2007-07-06 13:31	2007-07-06 15:14	103
HFM13:1	Tb	38.14	50.1	2007-07-06 13:27	2007-07-06 15:06	99
HFM15:1	Gd	35.67	51.8	2007-07-09 10:22	2007-07-09 12:05	103
HFM19:1	Dy	44.37	66.3	2007-07-09 11:00	2007-07-09 13:35	155
HFM32:3	Re	19.59	24.7	2007-07-09 16:07	2007-07-09 16:57	50
KFM10A:2	Ho	39.44	50.5	2007-07-06 10:00	2007-07-06 11:47	107

4.4.3 Tracer test with sorbing tracer

The additional tracer injection of Uranine and Cesium in HFM15 was performed with excess pressure. Some of the pumped water from HFM14 was re-circulated into HFM15 and concentrated tracer solution was added as a sub-flow. The total injection flow rate was c 2.6 l/min and the sub flow was 9.1 ml/min. The flow rate of the re-circulated water was less than 1% of the total pumping flow rate. Hence, the risk that any tracer content in the re-circulated water should increase the tracer concentration in the samples can be neglected. The injection lasted for 24 hours and was followed by injection of "clean" water from HFM14 at the same flow rate to maintain the pressure conditions. The "rinsing" continued throughout the test (two weeks). Some data on the injection is presented in Table 4-4. Also a schematic view of the injection procedure and equipment is shown in Figure 3-6 in Section 3.3.1.

4.4.4 Water sampling for chemical analysis

Water sampling for SKB chemical analysis Class 3 was performed by SKB at three occasions during the 15 weeks of pumping. The first was taken just after pump start, the second in the middle of the pumping period and the last one at the end. Table 4-5 shows the dates and times of the sampling together with the SKB sample number used for identification in the Sicada database.

4.5 Data handling/post processing

All samples analysed for Uranine were analysed at the Geosigma laboratory in Uppsala. The samples intended for analysis of metals were sent to ALS Scandinavia laboratory in Luleå.

The results were compiled in an Excel-file together with sample date for further processing, plotting and calculations.

4.6 Analyses and interpretations

4.6.1 Groundwater flow measurements

In the dilution method a tracer is introduced and homogeneously distributed into a borehole test section. The tracer is subsequently diluted by the ambient groundwater, flowing through the borehole test section. The dilution of the tracer is proportional to the water flow through the borehole section and the groundwater flow is calculated as a function of the decreasing tracer concentration with time, Figure 4-2.

Table 4-4. Data on tracer injection in HFM15 during the additional test.

Borehole: section	Tracer	Injection flow rate (l/min)	Volume tracer injected (l)	Injection start YYYY-MM-DD hh:mm	Injection stop YYYY-MM-DD hh:mm	Injection time (min)
HFM15:1	Uranine Cs	2.55	3,677	2007-09-24 14:22	2007-09-25 14:24	1,442

Table 4-5. SKB Class 3 water sampling.

Bh ID	Date and time of sample	Pumped section (m)	Pumped volume (m^3)	Sample type	Sample ID no	Remarks
HFM14	2007-06-28 12:49	0–150.5	43	WC080	12,819	
HFM14	2007-08-06 12:10	0–150.5	19,700	WC080	12,820	
HFM14	2007-09-20	0–150.5	42,400	WC080	12,821	

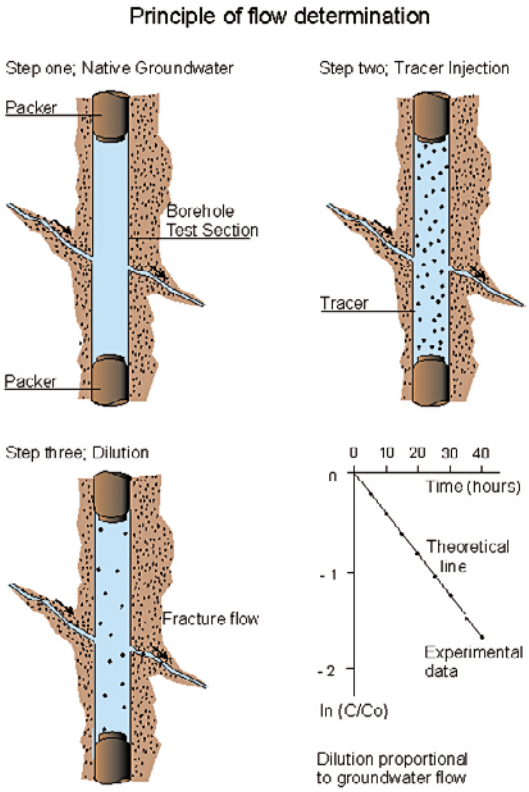

Figure 4-2. *General principles of dilution and flow determination.*

Flow rates were calculated from the decay of tracer concentration versus time through dilution with natural unlabelled groundwater, cf /9/. The so-called "dilution curves" were plotted as the natural logarithm of concentration versus time. Theoretically, a straight-line relationship exists between the natural logarithm of the relative tracer concentration (C/C_0) and time, t (s):

$$\ln (C/C_0) = - (Q_{bh} /V) \cdot \Delta t \qquad (4\text{-}2)$$

where Q_{bh} (m^3/s) is the groundwater flow rate through the borehole section and V (m^3) is the volume of the borehole section. By plotting ln (C/C_0) versus t, and by knowing the borehole volume V, Q_{bh} may then be obtained from the straight-line slope. If C_0 is constant, it is sufficient to use ln C in the plot.

The sampling procedure with a constant flow of 4–10 ml/h also creates a dilution of tracer. The sampling flow rate is therefore subtracted from the value obtained from Equation 4-2.

4.6.2 Tracer test

The total mass injected of each tracer was determined by weighing the cans before and after the injection and by analysing the concentration in each can. Since the injection was performed as an "exchange procedure" the cans with water pumped up from the section were also weighed and the water was analysed. The small mass of metal leaving the system through sampling of the injection section was also calculated and subtracted.

To control the analyses and the calculations of injected mass the total mass of tracer in the cans before injection (calculated by weighing and analyses) was compared to the total mass of each tracer that had been added (theoretical mass).

The sample bottles and tubes were weighed before being sent to the consulted laboratory. Then the results from the laboratory were recalculated to account for dilution by acid added in the samples. After this the concentrations of tracer were plotted against elapsed time since

injection start and the data were controlled. Some outliers were removed and the correct mean background concentrations of the different tracers were determined. The background was subtracted from the sample concentrations and the breakthrough curves from HFM14 were plotted as normalized mass flux against elapsed time. The normalized mass flux from HFM14 was calculated by multiplying the concentration measured at each time by the withdrawal rate and dividing with the total injected mass.

No correction for delay in tubes and hoses were made for samples from HFM14 since the flow rate is very high and the pump is placed at a moderate depth in the borehole.

It was assumed that tracer starts entering the fractures (e.g. leave the borehole section) when 0.5 section volume has been injected. This time was selected as t=0 and the elapsed time is related to this time in all calculations. The principle injection function was approximated as shown by the blue thick line in Figure 4-3. It is assumed that from time t=0 until the injection is stopped the concentration C_0 in the section equals the concentration in the cans (C_{00}). Then the tracer is diluted by the groundwater flow through the section.

The tracer dilution that occurs during a period after the injection stop was evaluated according to Equation 4-2 and the groundwater flow was calculated. The evaluated groundwater flow was compared to the flow obtained from the previous measurements. The calculated groundwater flow was then used together with data on tracer solution concentration (C_0=C_{00}), background concentration (C_b), and section volume (V) to calculate the decaying part of the injection function for each tracer according to Equation 4-3. The first part of the function depends on the injection time (t_{inj}). From t=*0* until t= t_{inj} C is assumed to be C=C_0=C_{00}.

$$C = -(C_b - C_0)e^{-\frac{Q}{V}t} + C_b \qquad (4\text{-}3)$$

For use in the model the injection function has to be discretisized with a start time, a stop time and a value for the given time period. The principle for this is shown by to the thin green line in Figure 4-3. Also the concentration-time relationship was converted into a function of normalized mass flux against time.

Modelling was then performed using the models described in Section 3.4. A further description of which model that was used for each breakthrough curve is found together with the results from the modelling in Section 5.2.2.

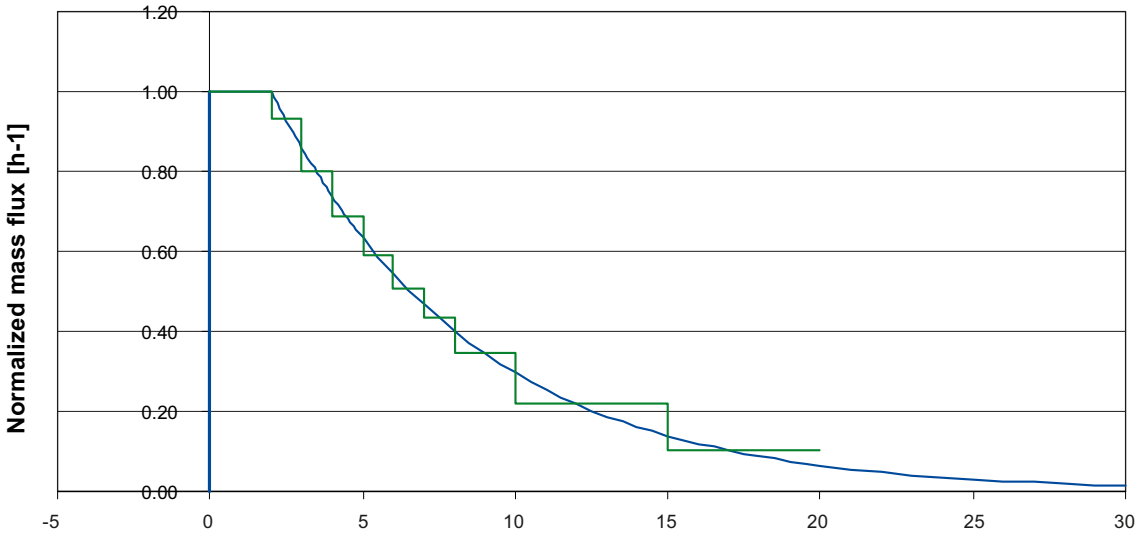

Figure 4-3. *Assumed shape of the injection function (blue) and the discretization used for modelling (green). This particular injection function is just an example.*

Some assumptions were made:

- Plug flow is assumed in the injection sections.
- Complete mixing during circulation.
- The pumping rate is assumed to be constant (the variation was c 1% from the desired value).

4.7 Nonconformities

The additional tracer test with Cs and Uranine in HFM15 was not mentioned in the Activity Plan (AP PF 400-07-020).

- There were several outliers in the tracer concentration data during a certain time period. These have been excluded from the evaluation. No explanation could be found. This did not affect the overall quality of the data.
- During a period of high temperature and high humidity some of the samples were diluted by drops of water (condensation). These samples were treated as outliers and were not included in the evaluation. This did not affect the evaluation of the data.
- A power failure caused the circulation and sampling in HFM01 to stop around July 10, after c 850 h since the injection start. Since the stop occurred after a relatively long time, when the tracer concentration in the section was low, it is not believed to have influenced the data.

5 Results

Original data from the reported activity are stored in the primary database Sicada. Data are traceable in Sicada by the Activity Plan number (AP PF 400-07-020). Only data in databases are accepted for further interpretation and modelling. The data presented in this report are regarded as copies of the original data. Data in the databases may be revised, if needed. However, such revision of the database will not necessarily result in a revision of this report, although the normal procedure is that major data revisions entail a revision of P-reports. Minor data revisions are normally presented as supplements, available at www.skb.se.

5.1 Groundwater flow measurements

The results obtained are presented in Table 5-1 including measured groundwater flow rates, together with transmissivity and volume for the section.

An example of a tracer dilution curve is shown in Figure 5-1. The flow rate is calculated from the slope of the straight-line fit. The other tracer dilution graphs are presented in Appendix 1. The groundwater levels during the entire test period are shown in Appendix 2, see also Table 5-1 for actual measurement period.

After the injection of tracers in the tracer test, the dilution of tracers in the injection sections were measured in the same way as during the groundwater flow measurements with Uranine. They were interpreted in the same way and the tracer dilution graphs are presented in Appendix 3. Generally there was good agreement between the two measurements.

An interesting observation is that in two of the measured sections, HFM01:2 and HFM32:3, concentrations are increasing a while after pump start, before decreasing. This is shown as a "bump" in the dilution graph (Figure 5-1). This phenomenon occurs when tracer is re-entering the borehole as a result of changing the direction of groundwater flow more than 90 degrees.

Table 5-1. Measured groundwater flow in the investigated sections.

Borehole/ section	Borehole length (m)	Transmissivity (m^2/s)	Volume (l)	Measured flow (ml/min) Natural gradient	Measured flow (ml/min) Stressed gradient [1)]
HFM01:2	33.5–45.5	*4.5E–5	39.55	7.8	52.2
HFM13:1	159–173	*2.9E–4	38.14	7.1	12.9/8.8
HFM15:1	85–95	*1.04E–4	35.67	2.6	79.5
HFM19:1	168–182	*2.7E–4	44.37	12.6	669/1,072
HFM32:3	26–31	*2.3E–4	19.59	1.1	28.5
KFM10A:2	430–440	**2.2E–5	39.44	10.0	16.9/10.4

* From HTHB measurements /10/, /11/, /12/ and /13/.

** From PSS measurements, transient evaluation, /14/.

[1)] Where two flows are given, the first occurs early and the other later. See each dilution graph in Appendix 1.

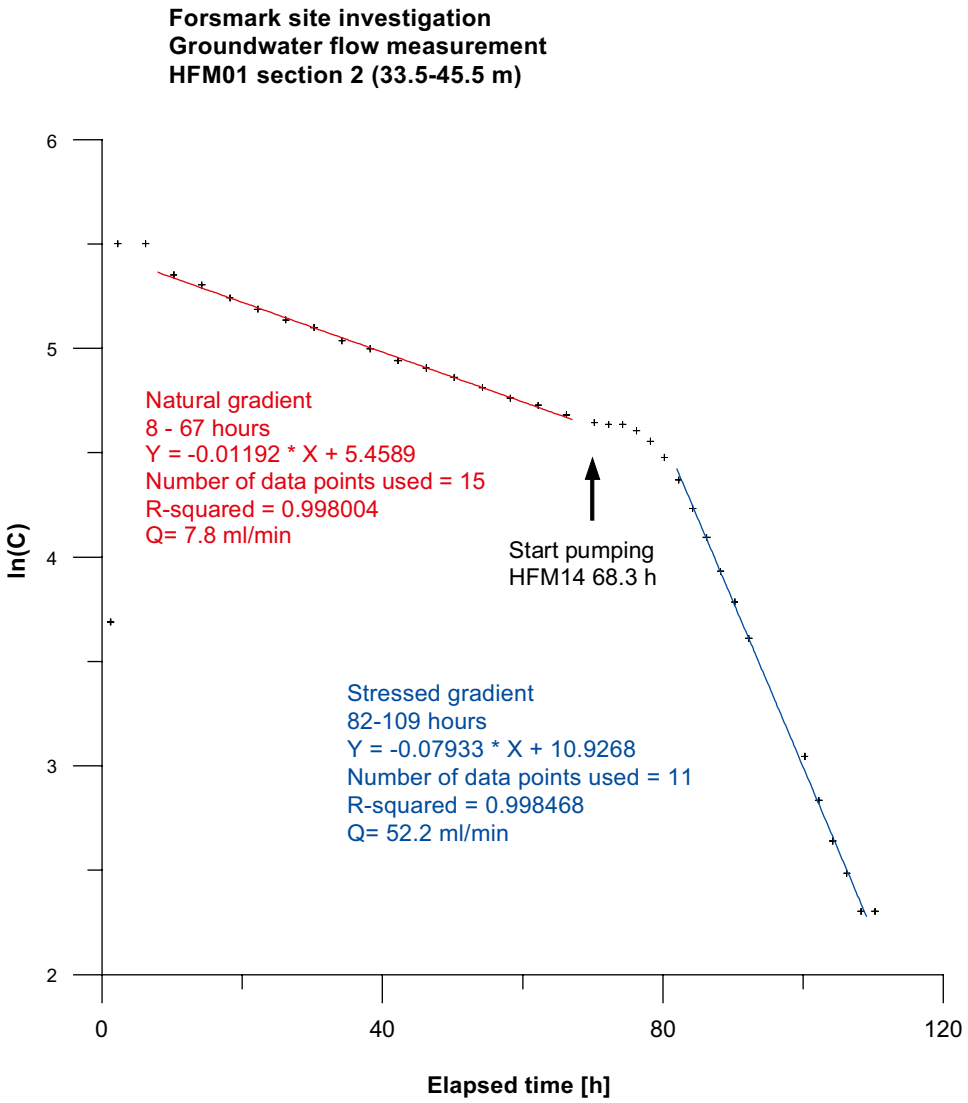

Figure 5-1. *Example of tracer dilution graph (logarithm of concentration versus time) for borehole HFM01, section 2, including straight-line fits during both natural and pumped conditions.*

Table 5-2. Comparsison between the two different measurements of groundwater flow during pumping in HFM14.

Borehole/ section	Borehole length (m)	Measured flow (ml/min) prior to tracer test [1)]	Measured flow (ml/min) during tracer test [1)]
HFM01:2	33.5–45.5	52.2	52.7
HFM13:1	159–173	12.9/8.8	12.6/7.3
HFM15:1	85–95	79.5	85.2
HFM19:1	168–182	669/1,072	459
HFM32:3	26–31	28.5	30.5
KFM10A:2	430–440	16.9/10.4	10.1

[1)] Where two flows are given, the first occurs early and the other later. See each dilution graph in Appendix 1 and 3.

5.2 Tracer test

5.2.1 Tracer breakthrough

The breakthrough curves for all tracers are shown in Figure 5-2. Separate breakthrough curves for each tracer are found in Appendix 4 (absolute concentrations) and in Section 5.2.2 below (normalized mass flux) where the curves are presented together with their model fits.

Tracer breakthrough was obtained from five of the six tested borehole sections. Only from HFM32 no breakthrough was obtained. The concentration peak seen after c 5 hours in the breakthrough curve for HFM32 is false and probably due to contamination caused by the breakthrough of Gd from HFM15. The distance to HFM32 is c 512 m, hence it is not likely that the arrival time for Re from HFM32 should be equal to the time for Gd from HFM15 which only has a distance to HFM14 of 72 m.

The groundwater levels in all injection sections for the whole pumping period are shown in Appendix 5.

The time for first arrival of each tracer is presented in Table 5-3 together with total injected mass and percentage recovery.

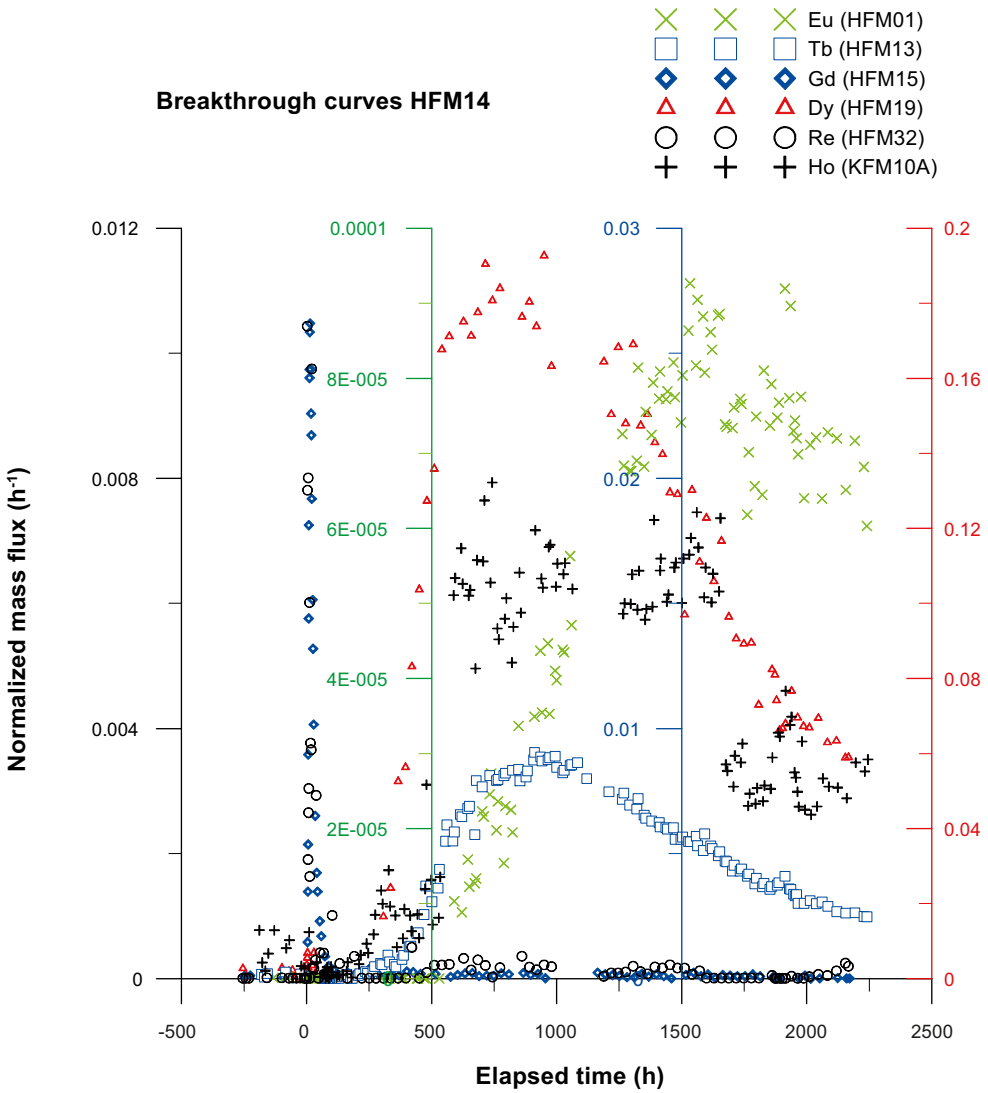

Figure 5-2. *Breakthrough curves for all six tracers. The colours of the symbols indicate the corresponding axis. The breakthrough of Re from HFM32 is, however, false, se explanation in the text.*

Table 5-3. First arrival, injected mass and mass recovery for the tracer test.

Borehole: section	Tracer	Mass of tracer injected (g)	First arrival (h)	Recovery at pump stop (%)
HFM01:2	Eu	19.9	580	6.6
HFM13:1	Tb	24.9	210	42.6
HFM15:1	Gd	7.9	3.5	91.1
HFM19:1	Dy	166.7	190	78.6
HFM32:3	Re	42.6	–	1.0
KFM10A:2	Ho	60.9	210	15.4

The recoveries at pump stop were calculated by integrating the mass-flux breakthrough curves and comparing the mass with the total mass injected. Note that at pump stop, the concentrations have not reached background levels again for any tracer except for Gd. Hence a mass recovery of 100% or almost 100% at pump stop is only expected for Gd.

$$Recovery\ (\%) = \frac{M_{pumphole}}{M_{inj}} \cdot 100 \qquad (5\text{-}1)$$

Additional tracer test

The breakthrough curves for Uranine and Cs from the additional tracer test are shown in Figure 5-3. The recovery at pump stop, together with time for first arrival is presented in Table 5-4. The time for first arrival for Uranine in the additional tracer test is consistent with that for Gd in the first experiment. These two breakthrough curves are plotted together in Figure 5-4.

The figure shows that the shapes of the Gd- and Uranine curves are slightly different. This is an effect of the different injection techniques and injection times used. Gd was injected without excess pressure during c 2 h, whereas Uranine and Cs were injected with excess pressure during 24 h.

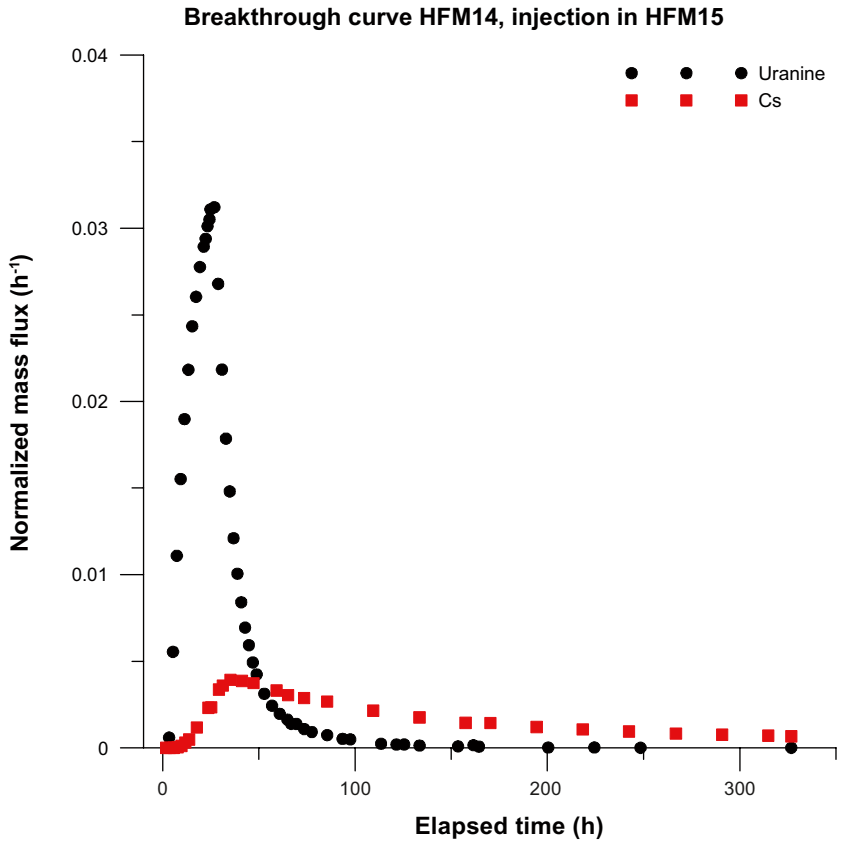

Figure 5-3. *Breakthrough curve for Uranine and Cs from the additional tracer test.*

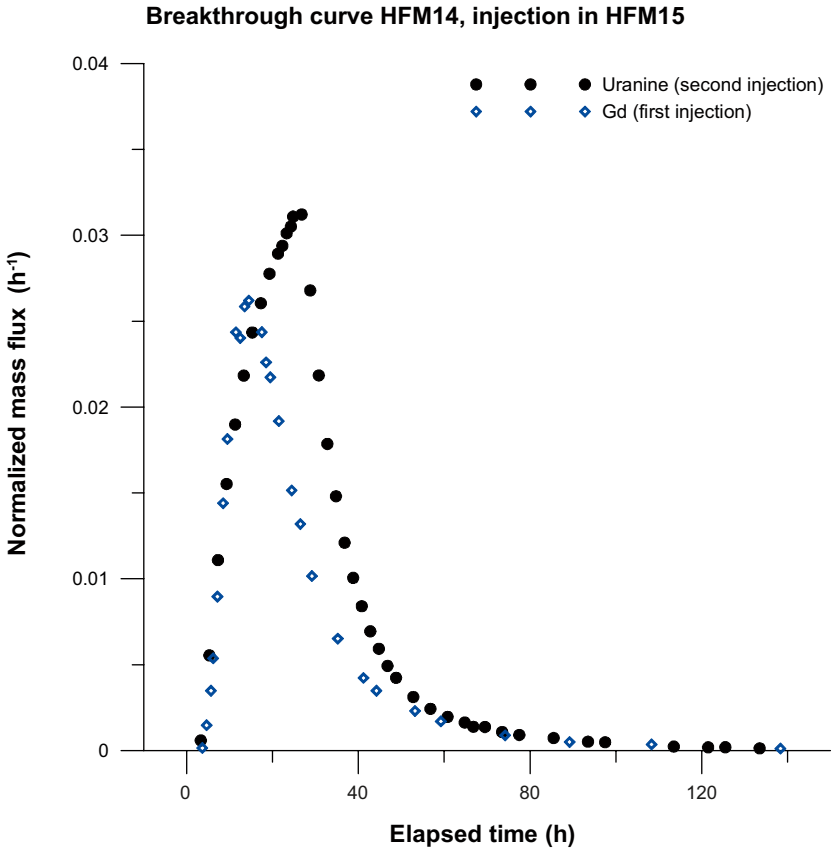

Figure 5-4. *Comparison of the breakthrough curves for the two non-sorbing tracers Gd and Uranine injected in HFM15 at different occasions and with different injection times and techniques.*

Table 5-4. First arrival, injected mass and percentage recovery for the additional tracer test.

Borehole: section	Tracer	Mass of tracer injected (g)	First arrival (h)	Recovery at pump stop (%)
HFM15:1	Uranine	187.5	3.5	89.4
HFM15:1	Cs	650.8	8	53.2

5.2.2 Model results and evaluated parameters

The models used in the evaluation of the tracer tests are presented in Section 3.4. The simulation procedure was to choose suitable starting values, then to run the selected model and finally examine the results mainly by considering the reasonableness, standard errors and correlation of the parameters as well as visual inspection of the model fit. The model used first was the AD model for a single pathway. After that, if needed, further simulations were tried with multiple pathways and/or the AD-MD model.

A simulation with the AD model was sufficient for the breakthrough from HFM01, HFM13 and KFM10A. When the fit is good using the AD-model it is often not possible to obtain a good fit using multiple flow paths or the AD-MD model. For HFM15, where the breakthrough was very fast and the "tail" of the curve very long, the AD-MD model provided a better model fit. Also for HFM19 the AD-MD model resulted in a better fit. Models for multiple pathways were tried for the breakthrough from HFM15 and HFM19. For HFM15 the multiple pathway simulation resulted in a reasonable fit, but for HFM19 this model did not converge.

The results from the model simulations are presented below in Figures 5-5 – 5-21, where estimated parameter values also are presented. The transport parameters that are extracted from the models are the proportionality factor (p_f), longitudinal dispersivity in terms of Peclet number (Pe) and mean residence time (t_m). For sorbing tracers, the retardation factor for the fracture (R) is also extracted and when using the AD-MD model also the lumped matrix diffusion parameter (A). For further description of the parameters see Section 3.4.

The data used in the simulations are normalized mass flux [h^{-1}] and time [h]. By using these units, the value of p_f directly indicates the recovery in the simulation as $p_f = 1$ implies 100% recovery in the simulation.

A number of simulations with different starting values were made in order to confirm the convergence of the simulation. All tracers used except Cs are assumed to be non-sorbing, hence the value of R is set to 1.

Generally, when the breakthrough curve is complete and has a tail, the fit using the AD model for a single pathway does not provide a sufficient fit. For HFM15, both the AD model with two pathways and the AD-MD solution give plausible fits to experimental data.

HFM01

Since the breakthrough curve is far away from complete when the pumping and sampling stopped, simulation using the AD-model for a single pathway was the only possible model to use. The background concentration and the concentration in the samples are both below the measurement limit until c 600 h which causes the horizontal line in Figure 5-5, before the concentration reaches above the measurement limit.

HFM13

A considerable part of the breakthrough curve is obtained and the model fit is good, see Figures 5-7 and 5-8. A simulation using the AD-model for a single pathway provided a good fit, hence no other models were tried.

HFM15

The breakthrough was fast and during most of the test the concentration is near the background value. Simulation was made both with the AD model and the AD-MD model, see Figures 5-9 and 5-10. The fit to experimental data for the tail is considerably better using the AD-MD model. This is most clearly seen in the log-log plot in Figure 5-10. Also, the AD-model with two pathways fits the data well and provides reasonable parameter values.

HFM19

Most of the injected tracer was recovered when the sampling and pumping stopped. Both the AD and the AD-MD models were used, and the fit was better using the AD-MD model, see Figures 5-11 and 5-12. The AD-model with two pathways was also tried but this did not provide any reasonable result. Hence, the AD-MD model is regarded to provide the best fit.

KFM10A

The data are somewhat scattered which makes the evaluation difficult. Furthermore the breakthrough curve is not complete. However, the fits shown in Figure 5-13 and 5-14 demonstrate a relatively good fit to the model data and reasonable model parameters are obtained.

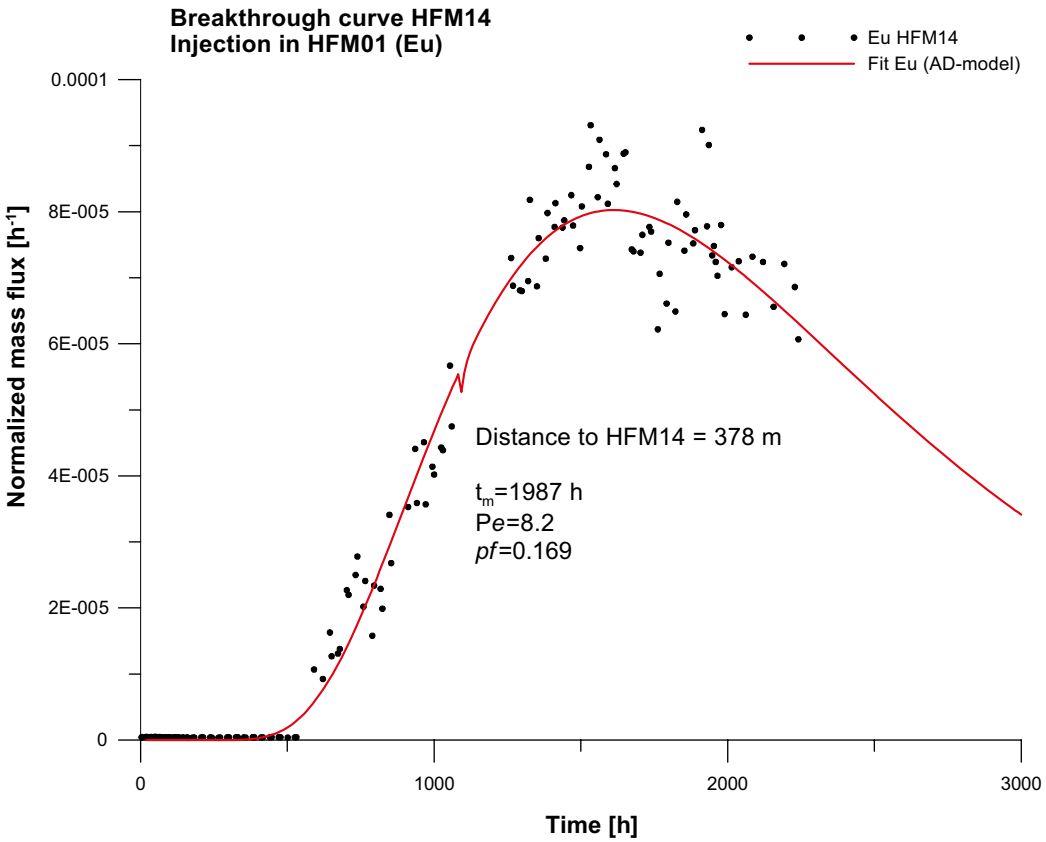

Figure 5-5. *Linear plot of model fit using the AD model to experimental data for Eu from HFM01.*

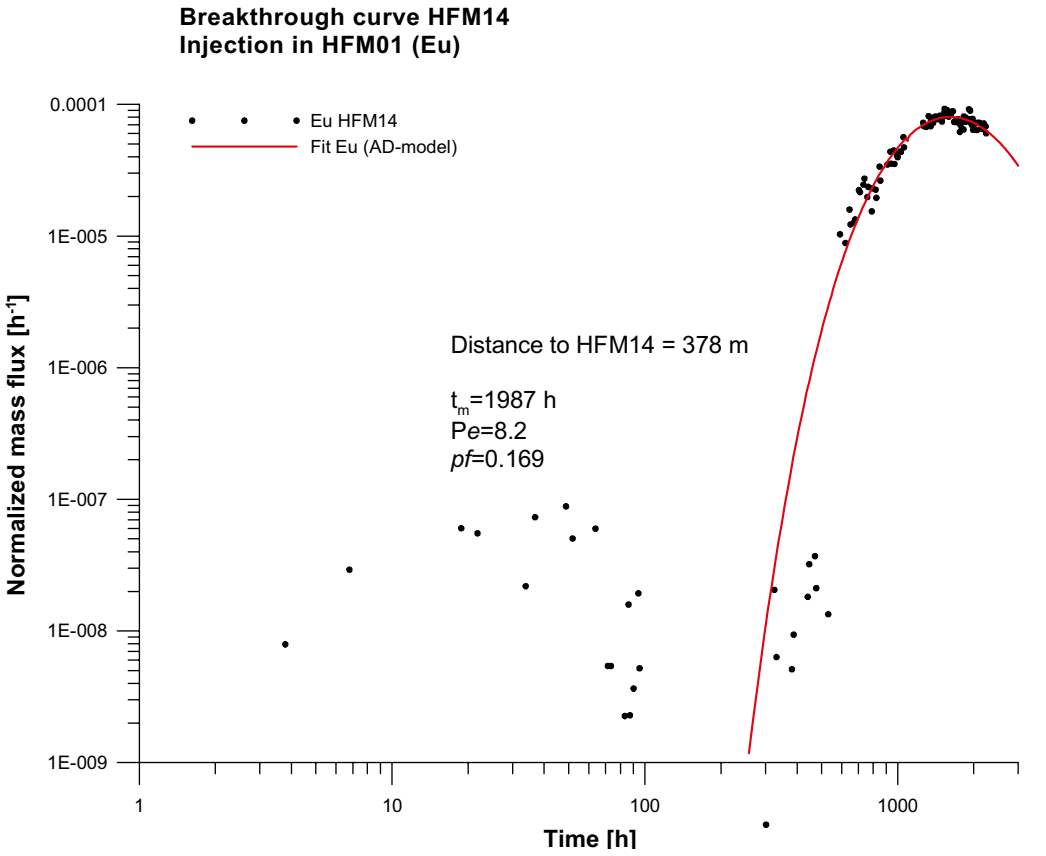

Figure 5-6. *Logarithmic plot of model fit using the AD model to experimental data for Eu from HFM01.*

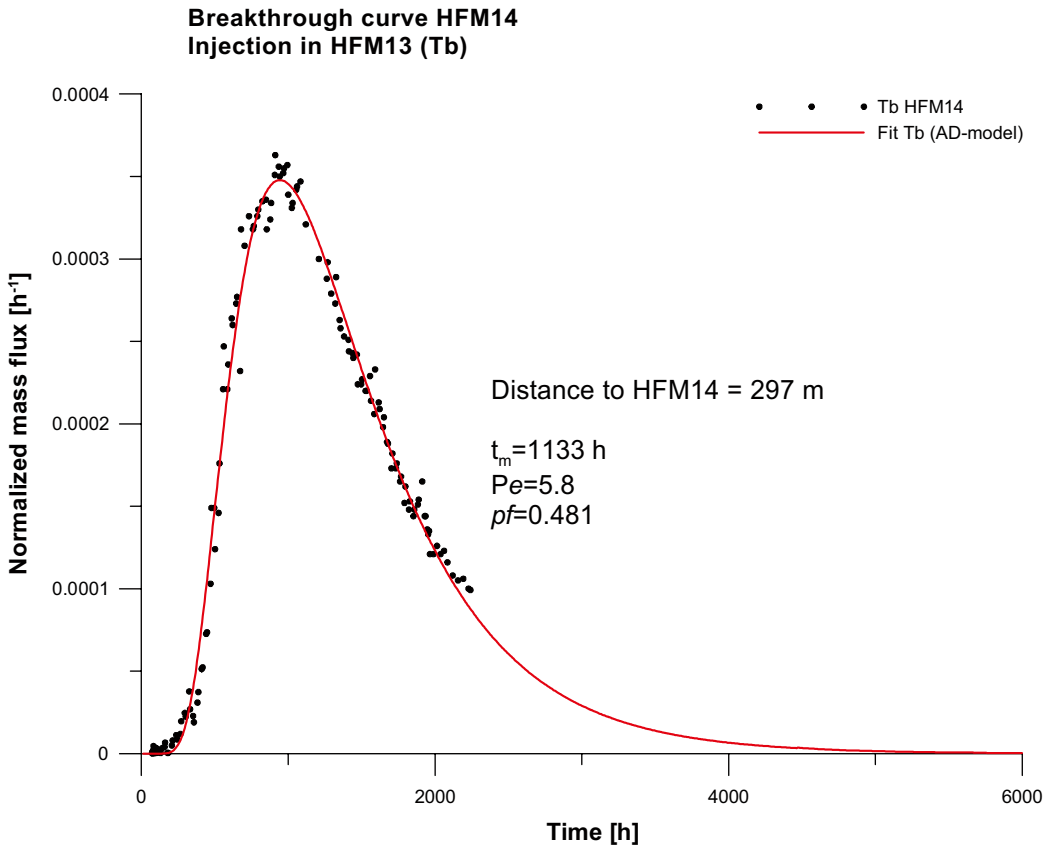

Figure 5-7. *Linear plot of model fit using the AD model to experimental data for Tb from HFM13.*

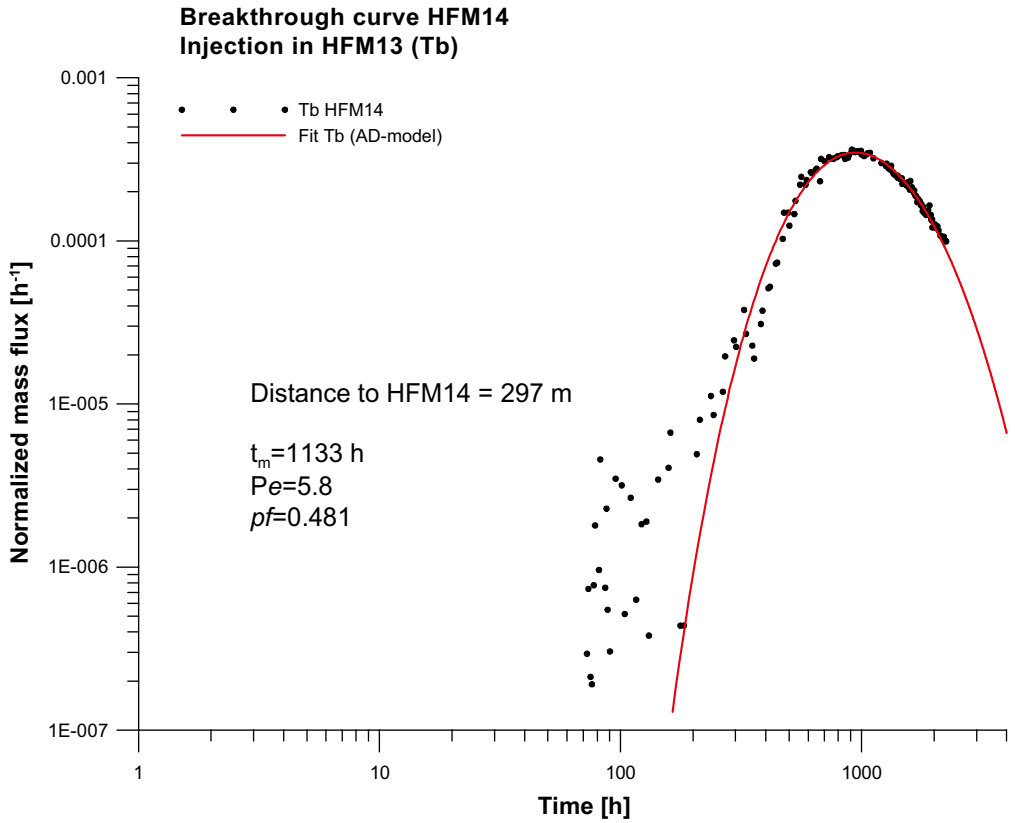

Figure 5-8. *Logarithmic plot of model fit using the AD model to experimental data for Tb from HFM13.*

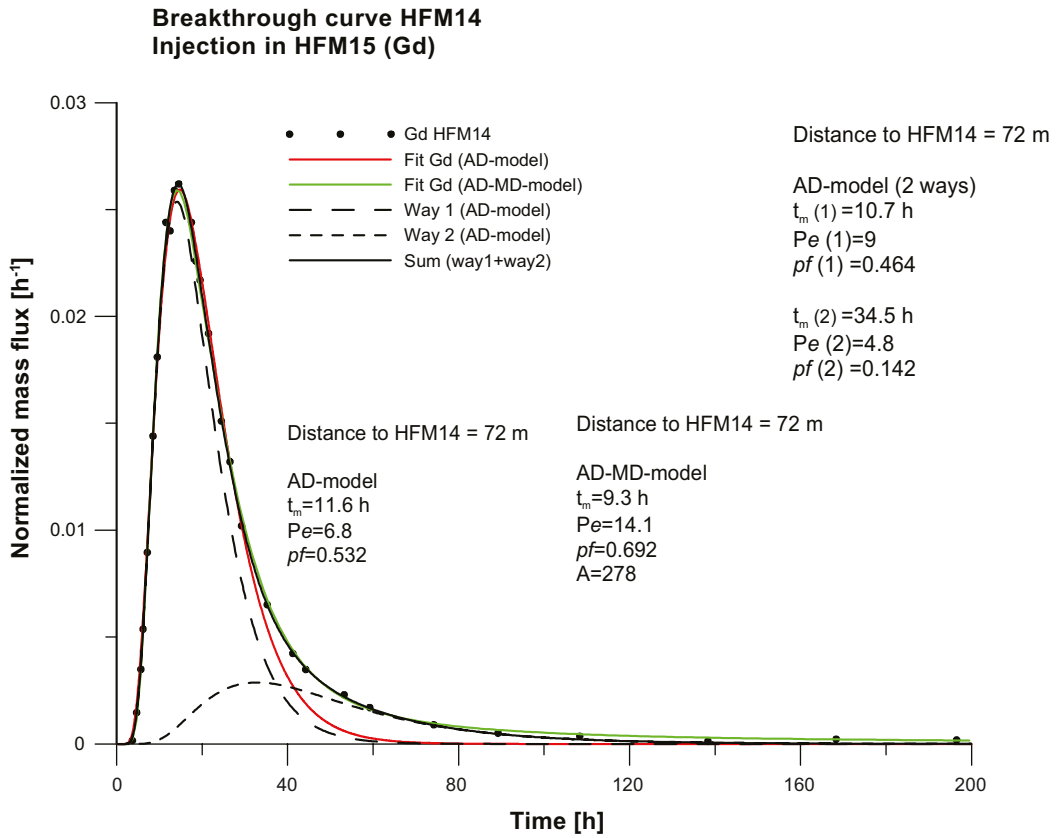

Figure 5-9. *Linear plot of model fit using the AD model, the AD-model with two pathways and the AD-MD model to experimental data for Gd from HFM15.*

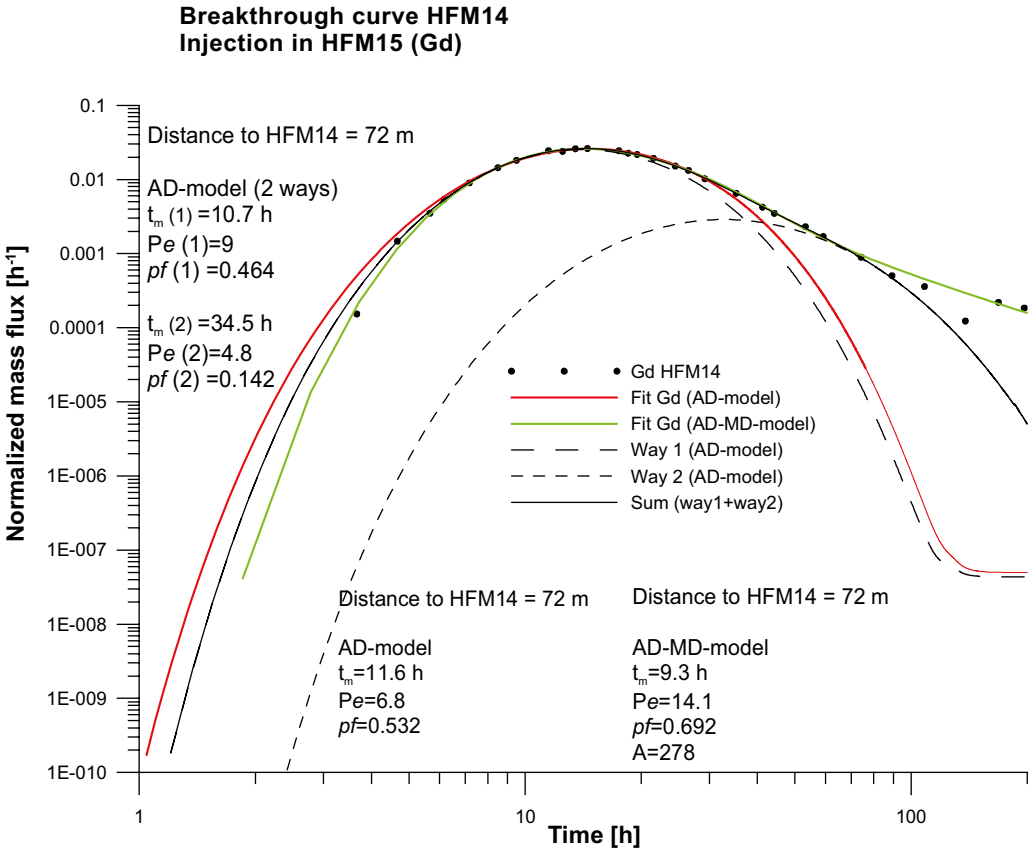

Figure 5-10. *Logarithmic plot of model fit using the AD model, the AD-model with two pathways and the AD-MD model to experimental data for Gd from HFM15.*

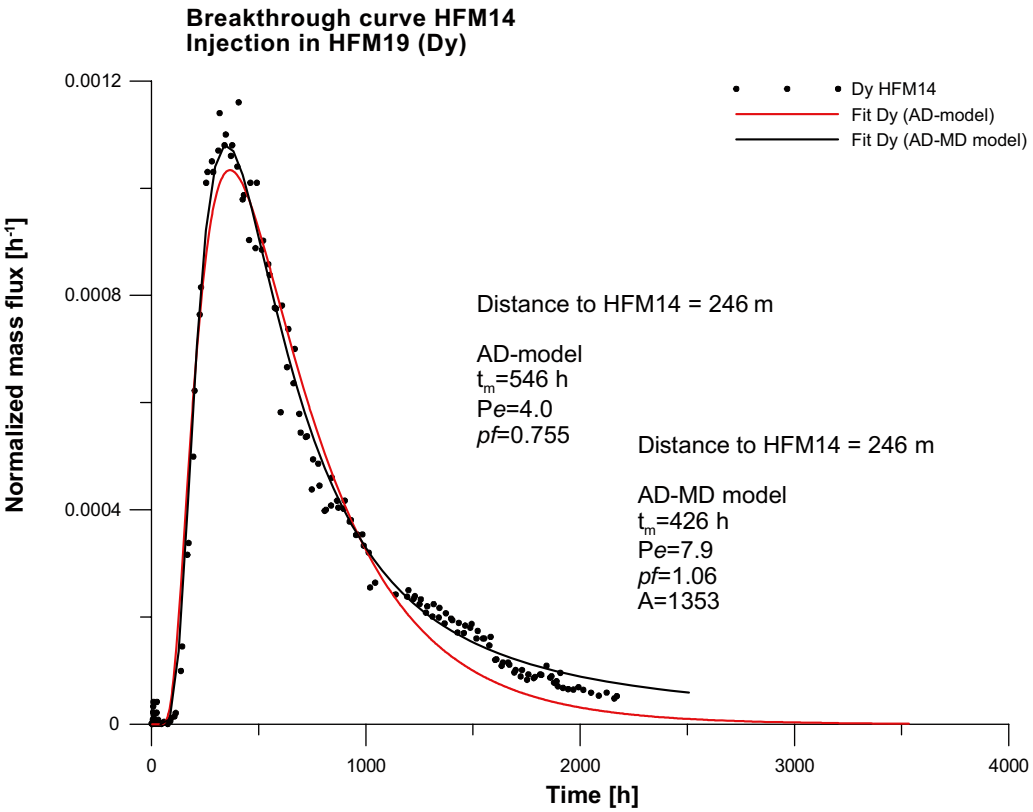

Figure 5-11. *Linear plot of model fit using the AD model and the AD-MD model to experimental data for Dy from HFM19.*

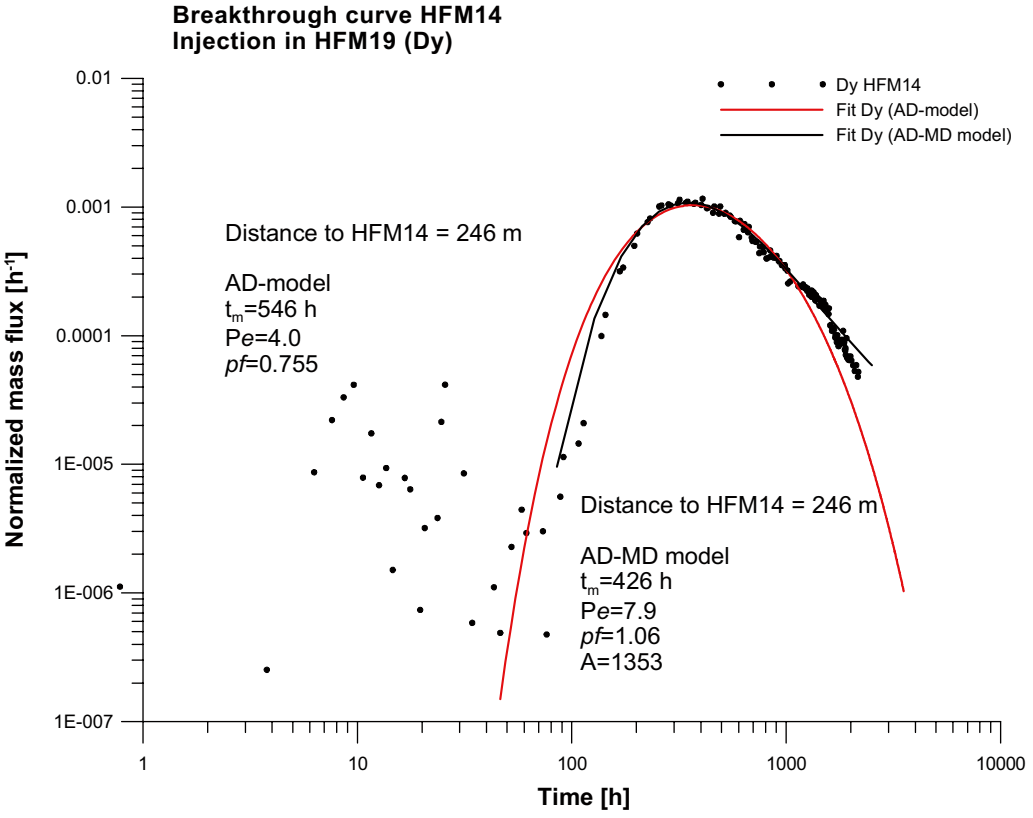

Figure 5-12. *Logarithmic plot of model fit using the AD model and the AD-MD model to experimental data for Dy from HFM19.*

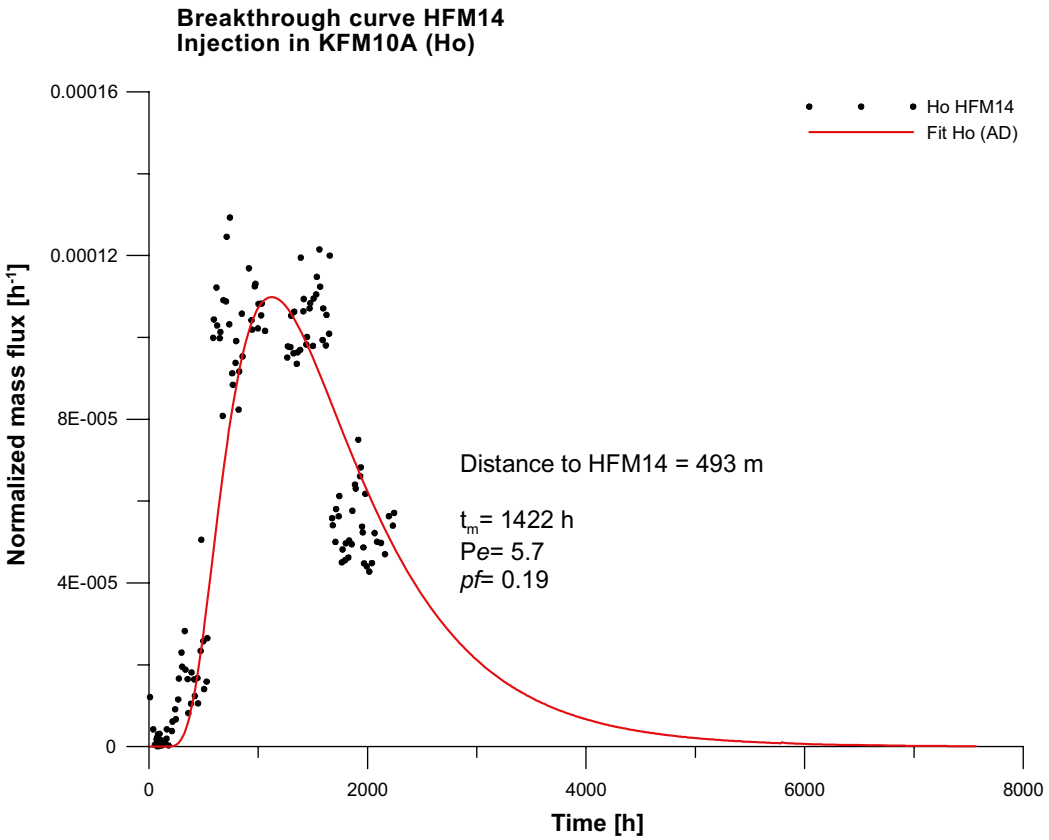

Figure 5-13. *Linear plot of model fit using the AD model to experimental data for Ho from KFM10A.*

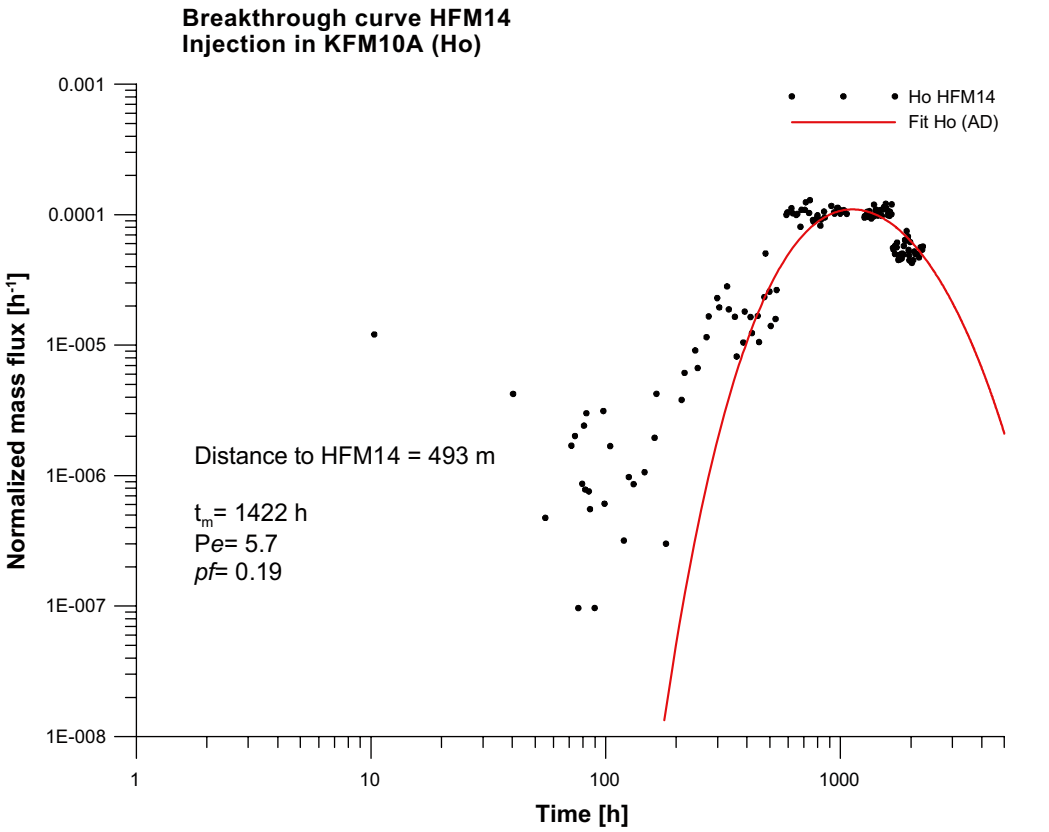

Figure 5-14. *Logarithmic plot of model fit using the AD model to experimental data for Ho from KFM10A.*

Summary of results

The results from the modelling are summarised in Tables 5-5, 5-6 and 5-7. Only the results regarded as reliable are presented in these tables.

Additional tracer test with sorbing tracer

Firstly the AD model was applied. Uranine and Cs were simulated simultaneously. In the first model run, all parameters were allowed to vary which resulted in different p_f for Uranine and Cs. Also, the fit was not very good for Cs, especially for the tail, see Figure 5-15. An additional simulation was made were p_f for Cs was restricted to be equal to p_f for Uranine, see Figure 5-16.

Restricting p_f for Cs to equal p_f for Uranine did not provide a good fit, Figure 5-16. Then the AD-MD model was applied which resulted in much better fits to experimental data. Firstly, a run letting all parameters be free was made. Then p_f for Cs was restricted to be equal to p_f for Uranine. Both fits are shown in Figure 5-17 and Figure 5-18; note that Uranine and Cs are plotted on separate axes. From the linear plot in Figure 5-17 it is seen that when p_f is free, a slightly better fit is provided (only seen for Cs). However, the estimated parameters are very similar. The fit where p_f is free is regarded to be the best one. In Figure 5-19 this fit is also shown with Uranine and Cs on the same axis.

For comparison with Figure 5-15 and 5-16 the best fit using the AD-MD model presented in Figure 5-18 is also shown in Figure 5-19 below where Uranine and Cs are plotted on the same axis.

Table 5-5. Results from the AD model.

Borehole: section	Tracer	Distance to HFM14 (m)	t_m (h)	Pe (–)	p_f (–)
HFM01:2	Eu	378	1,987	8.2	0.17
HFM13:1	Tb	297	1,133	5.8	0.48
KFM10A:2	Ho	493	1,422	5.7	0.19

Table 5-6. Results from the AD-MD model.

Borehole: section	Tracer	Distance to HFM14 (m)	t_m (h)	Pe (–)	p_f (–)	A (–)
HFM15:1	Gd	72	9.3	14.1	0.69	278
HFM19:1	Dy	246	426	7.9	1.1	1,353

Table 5-7. Results from the AD model with 2 pathways for HFM15.

Borehole: section	Path	Distance to HFM14 (m)	t_m (h)	Pe (–)	p_f (–)
HFM15:1	1	72	10.7	9.0	0.46
HFM15:1	2	72	35	4.8	0.14

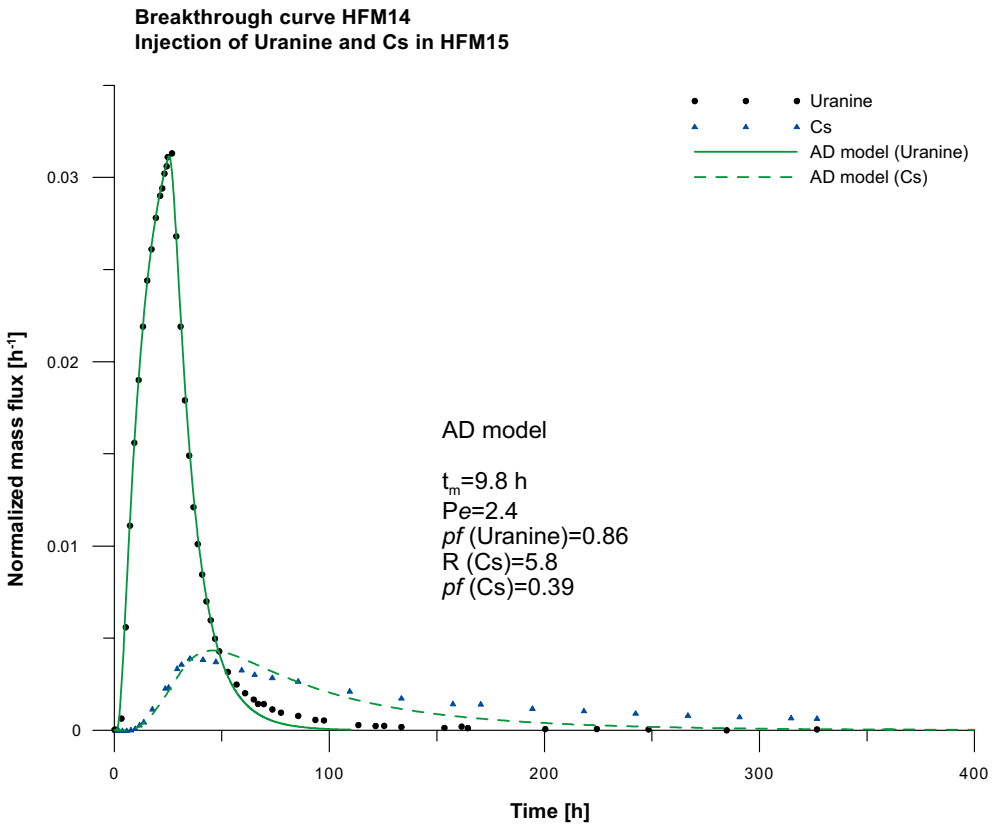

Figure 5-15. *Linear plot of model fit using the AD model to experimental data for Uranine and Cs from HFM15 in the additional tracer test. All parameters are free.*

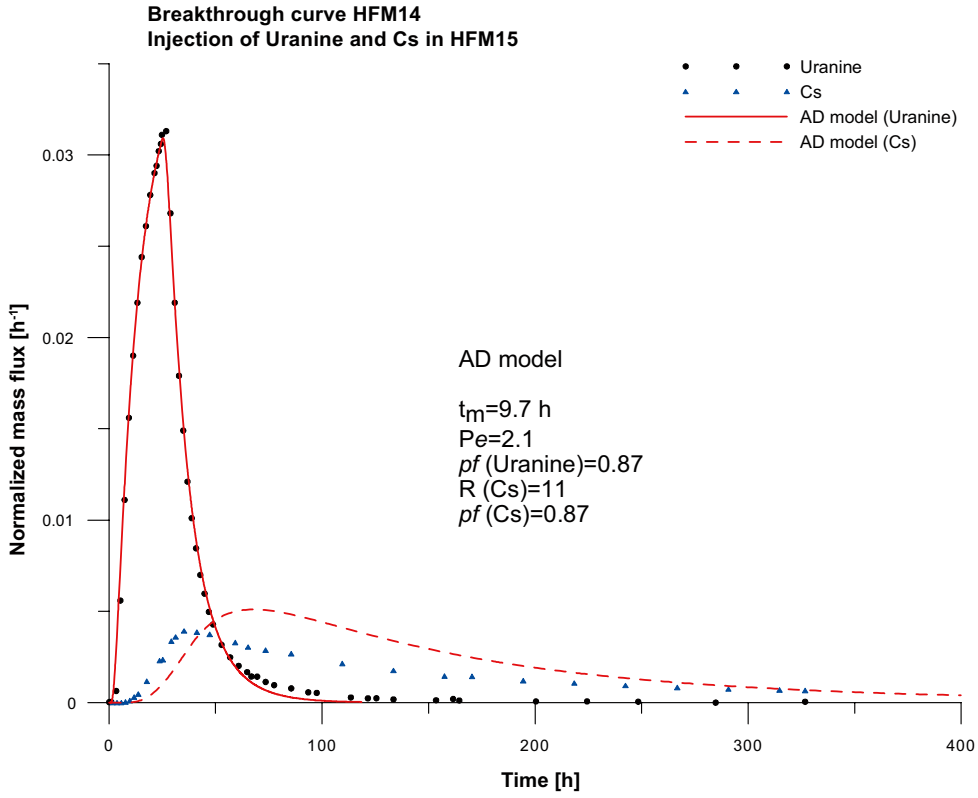

Figure 5-16. *Linear plot of model fit using the AD model to experimental data for Uranine and Cs from HFM15 in the additional tracer test. p_f for Cs is restricted to equal p_f for Uranine.*

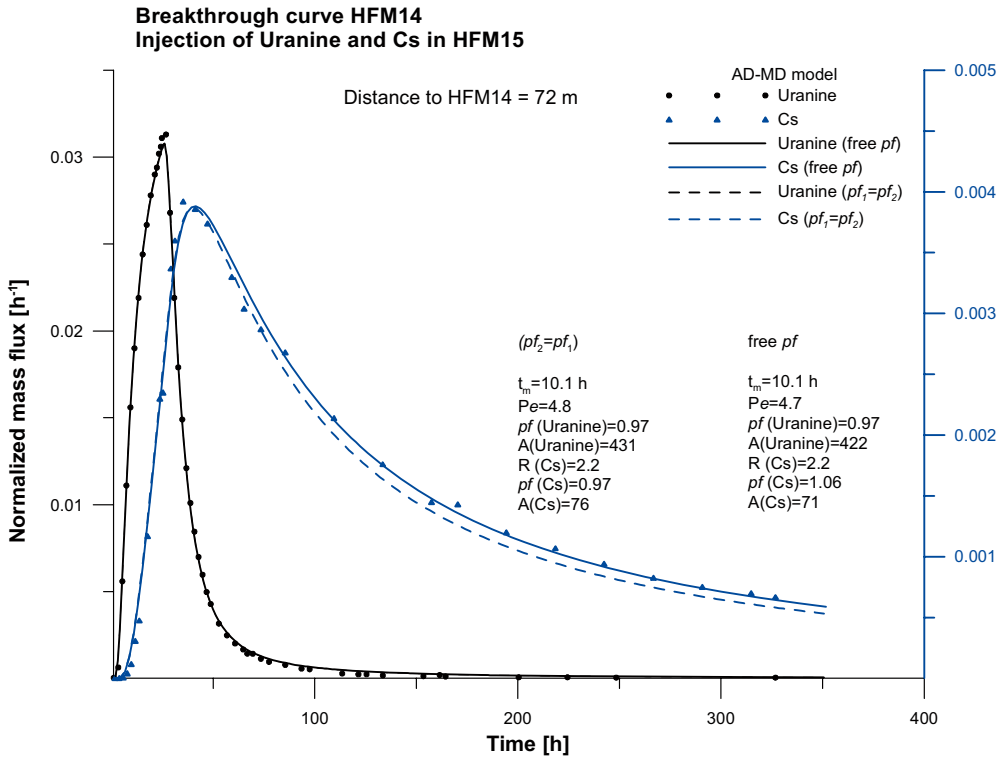

Figure 5-17. *Linear plot of model fit using the AD-MD model to experimental data for Uranine (black) and Cs (blue) from HFM15 in the additional tracer test showing Uranine and Cs on different axes. The figure shows the difference between free p_f for Cs (solid line) and when p_f for Cs is restricted to equal p_f for Uranine (dashed line).*

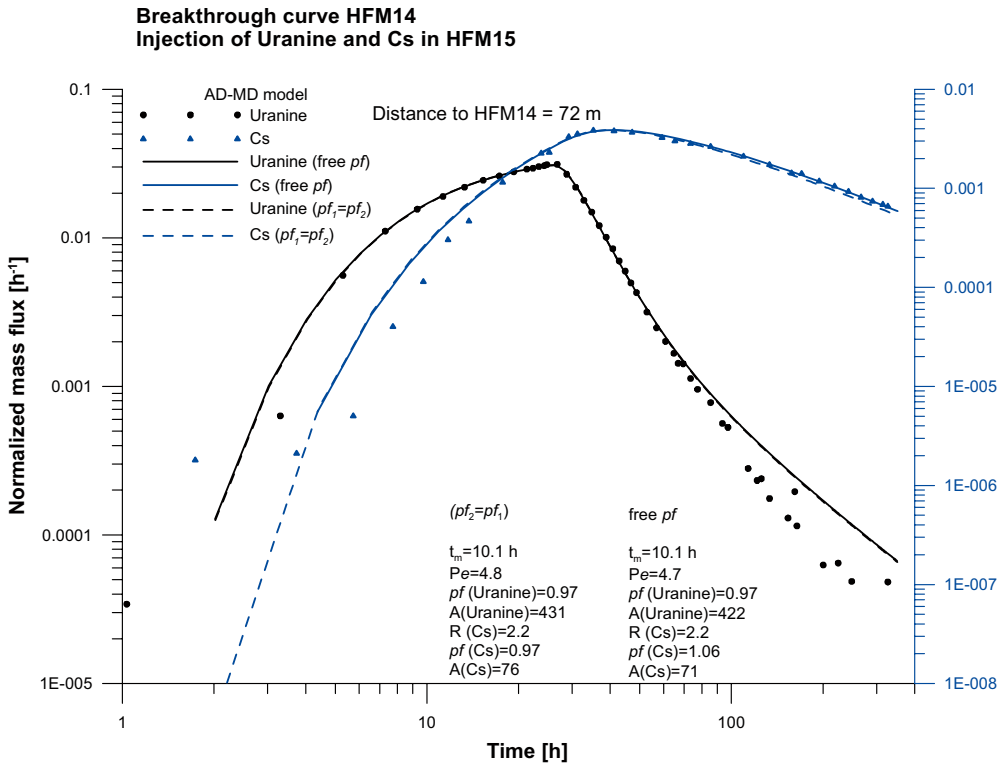

Figure 5-18. *Logarithmic plot of model fit using the AD-MD model to experimental data for Uranine (black) and Cs (blue) from HFM15 in the additional tracer test showing Uranine and Cs on different axes. The figure shows the difference between free p_f for Cs (solid line) and when p_f for Cs is restricted to equal p_f for Uranine (dashed line).*

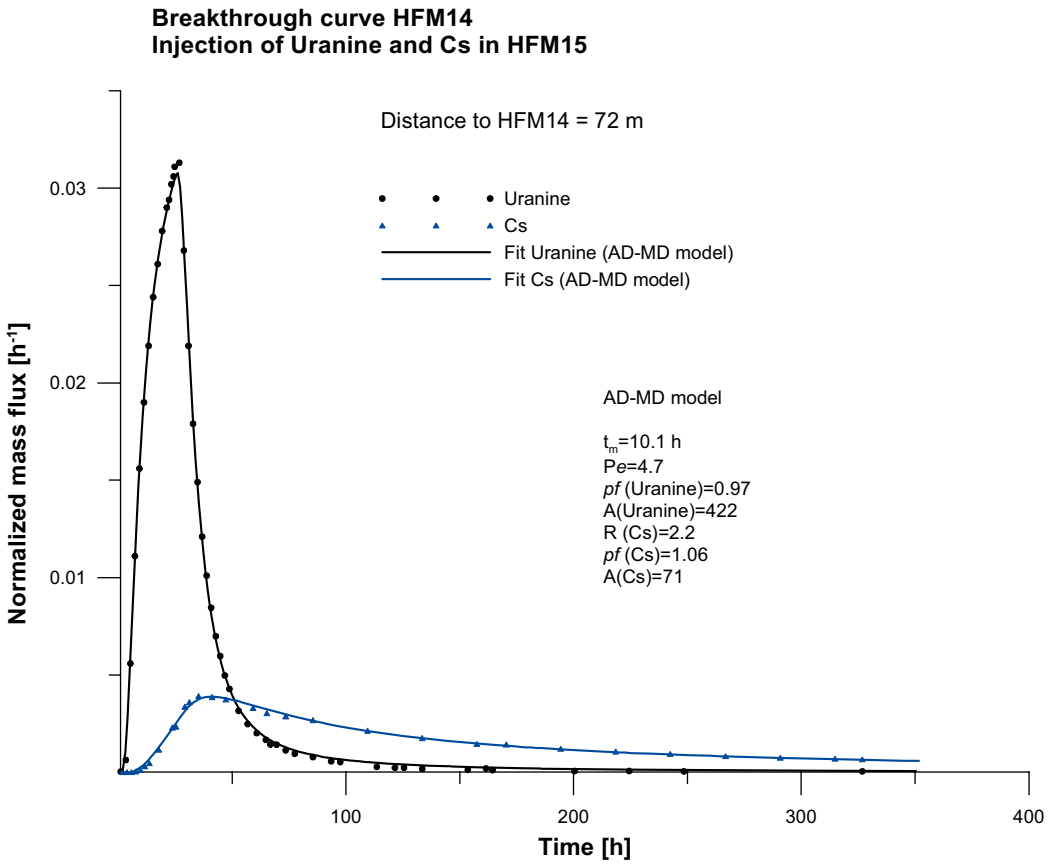

Figure 5-19. *Linear plot of model fit using the AD-MD model to experimental data for Uranine and Cs from HFM15 in the additional tracer. Free p_f.*

Table 5-8. *Results from the AD-MD model.*

Borehole: section	Tracer	t_0 (h)	Pe (–)	p_f (–)	R	A (–)
HFM15:1	Uranine	10.1	4.7	0.97	1.0	422
HFM15:1	Cs	10.1	4.7	1.06	2.2	71

Comparision between results from injection of Gd and Uranine in HFM15

Model runs were also performed on *only* the Uranine breakthrough curve using both the AD model and the AD-MD model. The results are shown in Figure 5-20 (linear plot) and Figure 5-21 (logarithmic plot). These results were compared with the corresponding simulations made for Gd in the first tracer test. They were also compared with the parameters obtained for Uranine when simultaneously modelling the Cs breakthrough curve. The AD model for a single pathway did not provide good fits for any of the two tracers.

The AD-model with two pathways was applied on both Uranine and Gd. This model provided a better fit than the AD model for a single pathway.

In the following table (Table 5-9) all the simulations using the different models of Gd and Uranine breakthrough data (alone and simultaneously with Cs) are compared.

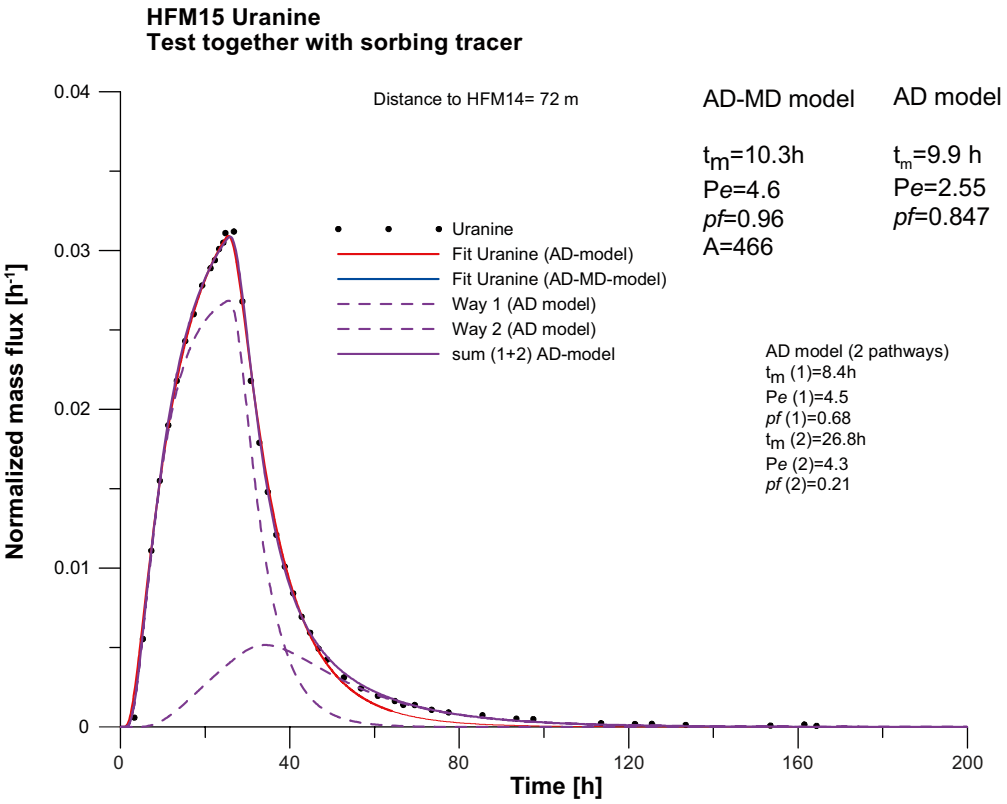

Figure 5-20. *Linear plot of model fit using the AD model with a single pathway and with two pathways and the AD-MD model to experimental data for Uranine only from HFM15 in the additional tracer test.*

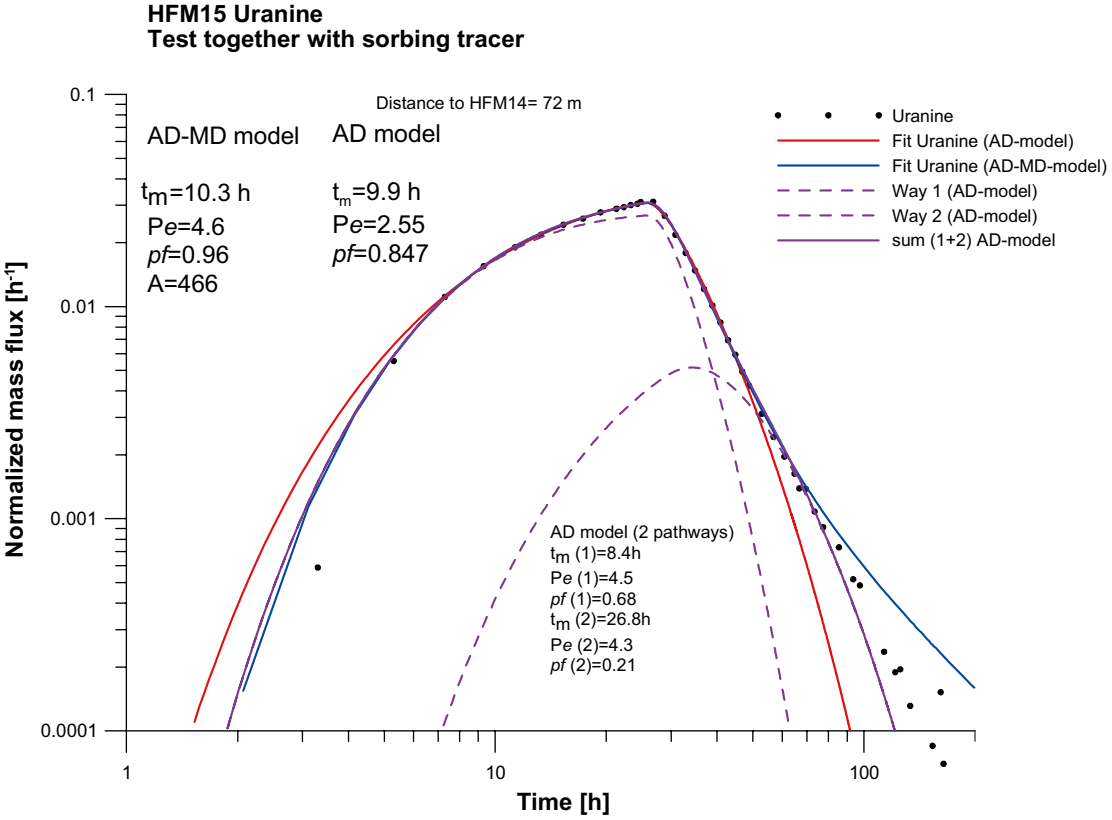

Figure 5-21. *Logarithmic plot of model fit using the AD model with a single pathway and with two pathways and the AD-MD model to experimental data for Uranine only from HFM15 in the additional tracer test.*

Table 5-9. Comparision of model results from fits to Gd and Uranine.

Model	Tracer	t_m (h)	Pe (–)	p_f (–)	A (–)
AD single pathway	Gd	11.6	6.8	0.532	–
AD single pathway	Uranine	9.9	2.6	0.85	–
AD two pathways	Gd (path 1)	10.7	9.0	0.46	–
AD two pathways	Uranine (path 1)	8.4	4.5	0.68	–
AD two pathways	Gd (path 2)	34.5	4.8	0.14	–
AD two pathways	Uranine (path 2)	26.8	4.3	0.21	–
AD	Uranine (with Cs)	9.8	2.4	0.86	–
AD-MD	Gd	9.3	14.1	0.69	278
AD-MD	Uranine	10.3	4.6	0.96	466
AD-MD	Uranine (with Cs)	10.1	4.7	0.97	422

5.2.3 Other derived transport parameters

A number of other transport parameters may be derived from the modelling results. In cases where more than one model was used, one of the simulations was selected to be the most representative one. The simulations with the AD-MD model for HFM15 and HFM19 presented in Figure 5-9 and 5-11, respectively, were considered to provide the best results.

The background data from the modelling used to calculate additional transport parameters are presented in Table 5-10. Fracture conductivity (K_{fr}), equivalent fracture aperture (δ) and flow porosity (ε_f) were calculated according to SKB's methods description (SKB MD 530.006). These calculated parameters are presented in Table 5-11.

In order to calculate the additional transport parameters the mean head difference, Δh (m) between injection- and pumping section has to be determined. The mean head differences were determined from head readings (pressure registrations) in both of the boreholes just before pump stop. The head difference, Δh, is shown together with the distance between the two borehole sections in Table 5-10.

For the flow porosity calculations according to Equation 3-25, an estimation of K (the conductivity from steady state evaluation of the interference test) is needed. This calculation is valid for a packed-off section, but in this case the pumping was made in an open hole. The section length can instead be approximated by the thickness of the zone A2 intersection in the borehole, which is the hydraulically dominating structure intersecting this borehole. This estimation can be made from geological interpretations where A2 is defined to intersect HFM14 at DZ1 and DZ2 /15/ which according to /16/ is at borehole length 68–76 m and 92–104 m, respectively. Alternatively, the estimation of the zone thickness can be made from flow logging /17/, which indicates that the flowing part of these structures are 67.5–68.5 m and 100–102 m, respectively. The two different ways of estimating the section length give rise to a difference in calculated flow porosity by a factor 5 (the larger flow porosity obtained when the shorter section length is used). In Table 5-11 the flow porosity presented is calculated by using the section length estimated from the flow logging /17/.

Table 5-10. Background data for calculations of transport parameters.

	Distance (m)	Mean head difference, Δh (m)
HFM01	377	9.1
HFM13	297	5.6
HFM15	72	4.5
HFM19	247	5.3
KFM10A	493	6.2

Table 5-11. Calculated transport parameters.

	Fracture conductivity, K_{fr} (m/s)	Equivalent fracture aperture, δ (m)	Flow porosity, ε_f [1] (–)
HFM01	1.20E–02	9.32E–02	1.37E–02
HFM13	2.05E–02	8.56E–02	7.99E–03
HFM15	1.59E–01	1.20E–02	1.04E–03
HFM19	3.92E–02	4.65E–02	4.19E–03
KFM10A	4.27E–02	3.90E–02	3.85E–03

[1] Section length estimated from flow logging /17/.

6 Summary and discussions

6.1 Tracer breakthrough

From Figure 6-1 it is seen that the mean residence time, t_m, is generally increasing with the distance to HFM14. The exception is HFM01 which has a longer mean residence time than KFM10A although the distance from KFM10A is c 100 m longer than the distance between HFM01 and HFM14.

All borehole sections used in the tracer test, except HFM13 and HFM32, are intersected by the deformation zone A2. HFM13 is interpreted as intersecting ZFMNE0401 /14/. The results indicate good connection between this zone and Zone A2. An interesting observation is that the residence time for HFM13 is c 850 h shorter than for HFM01. The distance between the pumping borehole and HFM13 is c 80 m shorter than the corresponding distance to HFM01. Despite this the dispersivity for these two sections is practically the same (*Pe* for HFM13 is lower). This may be due to a more complex pathway for the tracer from HFM13 since it only has a secondary connection to the Zone A2.

Since HFM32, from which breakthrough did not occur, is the most distant borehole from the pumping borehole, it is not clear whether it is the distance that is limiting or if it is because the section is not located in Zone A2. However, the difference between the distance to KFM10A and to HFM32 is only c 20 m, and breakthrough from KFM10A was obtained already after 210 h and the peak after c 1,200 h (the sampling continued for 2,200 h). These facts indicate that the less good connectivity observed is likely to be due to that the section is not intersected by Zone A2.

6.2 Model parameters

The Peclet numbers (*Pe*) range between 4 and 14, which is significantly higher than the value (*Pe* = 0.9) determined in a previous tracer test in Zone A2 between KFM02A and KFM02B /2/. These values correspond to dispersivities ranging between 5 and 86 m.

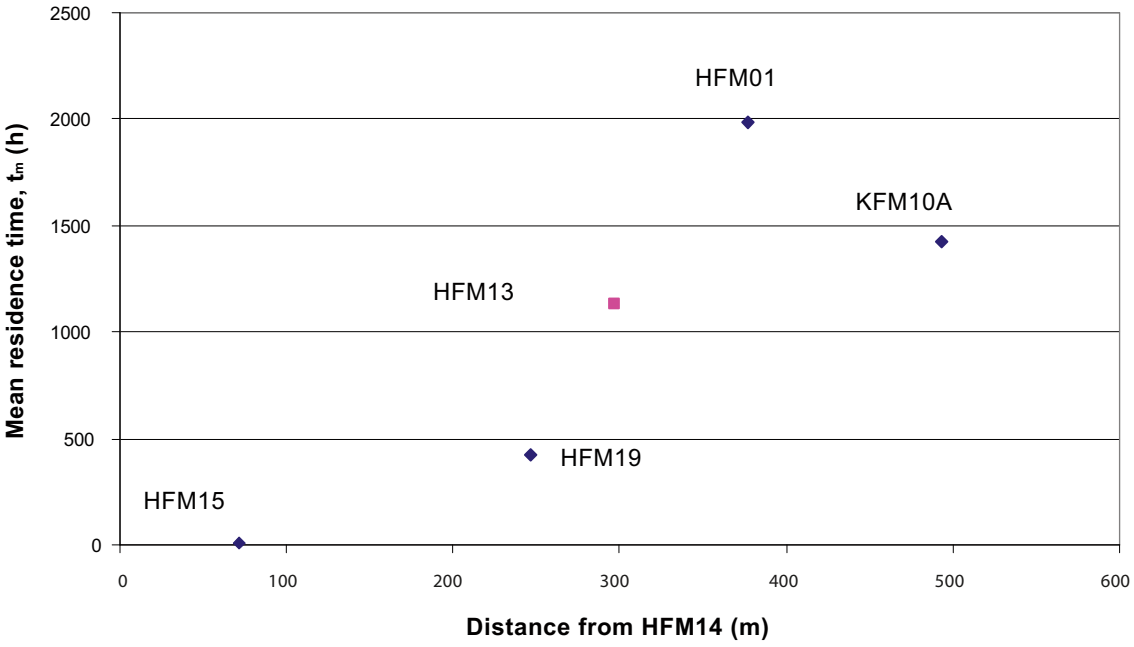

Figure 6-1. *Interpreted mean residence time plotted against distance from the pumping borehole HFM14. Since HFM13 is not interpreted to intersect Zone A2 it is denoted by a different symbol and colour.*

The estimated value of the retardation coefficient, R, for Cs (R=2.2) from the additional tracer test indicates a moderate retention along this flow path. This is consistent with the tracer test performed in another, deeper part of Zone A2 (in the previous tracer test between KFM02A and KFM02B /2/) where R=3.4 was estimated for Cs /2/.

When comparing the results from simulations of the Gd- and the Uranine breakthrough curves, the biggest difference is the larger *Pe* obtained for the fit to the Gd-curve. A larger *Pe* (less dispersion) can be expected for Gd since this tracer injection was performed without excess pressure, whereas the Uranine injection was.

Generally, when using the AD-MD model *Pe* is higher than for the AD model. This is reasonable since diffusion is included in the AD-MD model, which reduces the need for dispersion to explain the tailing.

6.3 Uncertainities and errors

The calculation of recovery presented in Section 5.2.1 is in some cases very sensitive to the determination of background concentration. One example is HFM15 where the breakthrough is fast and the "tail" of the breakthrough curve is very long and a large part of the mass is in the tail. Since the concentrations are rather low, the analyses are also somewhat uncertain which makes it difficult to determine the correct background concentration. In Figure 6-2 a detailed plot of the low concentrations of Gd in HFM14 is shown. The figure demonstrates a large spreading of the data and three possible background levels. In Table 6-1 the effect on recovery at pump stop using these different background levels is presented. The background level of 0.145 ppb was considered most likely and was used in the calculations.

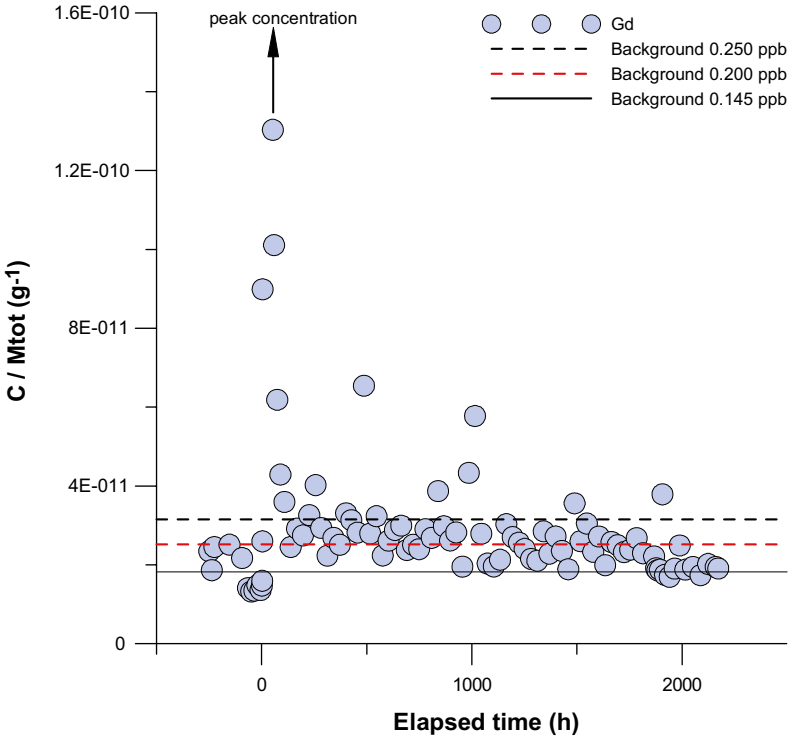

Figure 6-2. *Detailed picture of the low concentrations of Gd before injection and at the "tail" of the breakthrough curve, illustrating the difficulty to choose a correct background concentration. The arrow indicates the time when the peak arrives.*

Table 6-1. Example of effect on recovery by different background concentrations (HFM15).

Borehole: section	Tracer	Background (µg/l)	Recovery at pumpstop (%)
HFM15:1	Gd	0.145	91.6
HFM15:1	Gd	0.200	69.2
HFM15:1	Gd	0.250	59.8

The laboratory (ALS Scandinavia) reports that the analytical errors might in the worst case be as high as 20%.

In order to check the analyses and the calculations of injected mass, the total mass of tracer in the cans before injection (calculated by weighing and analyses) was compared with the total mass of each tracer that had been added in the preparation of the tracer solutions. When the agreement was bad, another set of samples was sent to the laboratory. In most cases the agreement between measured and theoretical mass was good (difference < 4%). However, for Eu (HFM01) and Gd (HFM15) the differences between theoretical and measured mass were 7% and 10%, respectively. The masses calculated by weighing and analyses were considered to be the most representative and were used for further calculations.

6.4 Groundwater flow measurements

The groundwater flow measurements performed before and during pumping in HFM14 were useful as an indicator of connectivity and as design parameter for the tracer test. Natural flow varied between 1–13 ml/min whereas flow during pumping increased with a factor 2–85 with no correlation to distance from HFM14, indicating a heterogeneous system.

The dilution measurements show a very high groundwater flow rate through the measured section in HFM19. Despite this, the transport time (mean residence time) from HFM19 to HFM14 is rather long which indicates that a large water volume is involved in the flow path.

6.5 Comparison of results with scoping calculations

The concentrations of tracers to be injected were designed in the scoping calculations so that the maximum concentration in HFM14 should be 100 times that of the expected background level if the recovery is total (100%), the dispersivity is equal to half the assumed travel distance (Peclet number = 2) and the aperture is 30 times the cubic law. When comparing the breakthrough curves with the time to maximum concentration indicated by the scoping calculations (see Table 4-1) and the maximum ratio C/C_0, it is clear that in most cases the time is underestimated in the scoping calculations and the peak concentration is overestimated. In Table 6-2 a comparison of the chosen prediction in the scoping calculations (Peclet number = 2 and aperture = cubic law*30) of C/C_0 maximum ratio and time to C_{max} and the results is presented. Also the actual ratio of $C_{max}/C_{background}$ is seen in Table 6-2 and is in most cases much lower than 100.

The reason for the difference between the scoping calculations and the actual results is the assumptions made in the scoping calculations. As seen in Table 6-3 the recovery was assumed to be 100% whereas the results actually varied between 19% and 110%. The assumption that the dispersivity is equal to a Peclet number of 2 was also incorrect since the modelled Peclet number ranges from 5.7 to 14.1. Finally the assumption of an aperture of 30 times the cubic law also seems rather underestimated in most cases.

Table 6-2. Results compared with scoping calculations assuming Peclet number = 2 and aperture = cubic law*30.

Borehole: section	C/C_0 max result	predicted	Time to Cmax (h) result	predicted	Cmax (Times Background)
HFM01:2	2.1E–07	5E–06	1,500	151	5.30
HFM13:1	6.1E–07	3E–06	1,000	215	22.50
HFM15:1	5.6E–05	5E–05	17	12	98.90
HFM19:1	3.7E–06	6E–06	400	103	65.79
HFM32:3	2.9E–07	5E–07	–	464	50.90
KFM10A:2	2.8E–07	3E–06	1,200	246	10.55

Table 6-3. Modelled results compared with assumption in scoping calculations.

Borehole section	Recovery	Dispersivity, Peclet number	Equivalent fracture aperture, δ divided by aperture according to the cubic law
HFM01:2 [1)]	17%	8.2	224
HFM13:1 [1)]	48%	5.8	111
HFM15:1 [2)]	69%	14.1	22
HFM19:1 [2)]	110%	7.9	61
KFM10A:2 [1)]	19%	5.7	112
Assumed in scoping [1)]	100%	2.0	30

[1)] AD model.

[2)] AD-MD model.

6.6 Comparison with hydraulic responses

The interference test performed in connection with the tracer test was carried out by pumping in HFM14 and at the same time monitoring pressure in several surrounding borehole sections. The results from and evaluations of the hydraulic interference test is reported in /1/.

The six observation sections involved in the tracer test as well as the pumping borehole were evaluated quantitatively using methods for transient evaluation.

The evaluation showed that three of the four sections standing out as responding most strongly are sections used in the tracer test (HFM15, HFM19 and KFM10A). Also, three more sections demonstrate responses that are distinct enough to be characterized as potential zone responses between HFM14 and the actual sections. One of these three is the injection section in HFM13. The results show that the connection between these boreholes and the pumping borehole is very good, which is also confirmed by the tracer breakthrough from these sections.

HFM32 and HFM01 do not stand out as the sections with strongest hydraulic responses. However, the connection between HFM01 and HFM14 is confirmed by the tracer breakthrough.

From the interference test evaluation a lag time (dt_L) is calculated. The lag time dt_L is based on a drawdown s=0.01 m in the observation section. Generally, the lag time increases with increasing distance to HFM14, see Figure 6-3. The exception is HFM01 which has a longer lag time than KFM10A despite a shorter distance from HFM14.

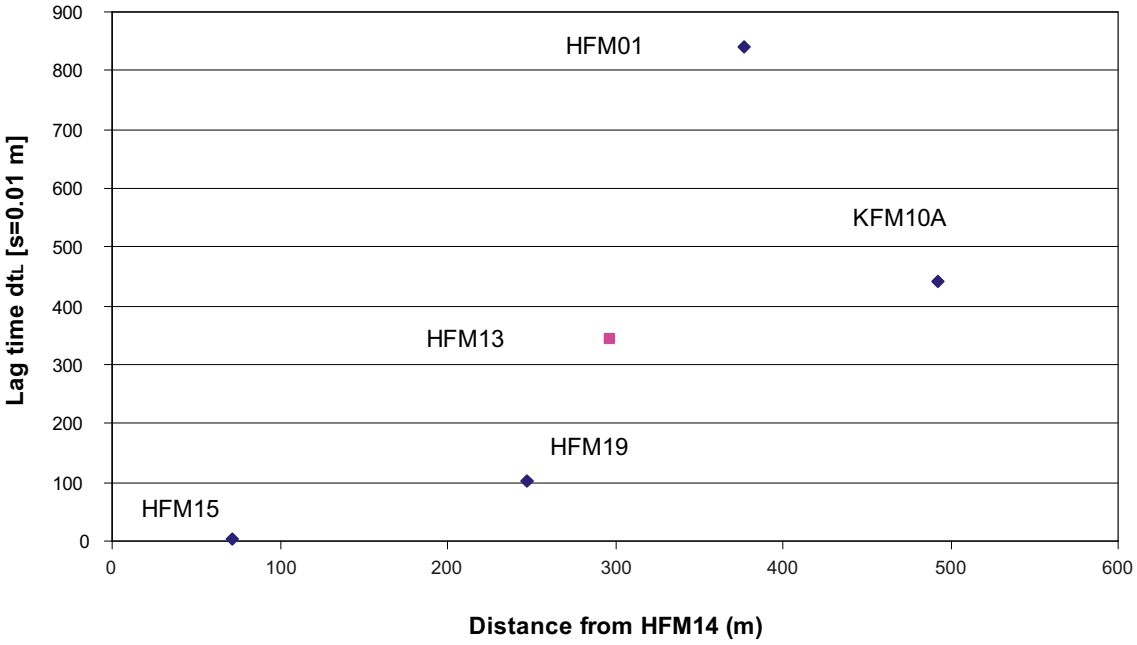

Figure 6-3. *Lag time from interference test evaluation plotted against distance from the pumping borehole HFM14. Since HFM13 is not interpreted to intersect Zone A2 it is denoted by a different symbol and colour.*

The estimated transmissivities from observation sections HFM01: 33.5–45.5 m and KFM10A: 430–440 m are significantly higher than the T-values obtained from single-hole tests from previous investigations /1/. Thus, the results from the interference test may not be quite representative of the formation close to the observation section but rather to an adjacent fracture zone, suggesting that the response may possibly be a strong secondary response rather than a primary response. The estimated T-values from the other observation sections correspond well to those from previous single-hole investigations.

The fact that the mean travel time from HFM01 is longer than from KFM10A despite the shorter distance is supported by the interference test which indicates a stronger response from KFM10A and also a shorter lag time.

HFM13 is not interpreted as intersecting the Zone A2. Despite this the hydraulic response is strong and tracer breakthrough is obtained. This indicates that the zone ZFMNE0401 which intersects HFM13 at 162–196 mbl /18/, /19/ has good connection with Zone A2. From HFM01 which intersects the Zone A2 one could maybe expect a stronger hydraulic response and a shorter mean travel time. The travel time from HFM01 is much longer than from HFM13 despite the fact that the distance is only c 80 m longer.

Figure 6-4 shows that there is a relationship between the lag time and the mean residence time of the tracer. This figure illustrates that there is a good agreement between the tracer test and the hydraulic interference test.

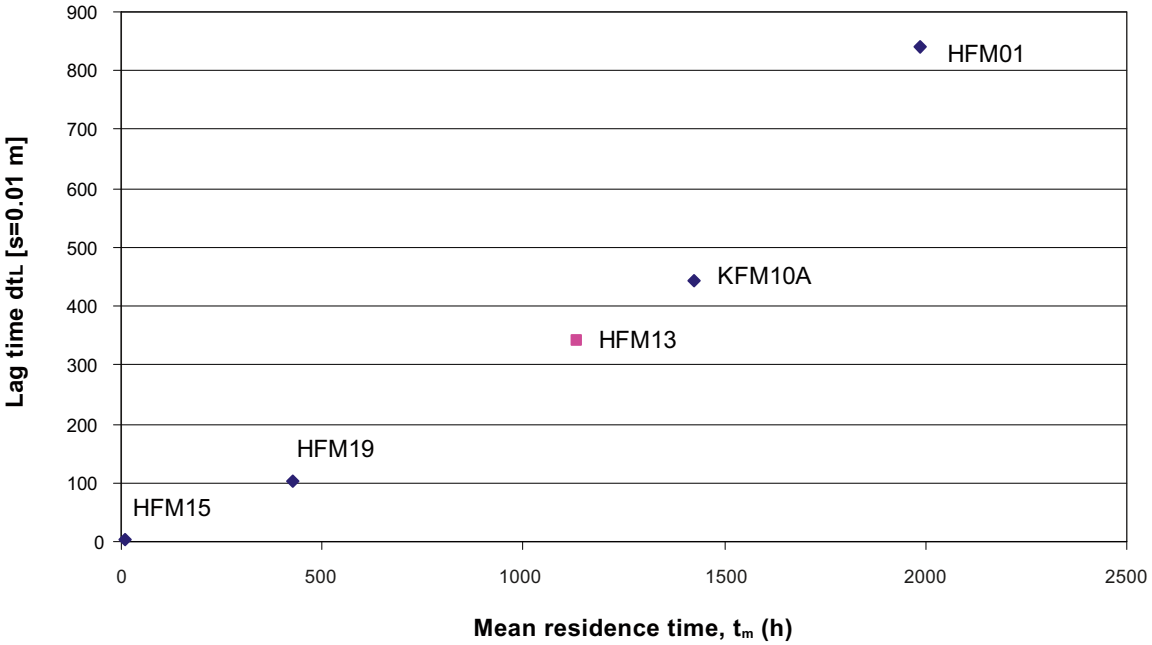

Figure 6-4. *Lag time from the interference test evaluation plotted against interpreted mean residence time. Since HFM13 is not interpreted to intersect Zone A2 it is denoted by a different symbol and colour.*

7 References

/1/ **Gokall-Norman K, 2007.** Forsmark site investigation. Hydraulic interference test in borehole HFM14, summer of 2007. SKB P-report in progress, Svensk Kärnbränslehantering AB.

/2/ **Lindquist A, 2007.** Forsmark site investigation. Confirmatory hydraulic interference test and tracer test at drill site 2. SKB P-08-13, Svensk Kärnbränslehantering AB.

/3/ **Lindquist A, Wass E, 2006.** Forsmark site investigation. Groundwater flow measurements in conjunction with the interference test with pumping in HFM14. SKB P-06-188, Svensk Kärnbränslehantering AB.

/4/ **Javandel I, Doughty C, Tsang C F, 1984.** Groundwater transport: Handbook of mathematical models. American Geophysical Union, Washington, D.C.

/5/ **Tang G H, Frind E O, Sudicky E A, 1981.** Contaminant transport in fractured porous media. An analytical solution for a single fracture. Water Resources Research, Vol 17, 555.

/6/ **Moreno L, Neretnieks I, Klockars C E, 1983.** Evaluation of some tracer tests in the granitic rock at Finnsjön. SKB TR 83-38, Svensk Kärnbränslehantering AB.

/7/ **Cooley R L, 1979.** A method of estimating parameters and assessing reliability for models of steady ground water flow. 2. Applications of statistical analysis. Water Resources Research, 15: 318–324.

/8/ **Moye D G, 1967.** Diamond drilling for foundation exploration. Civ. Eng. Trans. 7th. Inst. Eng. Australia.

/9/ **Gustafsson E, 2002.** Bestämning av grundvattenflödet med utspädningsteknik– Modifiering av utrustning och kompletterande mätningar. SKB R-02-31, Svensk Kärnbränslehantering AB.

/10/ **Ludvigson J E, Jönsson S, Levén J, 2003.** Forsmark site investigation. Pumping tests and flow logging – Boreholes KFM01A (0–100 m), HFM01, HFM02 and HFM03. SKB P-03-33, Svensk Kärnbränslehantering AB.

/11/ **Ludvigson J E, Jönsson S, Jönsson J, 2004.** Forsmark site investigation. Pumping tests and flow logging – Boreholes HFM13, HFM14 and HFM15. SKB P-04-71, Svensk Kärnbränslehantering AB.

/12/ **Ludvigson J E, Källgården J, Hjerne C, 2004.** Forsmark site investigation. Pumping tests and flow logging – Boreholes HFM17, HFM18 and HFM19. SKB P-04-72, Svensk Kärnbränslehantering AB.

/13/ **Jönsson S, Ludvigson J-E, 2006.** Forsmark site investigation. Pumping tests and flow logging – Boreholes HFM24, HFM32. SKB P-06-96, Svensk Kärnbränslehantering AB.

/14/ **Walger E, Hjerne C, Ludvigson J E, 2007.** Forsmark site investigation. Single-hole injection tests in borehole KFM10A. SKB P-07-31, Svensk Kärnbränslehantering AB.

/15/ **SKB, 2006.** Site descriptive modelling Forsmark stage 2.1. SKB R-06-38, Svensk Kärnbränslehantering AB.

/16/ **Carlsten S, Petersson J, Stephens M, Tunehed H, Gustafsson J, 2006.** Forsmark site investigation. Geological single-hole interpretation of KFM05A, HFM14-15 and HFM19 (DS5). Forsmark site investigation Revised October 2006. SKB P-04-296, Svensk Kärnbränslehantering AB.

/17/ **Lindquist A, Ludvigson J E, 2006.** Forsmark site investigation. Pumping tests and flow logging in borehole HFM14 and pumping test in KFM05A (0–114 m). SKB P-06-140, Svensk Kärnbränslehantering AB.

/18/ **SKB, 2006.** Site descriptive modeling Forsmark Stage 2.1. SKB R-06-38, Svensk Kärnbränslehantering AB.

/19/ **SKB, 2005.** Preliminary Site description. Forsmark area – version 1.2. SKB R-05-18, Svensk Kärnbränslehantering AB.

Appendix 1

Tracer dilution graphs- measurements prior to the tracer test

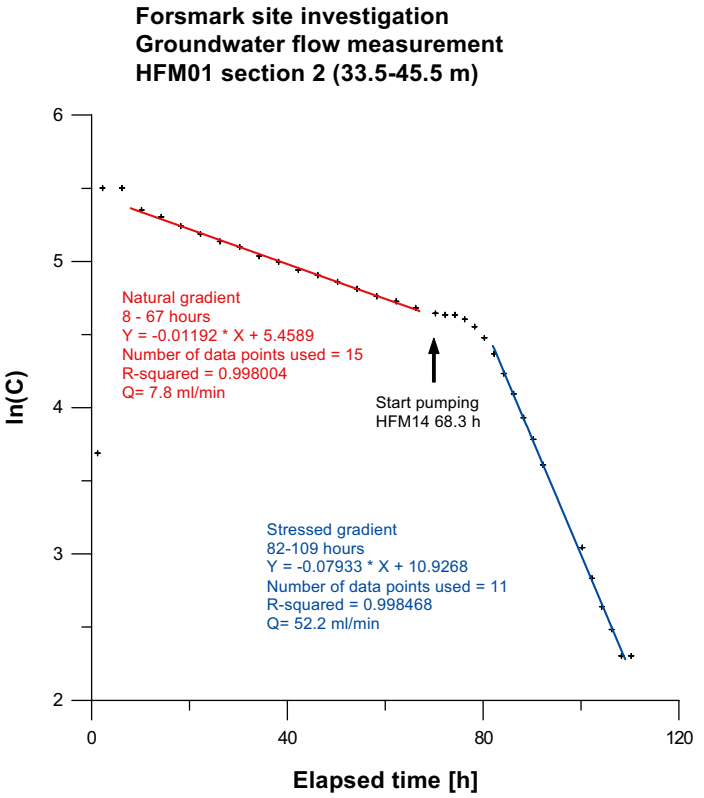

Figure A1-1. *Tracer dilution graph for section HFM01:2.*

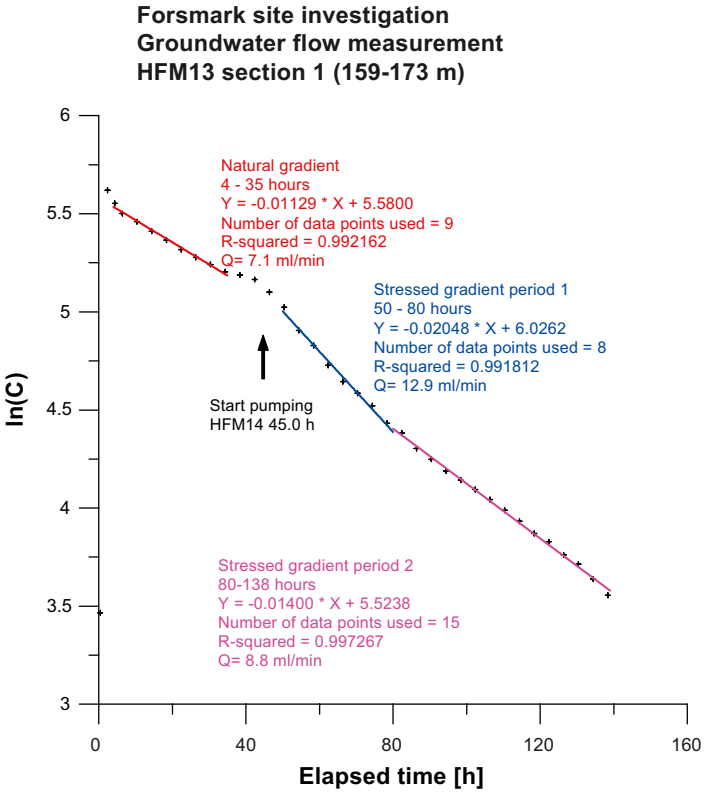

Figure A1-2. *Tracer dilution graph for section HFM13:1.*

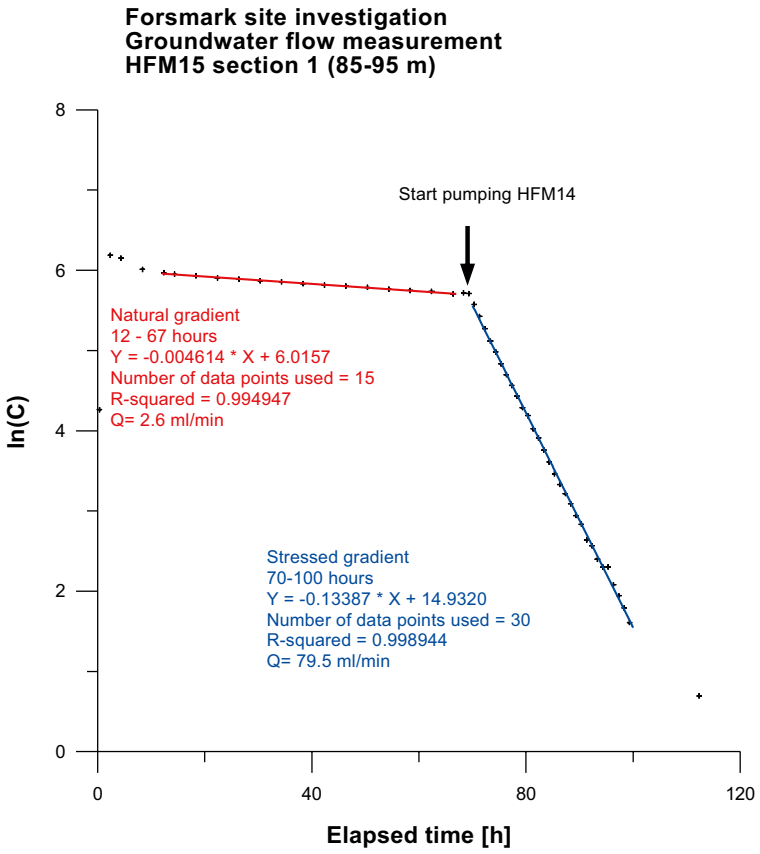

Figure A1-3. *Tracer dilution graph for section HFM15:1.*

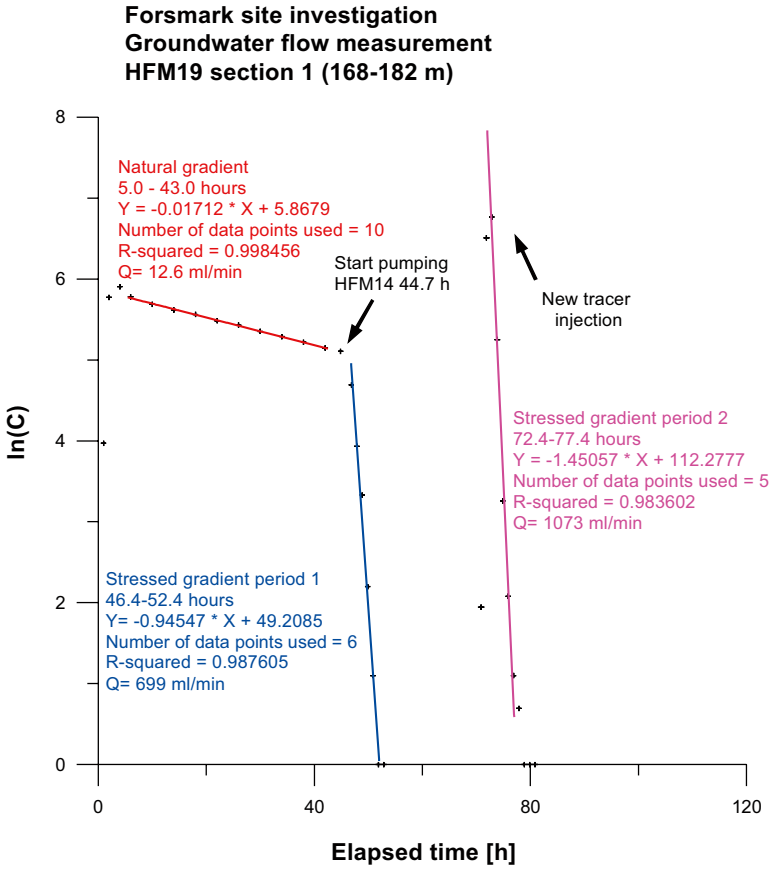

Figure A1-4. *Tracer dilution graph for section HFM19:1.*

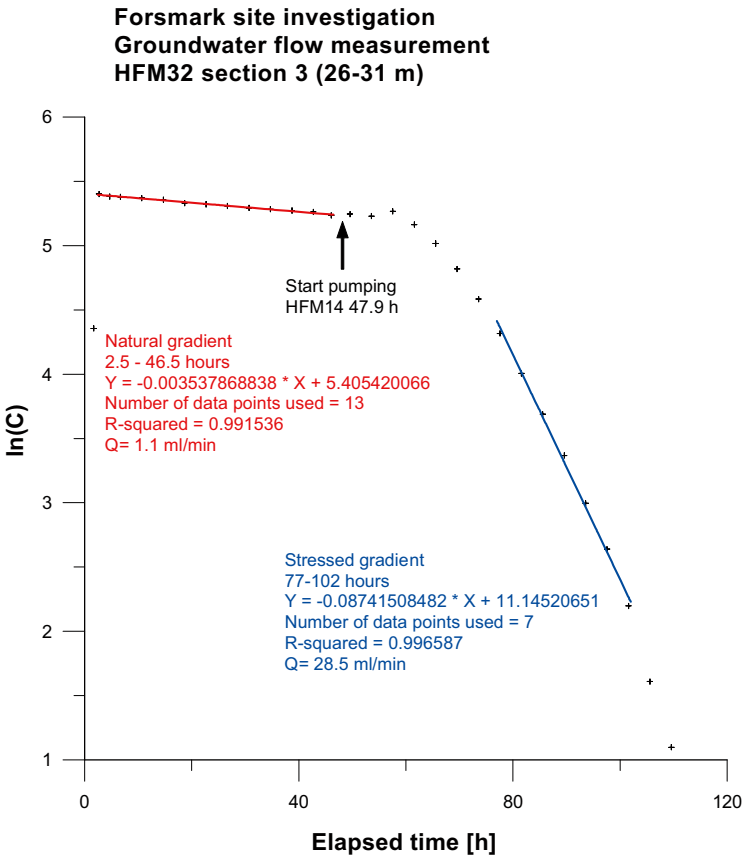

Figure A1-5. *Tracer dilution graph for section HFM32:3.*

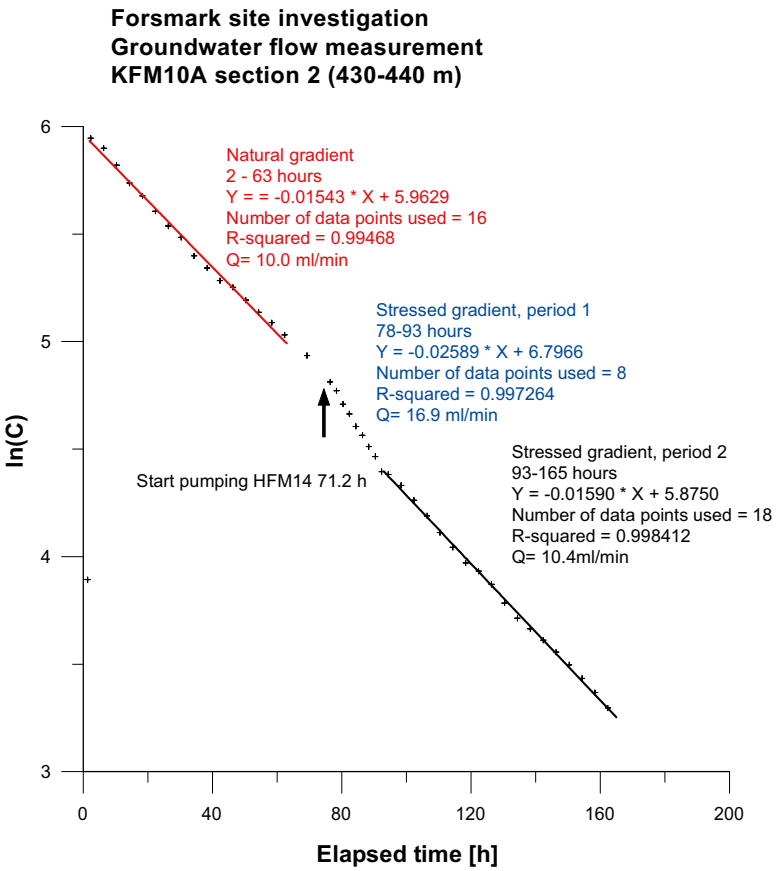

Figure A1-6. *Tracer dilution graph for section KFM10A:2.*

Appendix 2

Groundwater levels (m.a.s.l.) during groundwater flow measurements

2007-06-21–2007-07-06

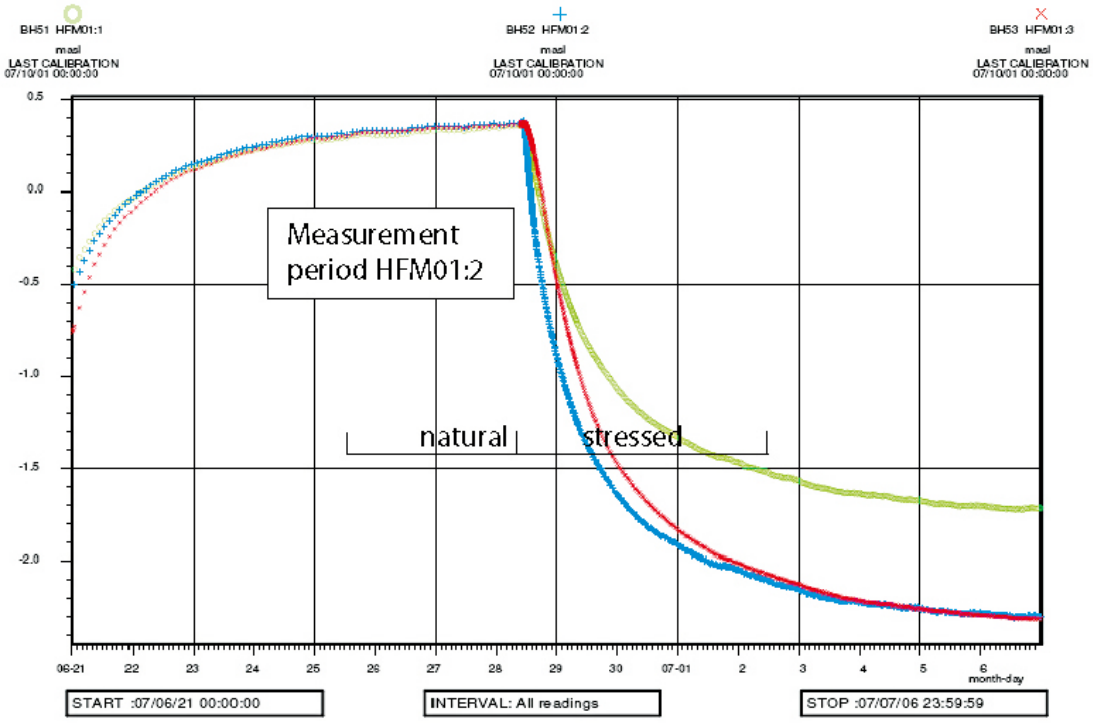

Figure A2-1. *Groundwater levels in borehole HFM01. Measured section HFM01:2 (blue).*

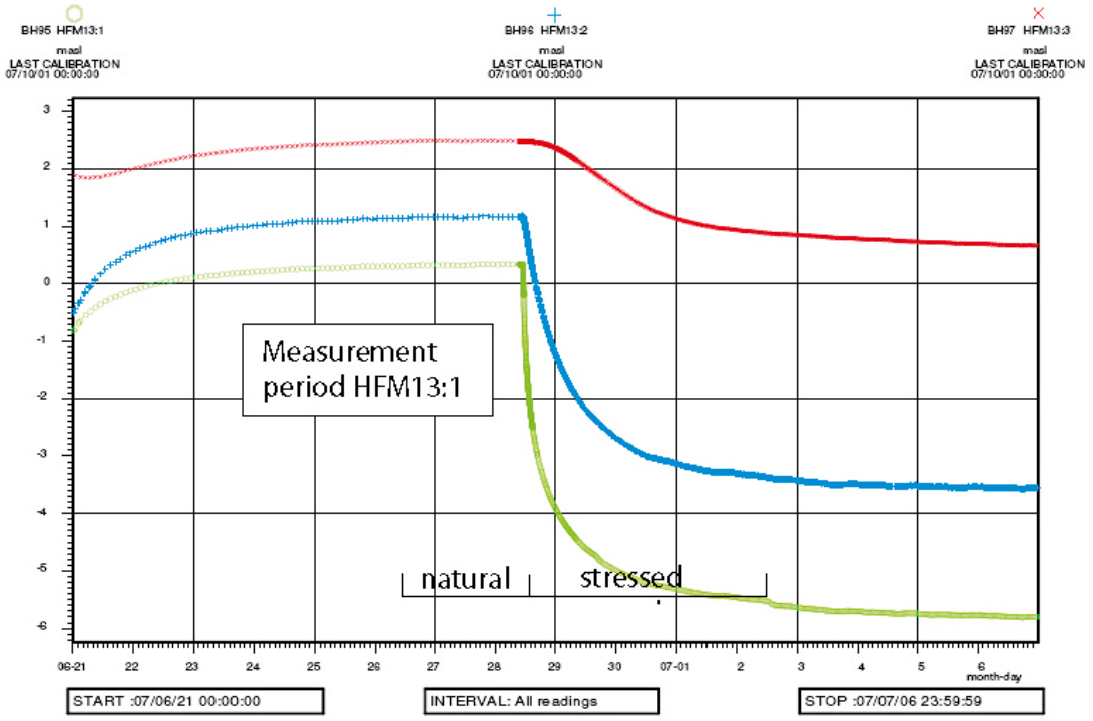

Figure A2-2. *Groundwater levels in borehole HFM13. Measured section HFM13:1 (green).*

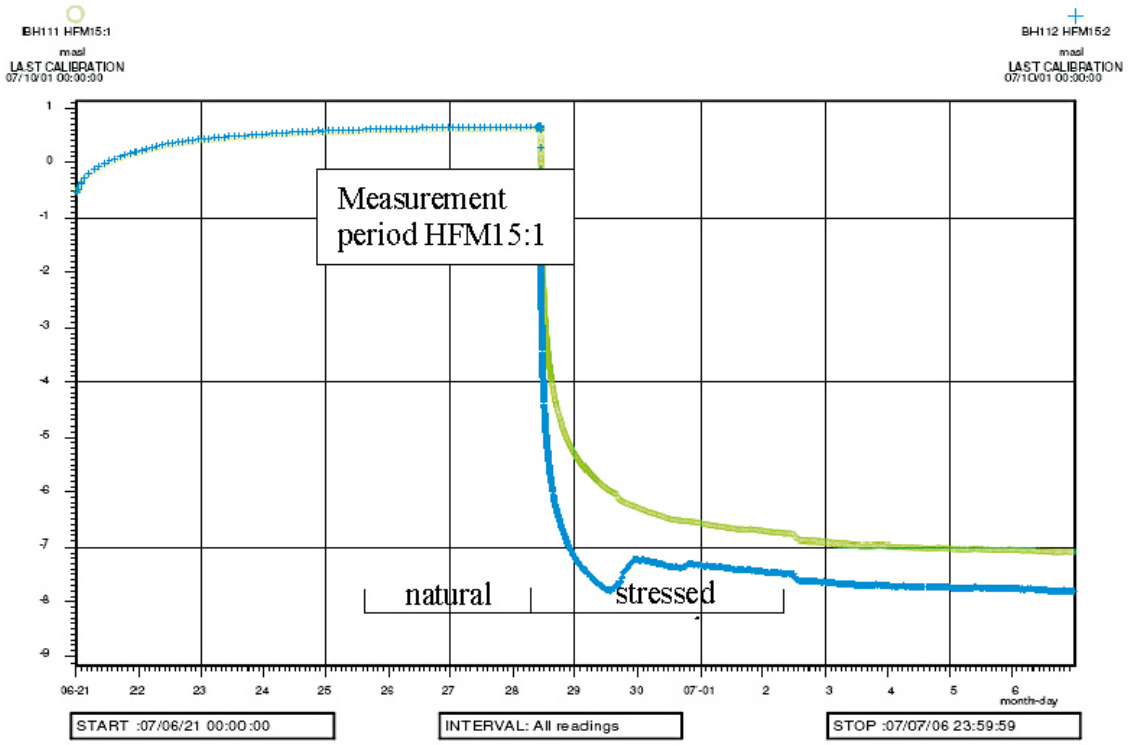

Figure A2-3. *Groundwater levels in borehole HFM15. Measured section HFM15:1 (green).*

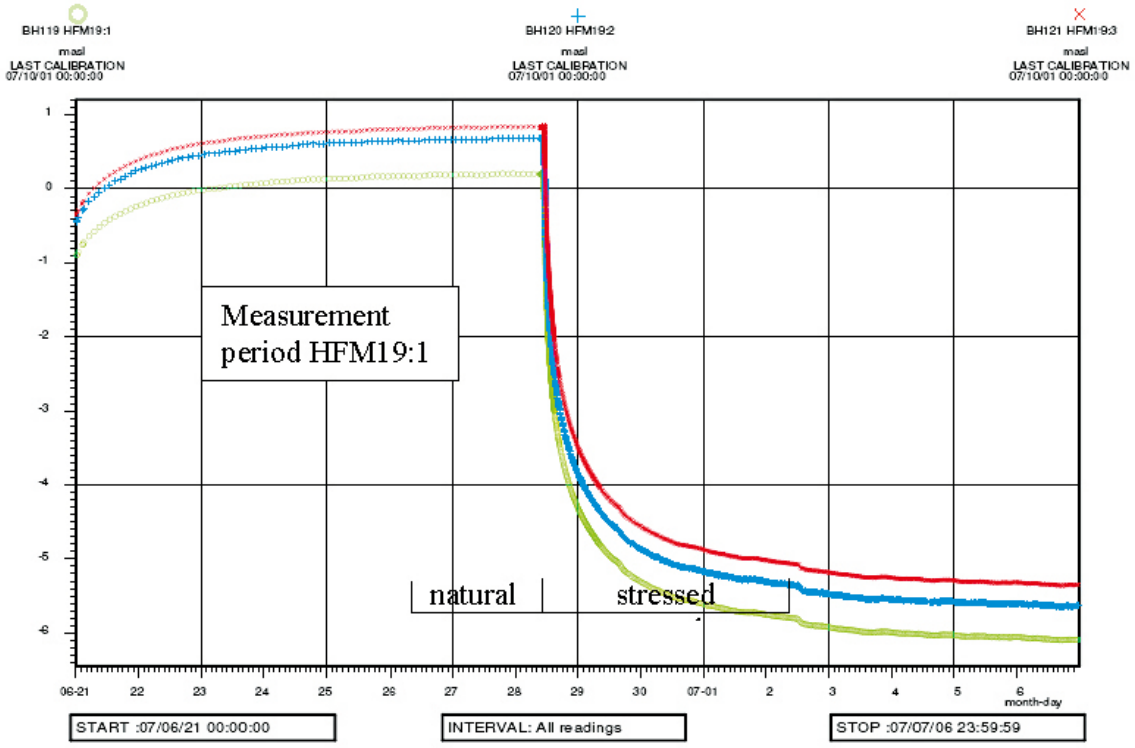

Figure A2-4. *Groundwater levels in borehole HFM19. Measured section HFM19:1 (green).*

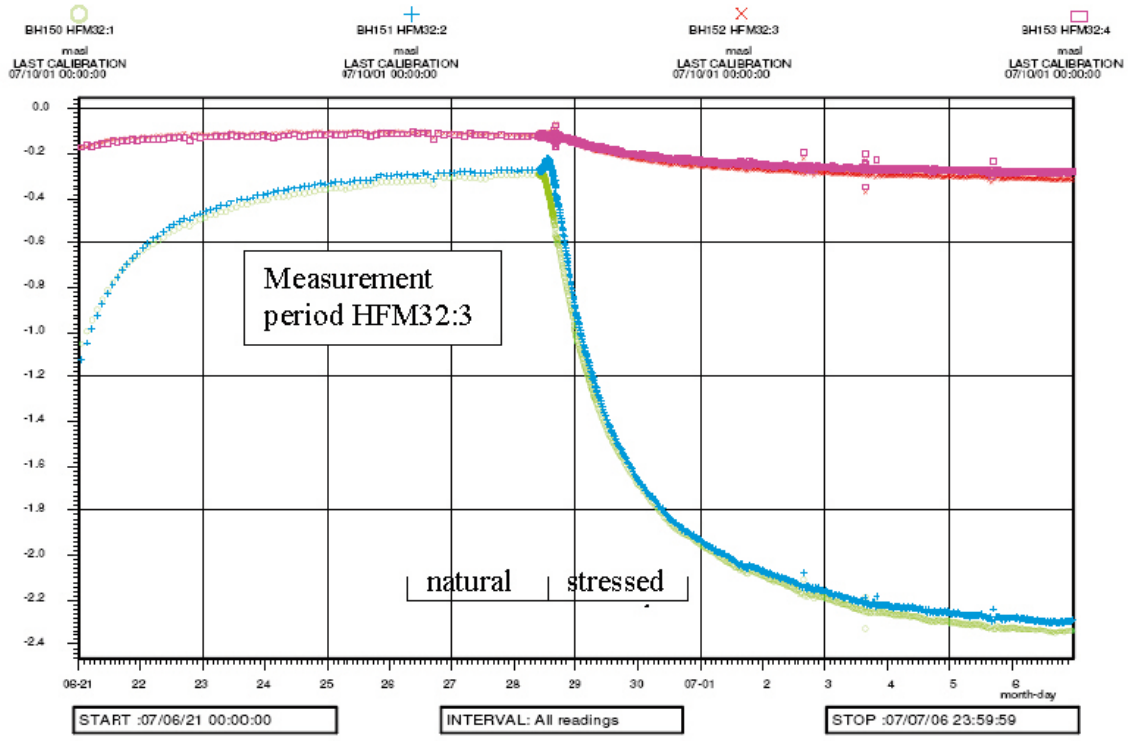

Figure A2-5. *Groundwater levels in borehole HFM32. Measured section HFM32:3 (red).*

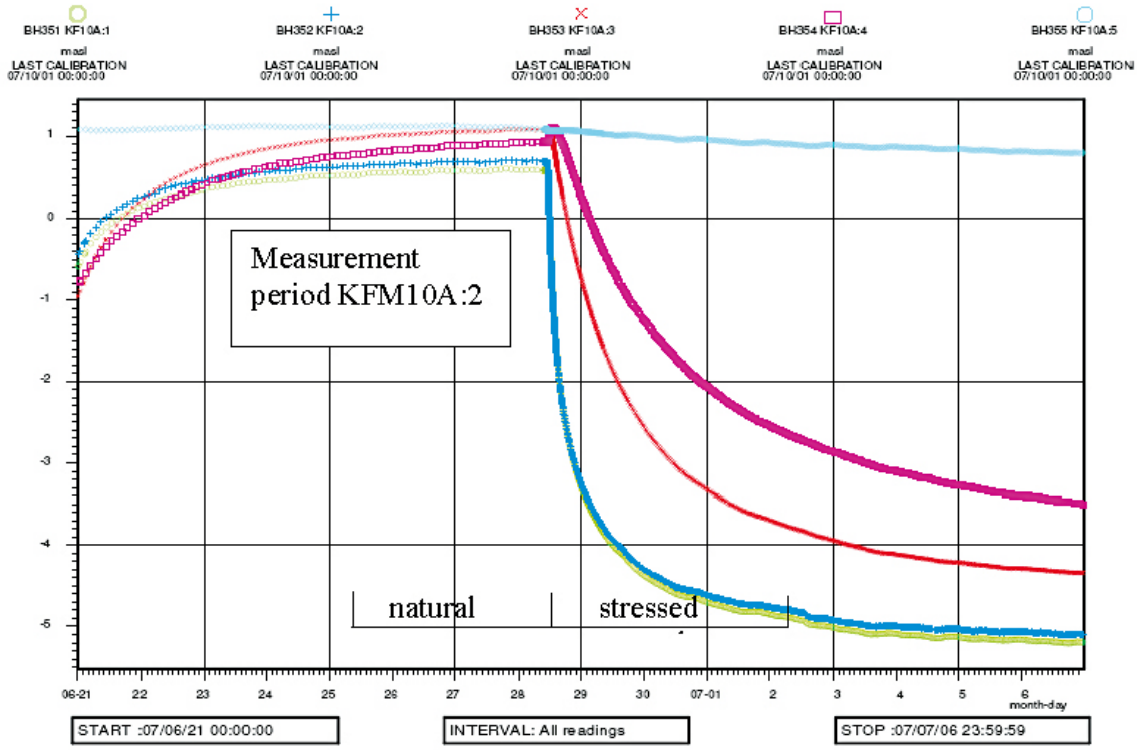

Figure A2-6. *Groundwater levels in borehole KFM10A. Measured section KFM10A:2 (blue).*

Appendix 3

Tracer dilution graphs- measurements after the tracer injection

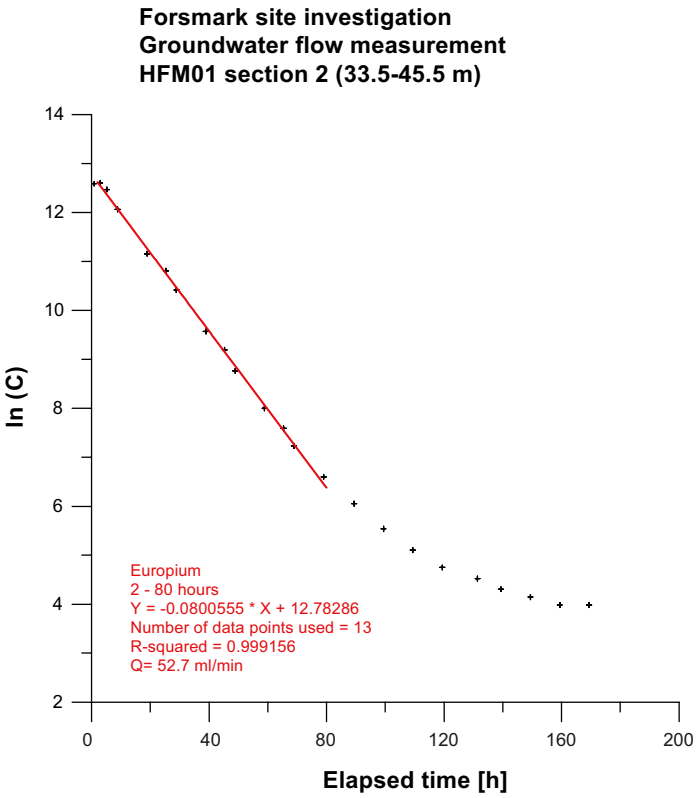

Figure A3-1. *Tracer dilution graph for section HFM01:2.*

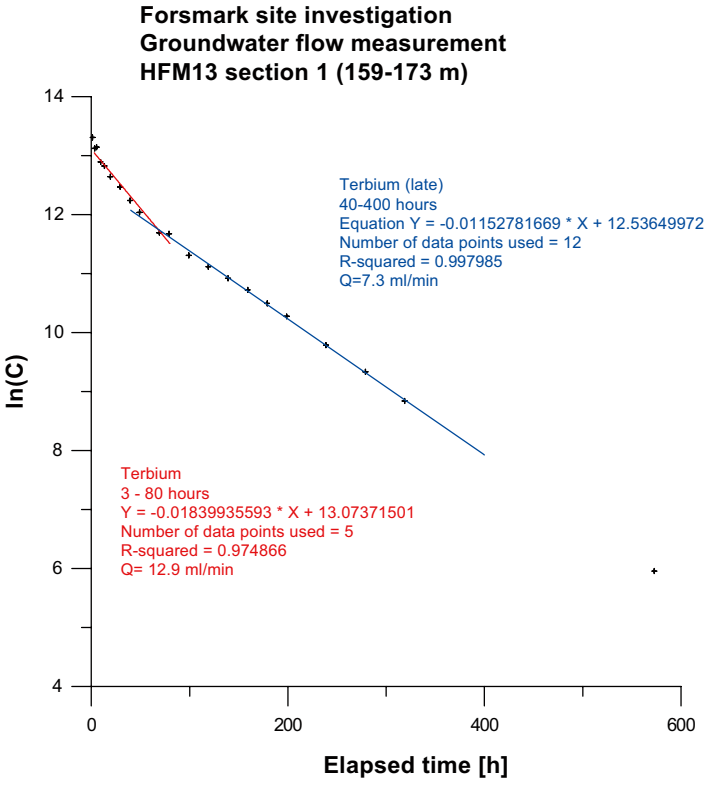

Figure A3-2. *Tracer dilution graph for section HFM13:1.*

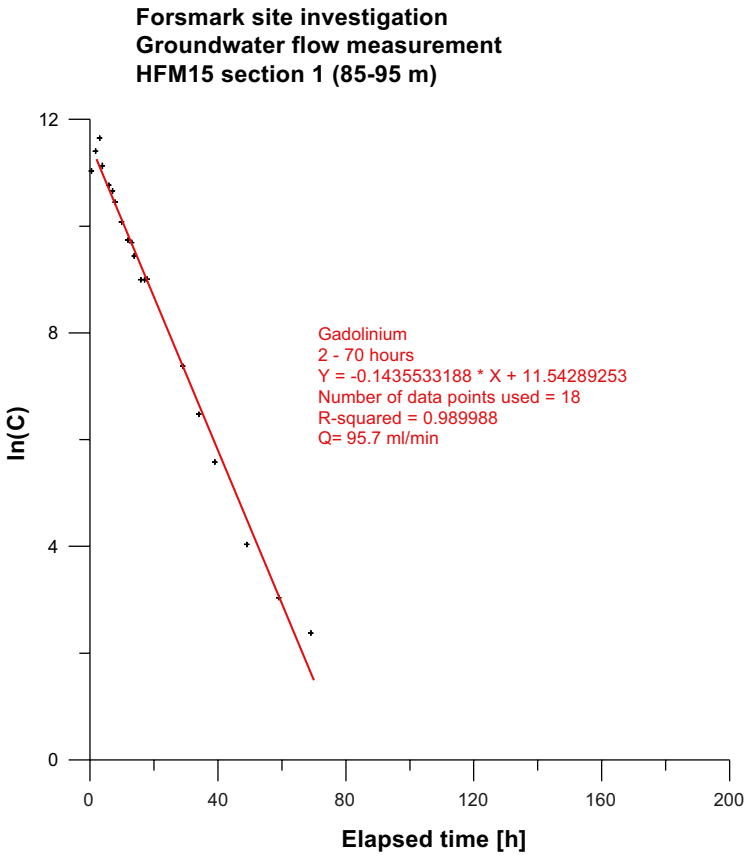

Figure A3-3. *Tracer dilution graph for section HFM15:1.*

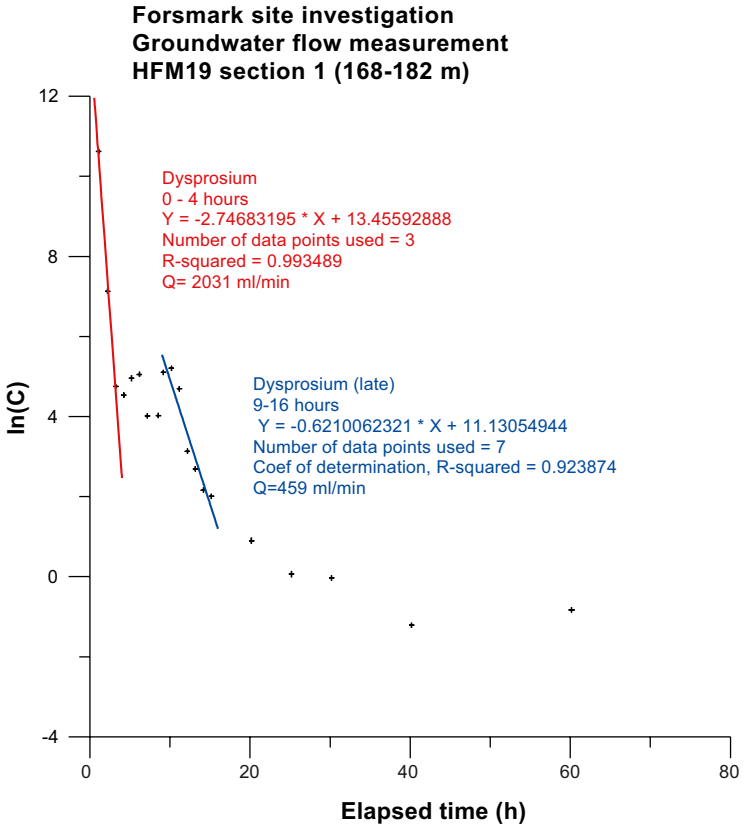

Figure A3-4. *Tracer dilution graph for section HFM19:1.*

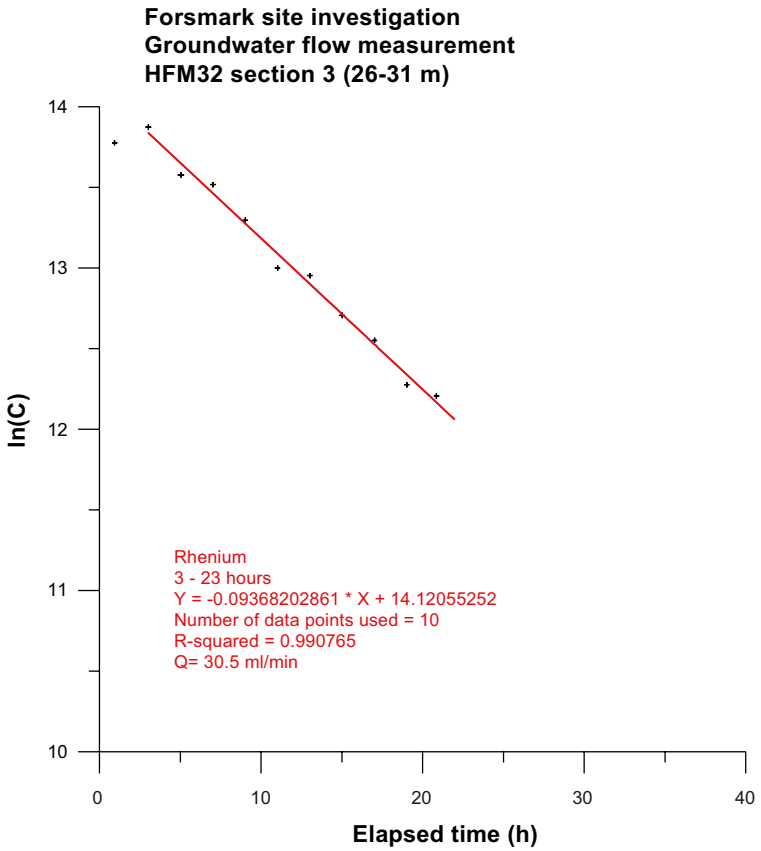

Figure A3-5. *Tracer dilution graph for section HFM32:3.*

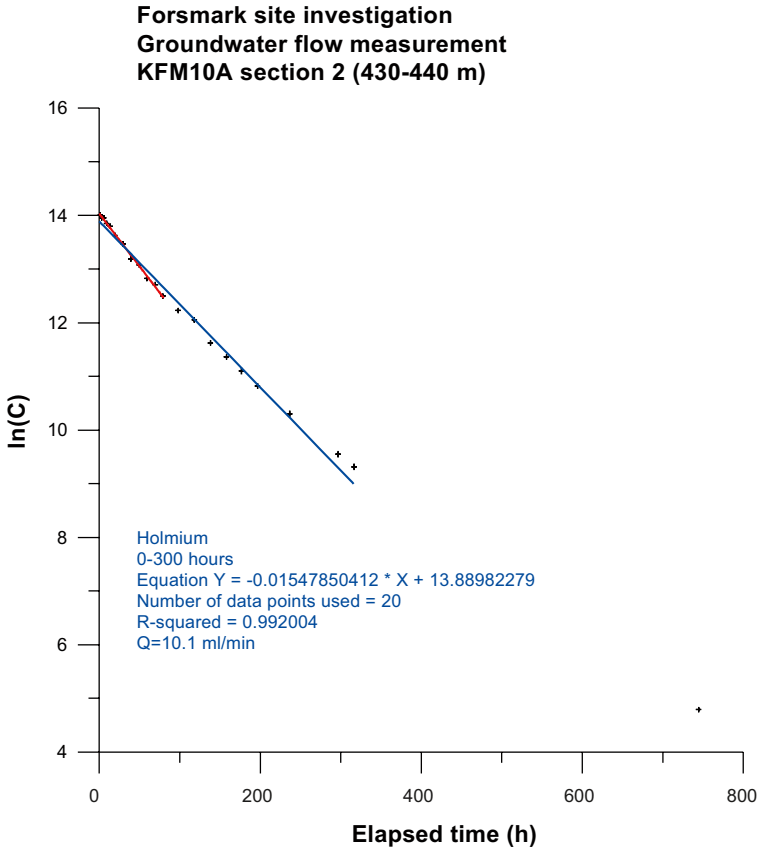

Figure A3-6. *Tracer dilution graph for section KFM10A:2.*

Appendix 4

Breakthrough curves (absolute concentrations, background concentration subtracted)

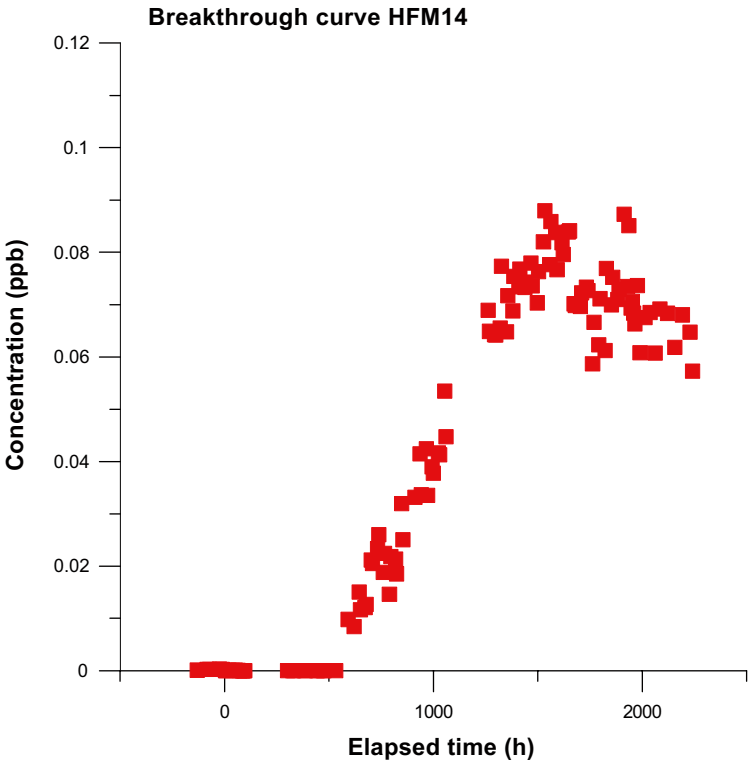

Figure A4-1. *Breakthrough curve for Eu from HFM01. Background concentration is subtracted.*

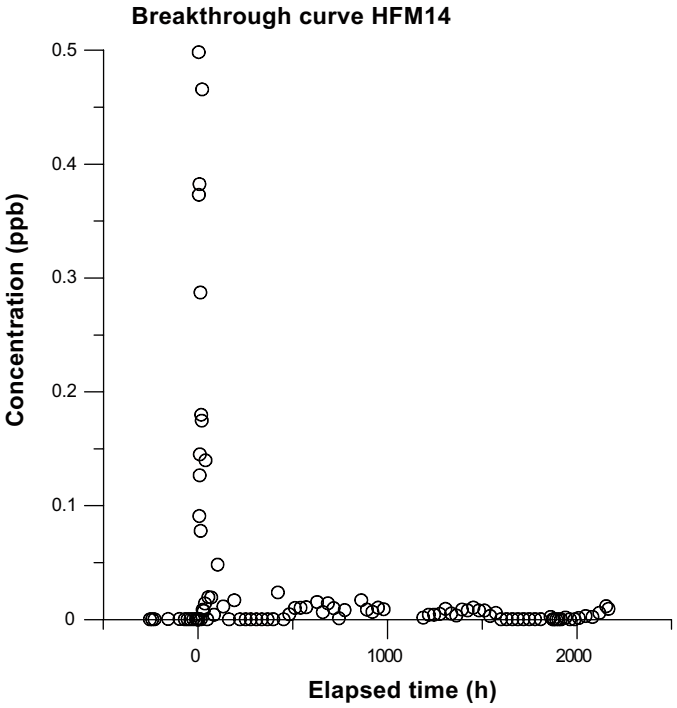

Figure A4-2. *Breakthrough curve for Re from HFM32. Background concentration is subtracted. The breakthrough is belived to be an artefact caused by contamination of Gd from HFM15, see Figure A4-6.*

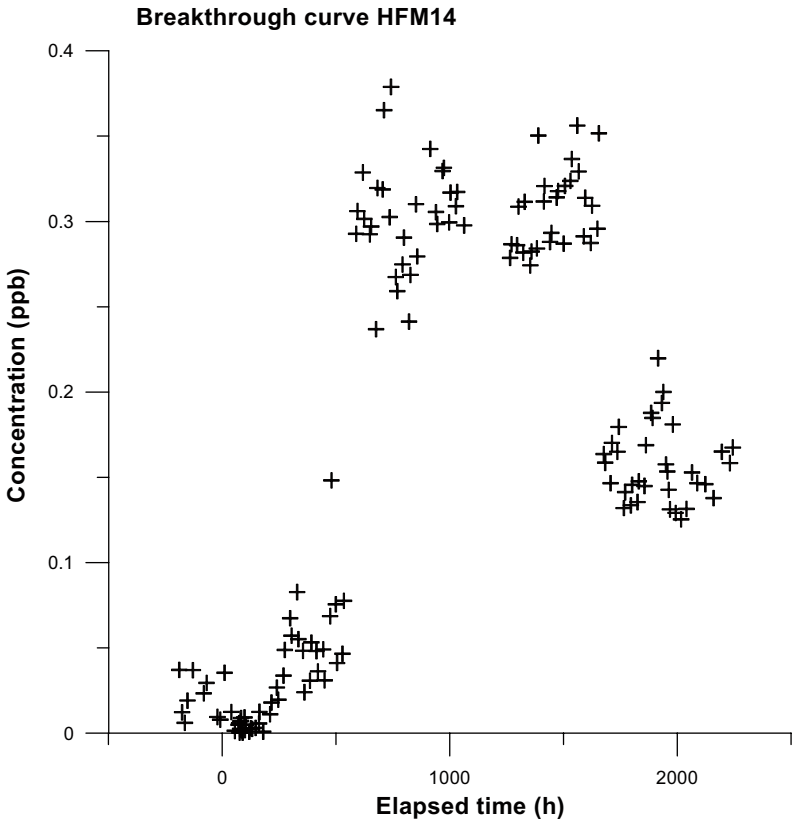

Figure A4-3. *Breakthrough curve for Ho from KFM10A. Background concentration is subtracted.*

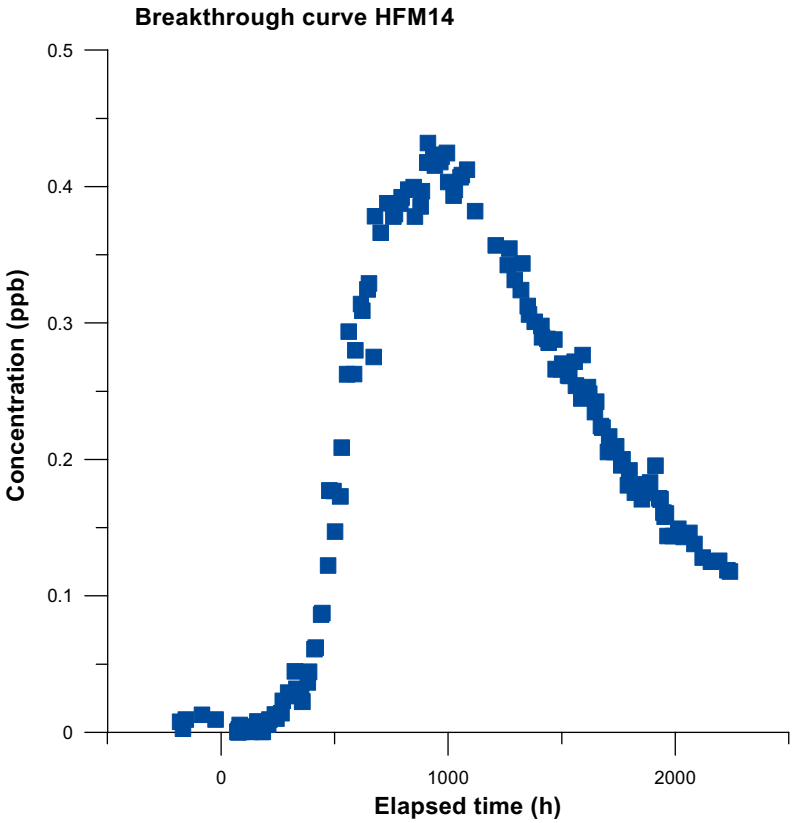

Figure A4-4. *Breakthrough curve for Tb from HFM13. Background concentration is subtracted.*

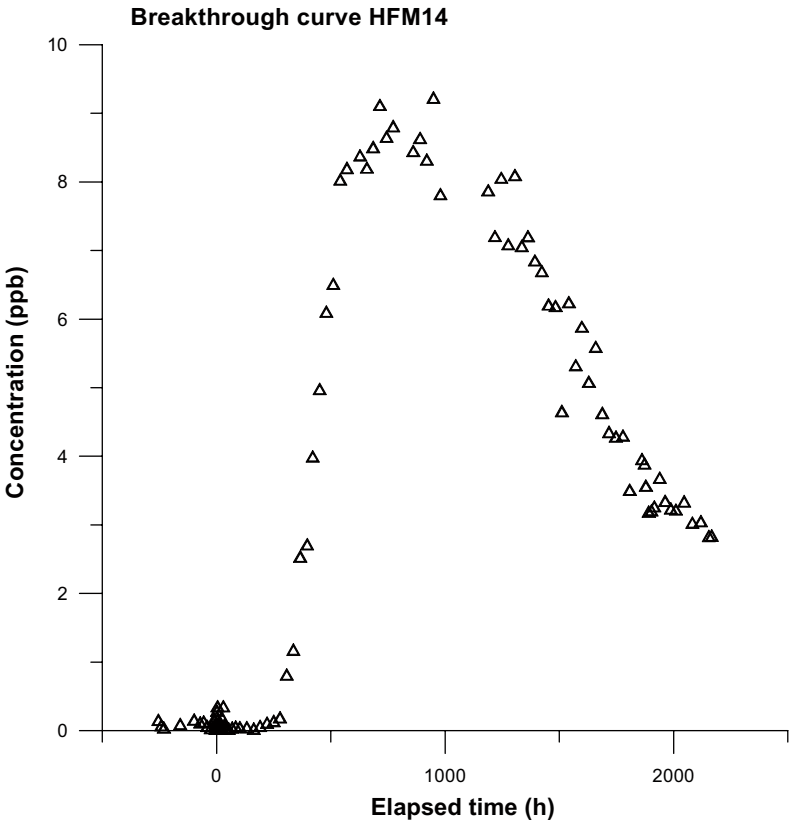

Figure A4-5. *Breakthrough curve for Dy from HFM19. Background concentration is subtracted.*

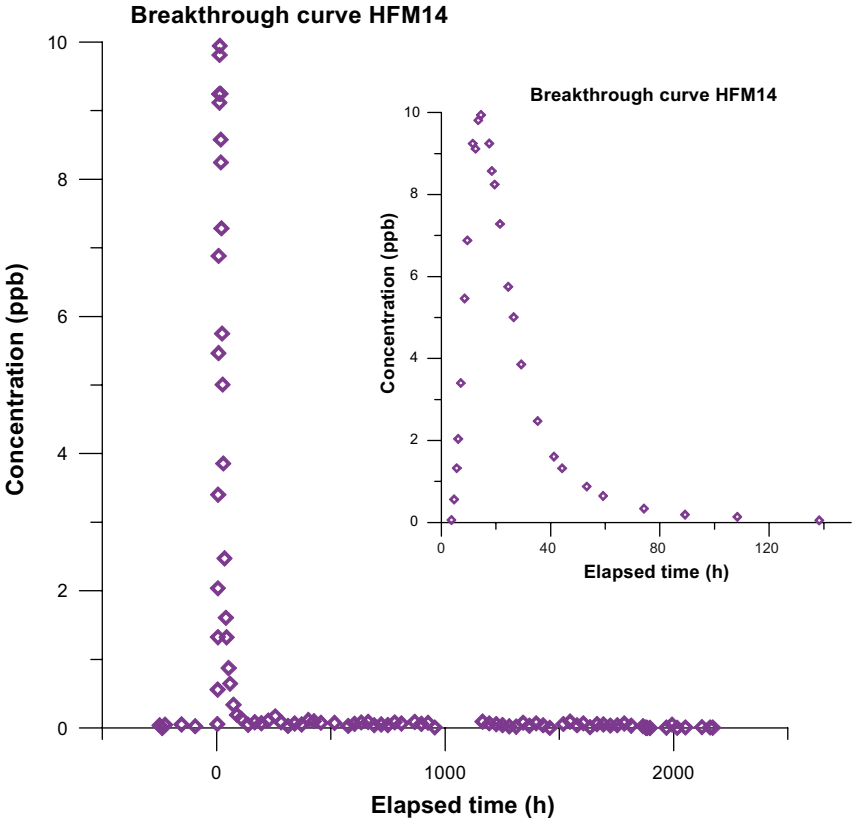

Figure A4-6. *Breakthrough curve for Gd from HFM15. Background concentration is subtracted. The small figure shows a more detailed resolution of the time scale at the time for breakthrough.*

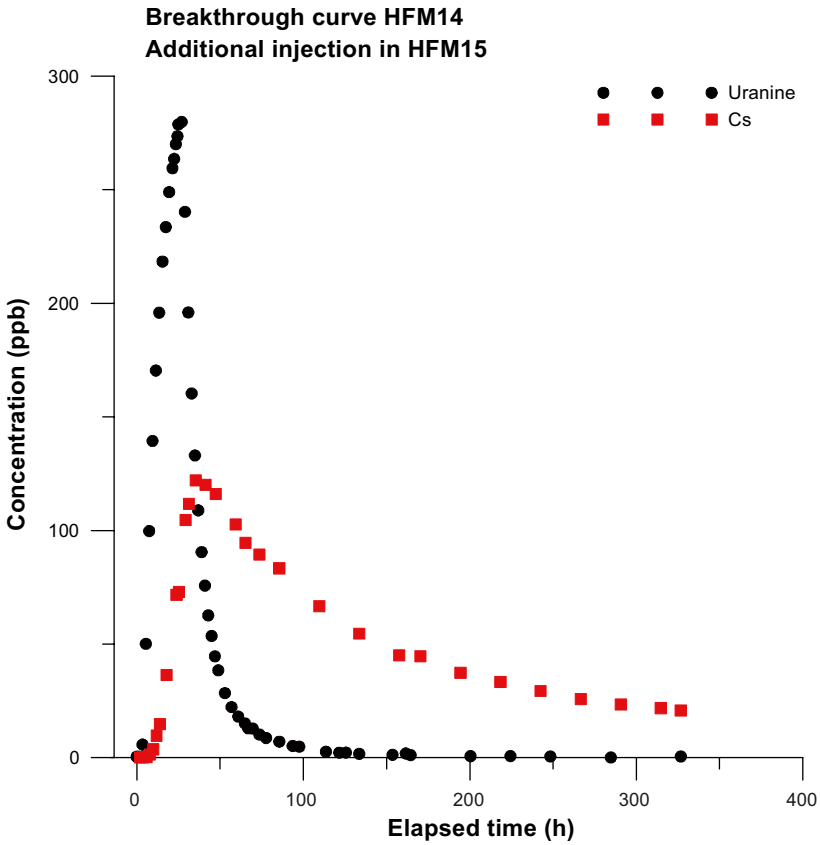

Figure A4-7. *Breakthrough curve for Uranine and Cs from HFM15. Background concentration is subtracted.*

Appendix 5

Groundwater levels (m.a.s.l.) during the whole test period

2007-06-15–2007-10-30

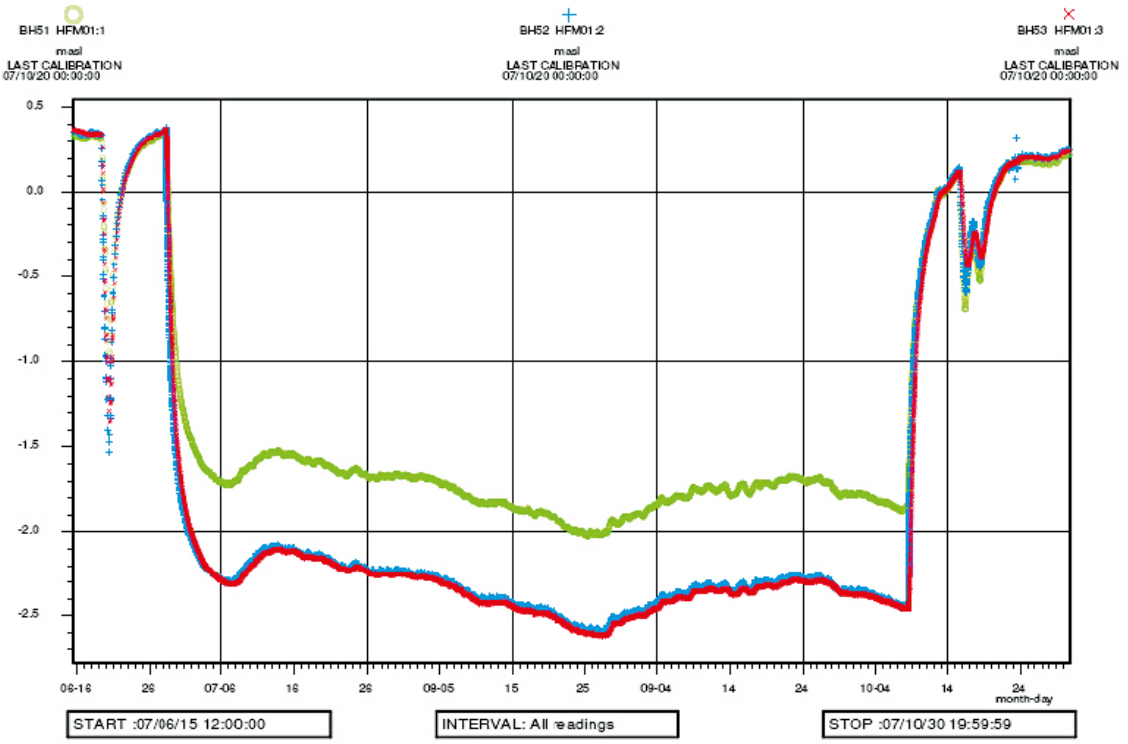

Figure A5-1. *Groundwater levels in borehole HFM01. Measured section HFM01:2 (blue).*

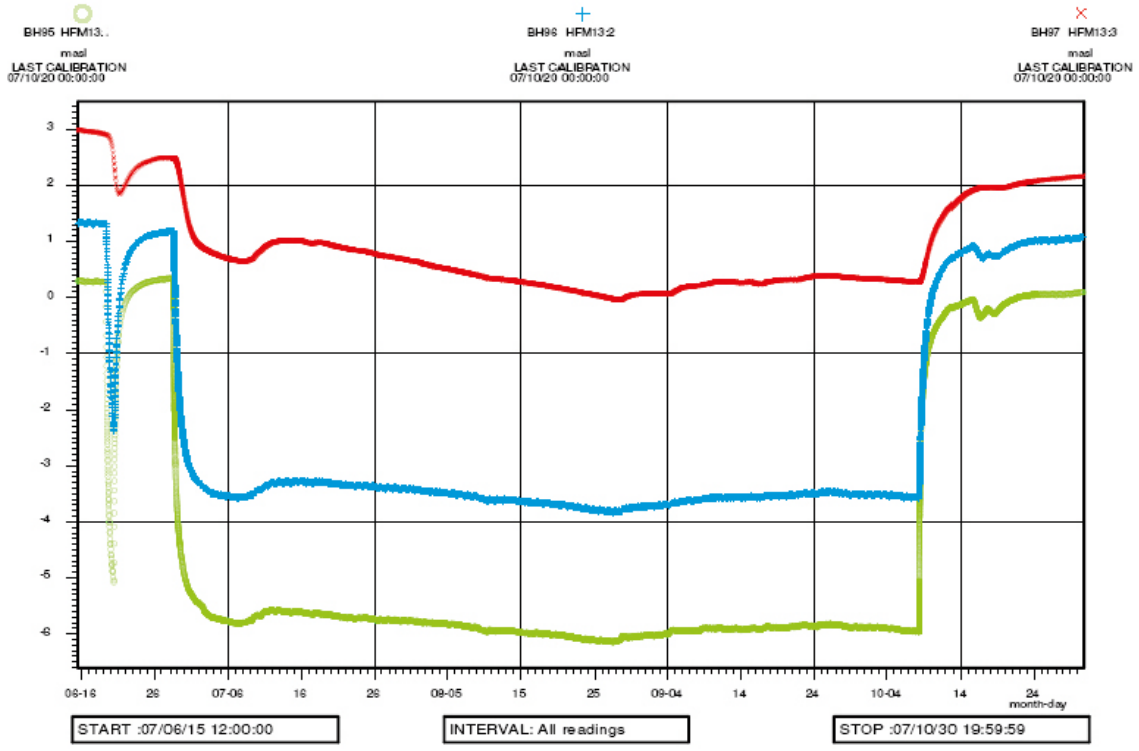

Figure A5-2. *Groundwater levels in borehole HFM13. Measured section HFM13:1 (green).*

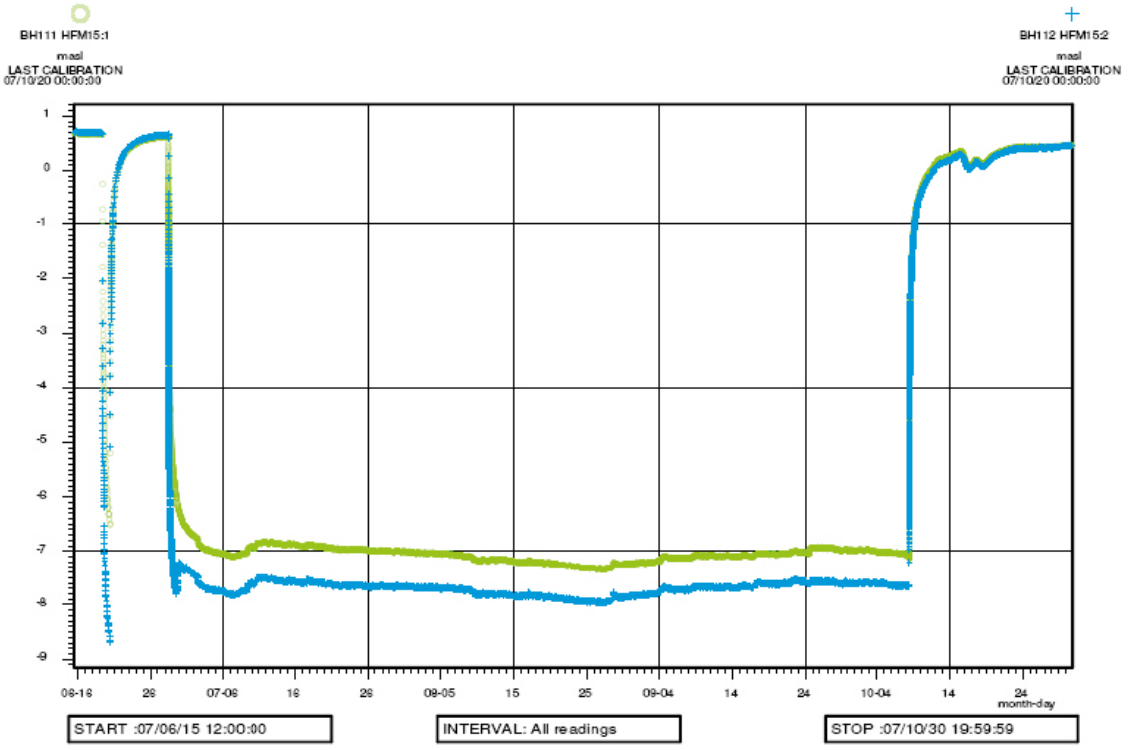

Figure A5-3. *Groundwater levels in borehole HFM15. Measured section HFM15:1 (green).*

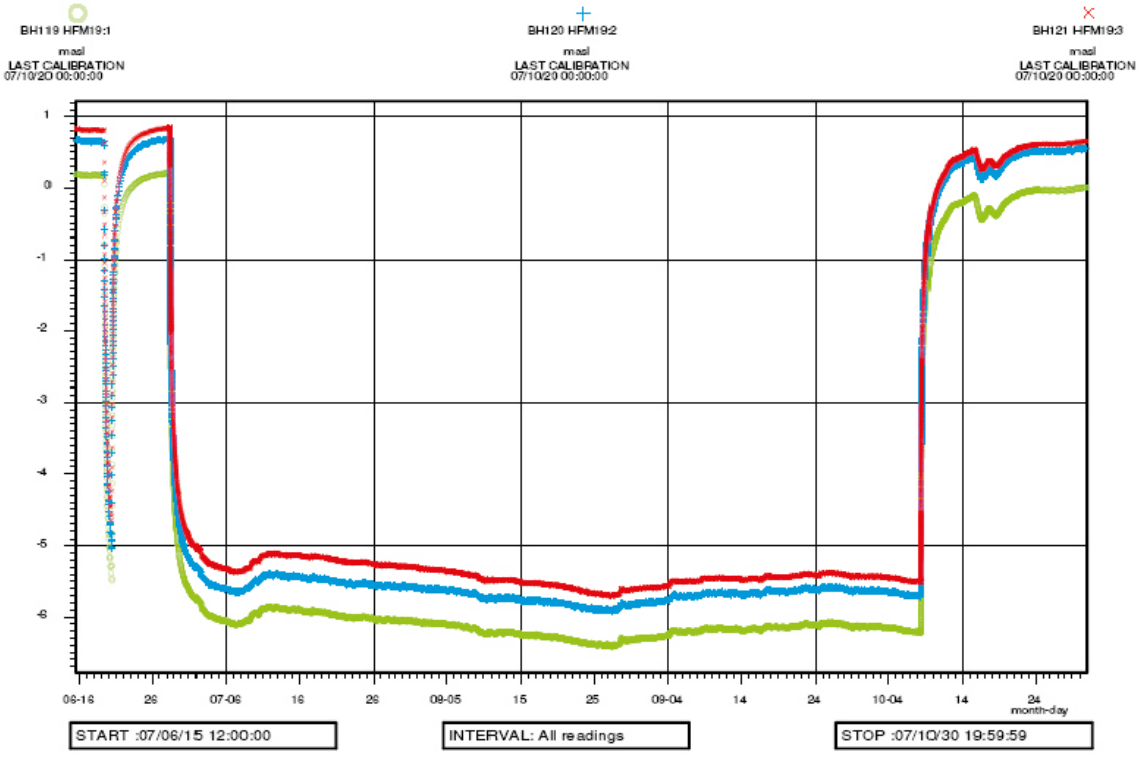

Figure A5-4. *Groundwater levels in borehole HFM19. Measured section HFM19:1 (green).*

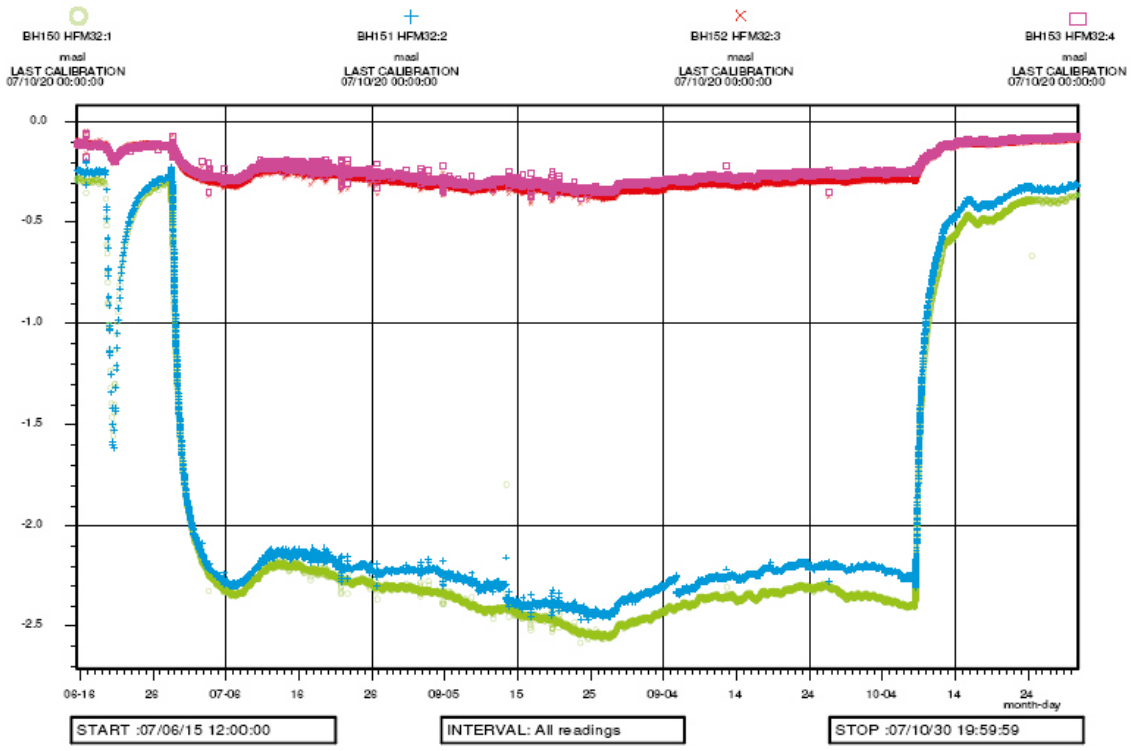

Figure A5-5. *Groundwater levels in borehole HFM32. Measured section HFM32:3 (red).*

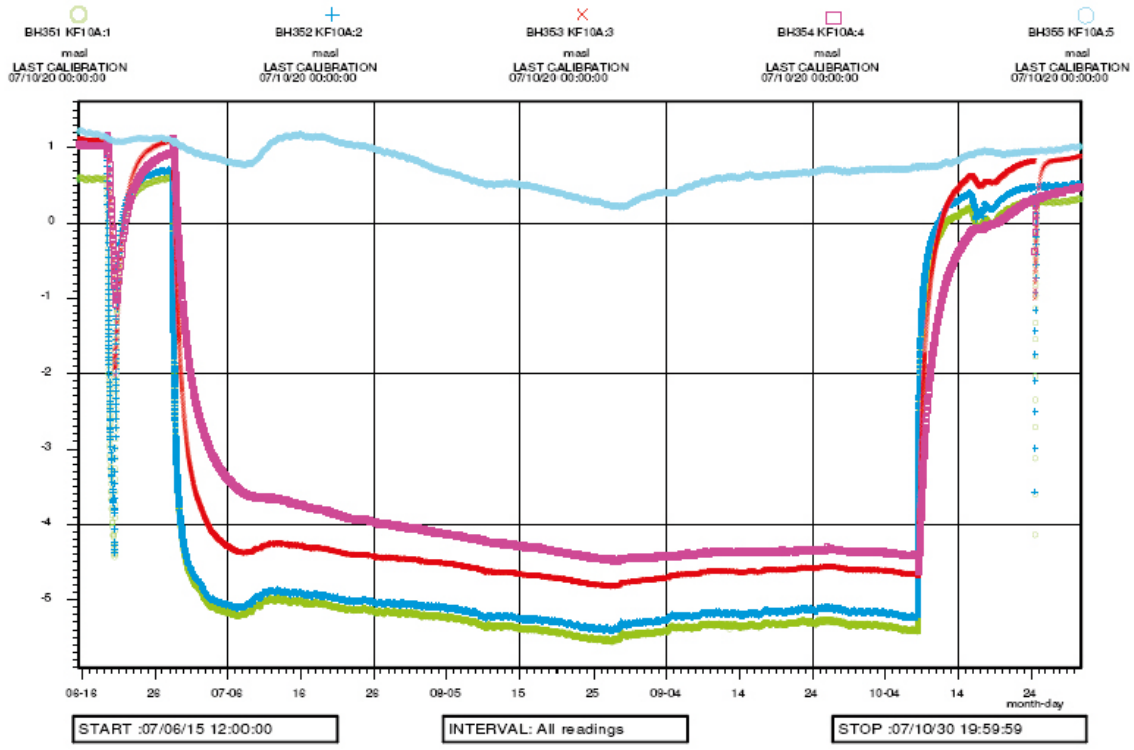

Figure A5-6. *Groundwater levels in borehole KFM10A. Measured section KFM10A:2 (blue).*